Fall 10-12-2023

HYDROCHEMISTRY OF AN ALPINE KARST SYSTEM, NORTHERN NEW MEXICO: LAS HUERTAS

Kambray A. Townsend
The University of New Mexico

Kambray Townsend
Candidate

Earth and Planetary Sciences
Department

This thesis is approved, and it is acceptable in quality and form for publication:

Approved by the Thesis Committee:

Laura Crossey, Chairperson

Rebecca Bixby

Karl Karlstrom

Tobias Fischer

HYDROCHEMISTRY OF AN ALPINE KARST SYSTEM, NORTHERN NEW MEXICO: LAS HUERTAS

By

KAMBRAY TOWNSEND

B.S. EARTH AND SPACE EXPLORATION (GEOLOGICAL SCIENCES), ARIZONA STATE UNIVERSITY

THESIS

Submitted in Partial Fulfillment of the Requirements for the Degree of

Master of Science

Earth and Planetary Sciences

The University of New Mexico

Albuquerque, New Mexico

December 2023

Acknowledgments

I would like to thank my advisor, Dr. Laura Crossey, and my committee members, Drs. Becky Bixby, Karl Karlstrom, and Tobias Fisher for their guidance and mentorship during my journey through the Master's program. Also, I want to thank Dr. Mehdi Ali for his patience and understanding while working in the chemistry lab and Dr. Laura Berkemper and Dr. Viorel Atudorei for their help running stable isotopes. I also thank Mr. Jim Daley for accompanying us and providing access to Las Huertas springs. Thanks to the Diagenesis Team, especially Dan Lavery, for assisting me in the field and the lab. Cibola National Forest provided funding to Dr. Crossey for analysis and fieldwork. I benefitted from the UNM Center for Water and the Environment workshops and networking opportunities. Financial support was provided by CREST NSF #1914490, EPS Alumni Scholarships, and a New Mexico Geological Society Grant-in-Aid.

HYDROCHEMISTRY OF AN ALPINE KARST SYSTEM, NORTHERN NEW MEXICO: LAS HUERTAS

Kambray Townsend

B.S. Earth and Space Exploration (Geological Sciences)

M.S. Earth and Planetary Sciences

ABSTRACT

Las Huertas in the Sandia Mountains relies on snowmelt, monsoonal recharge, and groundwater inputs. Our hypothesis, the proportion of groundwater contribution varied spatially and temporally, was assessed by observing travertine and multiple geochemical tracers to differentiate water balance components. We report 26 samples from 13 locations (sampled between 2021-2023). Major ion and isotopic analysis indicated Las Huertas headsprings vary spatially. Capulin Spring has higher salinity; major ions suggest recharged waters are a mix of $CaCO_3$-rich and sulfate-chloride-containing water. The proportion of groundwater to spring discharge is a mix of winter and summer precipitation. Travertine supersaturation is seasonal, with variations downstream, suggesting seep from near-surface karst. Major ions show greater dissolved ions in baseflow seasons and less in runoff seasons. Las Huertas springs differ from springs down the Madera dip-slope – by CO_2 manifested by travertine deposition - high CO_2 is from the limestone aquifer and external CO_2, likely from deep sources.

Table of Contents

List of Tables

List of Figures

Introduction

Persistent drought conditions, increased water use, and anthropogenic modifications of water resources have made wetlands in the southwest vulnerable to a changing climate. Spring-fed waterbodies in mountain recharge zones, such as Las Huertas Creek in the Sandia Mountains, New Mexico, rely on surface recharge and often have intermittent groundwater inputs along flow paths. Connections between surface water and groundwater in the Las Huertas watershed must be better understood for effective management. Las Huertas headwaters emerge within the southern portion of Las Huertas Canyon, where springs feed into the streamflow. Las Huertas waters are the primary water source for the acequias in the Village of Placitas, where most base and peak flows are used (Johnson and Campbell, 2002; Frus, 2016), including for irrigation by the San Felipe Pueblo. A small community comprised of camp facilities and private residential homes near the Las Huertas Springs, also uses Las Huertas waters in the northern portion of the watershed within the northern Sandia Mountains (Frus, 2016).

Previous workers have shown that the Las Huertas watershed receives recharge by snowmelt, summer precipitation, and infiltration into the regional karst aquifer (Johnson and Campbell, 2002; Frus, 2016; DeLay et al., 2021). The Las Huertas watershed includes CO_2-rich springs emerging at a high elevation in an arid land region, actively precipitating travertine in some reaches but not others, which may indicate variable fluid inputs and geochemistry along the flow path. The climate of the Sandia Mountains has a bimodal source of precipitation. Snowfall occurs from December through March, with monsoonal rainfall occurring from July through September. Sandia Crest receives an annual average rainfall of 560 mm and about 304 mm at the base (Johnson and Campbell, 2002; McCoy and Blanchard, 2008).

An inventory of springs located within Cibola National Forest was performed in 2012-16 by Rebecca Frus as part of her doctoral work (Frus, 2016). Forty-two water samples from 19 spring locations were collected (Table 1). Monitoring of these springs was continued by Kathryn Mendoza in Spring 2016 and Spring 2017 as part of a professional project for her Master of Water Resources degree (Mendoza, 2017). In the Summer of 2017, Spring Ecological Assessment Protocol (SEAP) forms were completed for ten springs locations, and seven water samples were collected from the Sandia and Manzano mountains (Table 1) (DeLay et al., 2021).

Legacy data from prior University of New Mexico (UNM) reports and papers for the Sandia and Manzano regions (work mentioned above) were used for a Springs Inventory Report on behalf of Cibola National Forest (DeLay et al., 2021). Selected data are summarized in a report focusing on the geochemical data from Brittany Griego (Sandia Mountains) and Naomi DeLay's spring research in 2019-2022 (Griego, 2023). Monitored springs were visited seasonally to understand flow paths and synthesize the geochemical dataset collection utilized as legacy data for this study (Table 1) (DeLay et al., 2021). This study also continues monitoring Capulin Spring and Las Huertas Springs in the Sandia Mountains.

Las Huertas watershed springs emerge within the upper portions of the watershed downslope from Sandia Crest. Capulin Spring is about 3.26 km northeast of Sandia Crest and is at an elevation of approximately 2,670 m. Capulin Spring is about 560 m downgradient. The Las Huertas Springs is about 3.27 km from Sandia Crest and about

709 m downgradient from Sandia Crest (Figure 1) (Read, A. et al. 2000). Several surface water collection locations are located at the Las Huertas Picnic Site. The Las Huertas Picnic Site, established in the 1930s, consists of walking trails and provides recreational activities such as picnicking and bird watching (USDA NFS). Five sample locations within the Las Huertas Picnic Site consist of waters from Capulin Canyon converging with the Las Huertas mainstem water (Read. et al., 2000) (Figure 2). Las Huertas then traverses north towards Tecolote, crosses the San Francisco faults (described below), and traverses west-northwest into the lower subbasin (Connell et al., 2000; Read et al., 2000; Johnson and Campbell, 2002).

Travertine-precipitating springs that feed the Las Huertas watershed emerge from the limestone aquifer with calcium carbonate-rich waters (Frus, 2016). Downstream from the springs, travertine deposits, forming dams and pools, are evident with intermittent occurrences along the Las Huertas Creek flow path (Figure 3). Regionally, Crossey and others (2009) have shown that carbonic springs and associated travertines record deep geologic inputs of CO_2 via transport along fault structures. Typically, springs precipitating travertine have waters with high concentrations of calcium carbonate and higher TDS values compared to non-travertine precipitating springs (McCoy and Blanchard, 2008).

Evaluating groundwater mixing regimes, CO_2-richness, and snowmelt infiltration in a high-elevation, spring-fed watershed in the regional karst aquifer and surface waters is essential for effectively managing the water resource. In the United States, forty percent of the groundwater used for drinking water comes from karst aquifers, and given increased water demands, karst aquifers are significant water reservoirs at risk of depletion (Green et al., 2006; Quinlan and Ewers, 1989). Karst terrains exhibit complex groundwater flow paths caused by depositional heterogeneities and fracturing (Quinn et al., 2006). Dissolution also affects carbonate aquifers, and groundwater flow may comprise diffuse, fracture, and conduit flows. These aquifers present focused and fast groundwater transport. Losing streams may also be present in a karst aquifer terrain (Bailly-Comte et al., 2009). Las Huertas has both perennial and dry reaches along the flow path, possibly due to the karst aquifer in the mountain recharge zone. The Las Huertas main stem mirrors karst aquifer chemistry and structure through intermittent flows and active travertine deposition along the flow path. Spring ecosystems can be classified using a site-specific geomorphological diagnostic approach (Stevens et al., 2021). Stevens et al., 2021 developed an illustrated key for terrestrial spring ecosystem types; Based on our visit to the Ellis Spring and Camp Spring emergence locations, in the upper most reaches of the watershed, in the Fall of 2021, the springs are classified as limnocrene or helocrene springs.

Study Approach

This study evaluates the hypothesis that the proportion of groundwater contribution to spring discharge of Las Huertas Springs and Capulin Spring varies spatially and temporally, using the most extensive sampling of the upper watershed to date. We hypothesize that the supersaturation of the Las Huertas waters with respect to calcite (travertine accumulation) will change seasonally, with greater potential for calcite precipitation during the fall season, reflective of baseflow condition, and less potential for calcite precipitation during the spring season, due to snowmelt runoff, along the Las Huertas stream flow path. We also hypothesize that stable isotopes and major ion concentrations will vary and that these patterns may allow the differentiation of the components (e.g., winter precipitation or snow, the short residence time of groundwaters or the underflow on a seasonal time scale, and the long residence time of regional karst groundwaters) in the water balance along the Las Huertas flow path. The geochemical modeling will be used to assess whether external carbon dioxide sources are required to produce the observed travertine occurrences. Major ion analysis for stream and spring waters allows us to gain insight into the Las Huertas watershed potential flow paths and general water quality. Additionally, stable isotope geochemistry helps investigate recharge mechanisms and evaporation effects (Sharp, 2017).

Geologic Setting

Regional Geology

The Sandia Mountains are located along the eastern flank of the Rio Grande Rift, comprised of the Sandia granite, an uplifted granite block of Paleoproterozoic granites and metavolcanic rocks overlain by the Arroyo Peñasco Group (sandstone), Sandia Formation (limestones and sandstone), and east-dipping interbedded limestone (Madera limestone) (Karlstrom et al., 1997; Lucas et al., 1999; Connell et al., 2000; Read et al., 2000; Frus, 2016) (Figures 4 and 5). Permian, Pennsylvanian, and Mississippian formations are distributed within the Placitas fault zone, higher elevation regions of the Sandia Mountains, and the bottom of the Las Huertas Canyon. Shales in the Upper Madera Group and finer-grained components in the Abo formation are confining beds isolating the Madera limestone aquifer (Figure 5). The Madera Limestone has been identified as the primary hydrostratigraphic unit for this region (Johnson and Campbell, 2002) (Figure 5).

The complexity of the fault network of this region plays a significant role in the hydrologic setting. The Madera limestone makes up the fractured regional aquifer, thus allowing groundwater to move through fault-related fracture systems, fractures formed from solution, and bedding planes (Johnson and Campbell, 2002; Connell et al., 2000; Read et al., 2000). The steep dipping, normal West Las Huertas fault and the north-trending, moderately dipping East Las Huertas normal fault bound Las Huertas Canyon (Figure 4; Johnson and Campbell, 2002; Connell et al., 2000; Read et al., 2000). The South Montezuma fault is an east trending steeply dipping reverse fault that joins the East Las Huertas fault at Tecolote (LeFevre, 1999). The faults within the Las Huertas system are parallel to the direction of stream flow and influence groundwater to flow in a fault-parallel direction (Johnson and Campbell, 2002). See geologic map shown in Figure 4.

Hydrologic Setting

Johnson and Campbell (2002) have characterized the hydrologic setting of the Las Huertas watershed, and this section draws from their work. Fed by spring discharge from the northwest portion of Capulin Peak and Sandia Crest runoff, Las Huertas traverses north towards Tecolote, crosses the San Francisco faults, and traverses west-northwest into the lower subbasin. Three major drainage basins, Las Huertas, Arroyo Agua Sarca, and Arroyo de San Francisco, comprise the Placitas area. Las Huertas, which drains much of the northern portion of the Sandia Mountains, is the largest of the three basins. Las Huertas begins near Sandia Crest at about 10,678 feet (about 3.25 km) (Figures 1 and 4). Note that streamflow drainages flow eastward directly downdip south of the Las Huertas watershed divide. North of the drainage divide, all the drainages are routed northward toward Placitas along the faults.

Arroyo del Ojo del Orno operates as the main tributary to the lower Las Huertas drainage and merges with Las Huertas approximately 4,828 meters (about 3 mi) west of Tecolote. Las Huertas drainage basin has two acequias, Las Huertas-La Jara Ditch Association within the upper portions of Las Huertas Creek and Las Acequias of the Village of Placitas in the Arroyo del Ojo del Orno subbasin. The latter acequias rely solely on spring discharge for irrigation and domestic water supply for the Village of Placitas. Additionally, the San Felipe Pueblo uses water from Las Huertas's lower reaches for irrigation. About 48 percent of the stream flow is in the upper reaches of Las Huertas between the Las Huertas Picnic Area and the ditch diversion. Discharge rates were determined by Johnson and Campbell (2002) for Las Huertas, approximately 0.3 miles south of Sandia Cave. For their period of study, stream flow was between 30 cubic feet per second (cfs) to less than two cfs (Figure 6). The Abo and Madera formation aquifers within Las Huertas Canyon receive recharge through the infiltration of streamflow from Las Huertas Creek and snowmelt. A study of the Placitas area hydrogeology shows that water level increases occurred in wells in Las Huertas Canyon in the spring and early summer from snowmelt runoff increasing flows in Las Huertas Creek. Data from this 2002 study shows that Las Huertas plays a significant role in the annual recharge of the aquifers of Las Huertas Canyon.

Many streams that drain the major basins are intermittent or ephemeral and flow in response to snowmelt or storm runoff (Johnson and Campbell, 2002; Frus, 2016; DeLay et al., 2021). Perennial reaches of these streams are evident along Las Huertas and Arroyo de San Francisco. They are fed by springs that discharge groundwater from the Madera limestone or springs and seep along the flow path. Las Huertas is an essential source of water for the Placitas area. This resource is vital as it supports riparian areas, consisting of dense tree canopy cover and macroinvertebrates within the stream such as mayflies, snails, stoneflies, and other, and supports irrigation; it is critical for redistributing groundwater and surface water systems in an unconnected or poorly connected groundwater aquifer (Johnson and Campbell, 2002; Frus, 2016; Noe et al., 2021; DeLay et al., 2021).

Las Huertas is perennial along spring-fed reaches within the upper portions, lower portions below Tecolote, and the Arroyo del Ojo del Orno. The upper reaches of Las Huertas, nestled within a private residential community in the Sandia Mountains' northern portions, are spring fed except for snowmelt and stormwater runoff occurrences. A 4 km stream stretch was identified as perennial between the springs and the Las Huertas – La Lara Ditch Association diversion area. Streamflow is typically continuous in the upper regions of Las Huertas by snowmelt from April through June. Monsoonal rains during the summer months can extend this continuous flow into the fall season. Discharge from springs contributes to a 2 km reach of perennial flow along the lower portion of Las Huertas. Waters from the Lower Santa Fe Group are discharged through springs and seep into the downstream reaches of Las Huertas (Johnson and Campbell, 2002). Despite this detailed work, there are few comprehensive descriptions of water quality in the watershed's upper reaches; this study aims to mitigate that gap. This study is the first to look at the geochemistry of the upper reaches of Las Huertas (both springs and stream) and the confluence of waters from Capulin Canyon to the Las Huertas mainstem and contributes towards a more comprehensive look at these surface water-groundwater connections within the watershed from a multiple geochemical tracer approach to further our understanding of groundwater contribution to streamflow and seasonality patterns within the Las Huertas watershed.

Methods

Water Sampling

Springs and portions of Las Huertas' surface water were collected in November 2021, May 2022, November 2022, and May 2022, attempting to gather samples at least once seasonally (Figures 1 and 2). Water collection includes samples from Las Huertas springs (Ellis Spring and Camp Spring), Capulin Spring, and downstream surface waters, including the Capulin Canyon and Las Huertas mainstem confluence, along the stream when present. One snow sample was collected near the Capulin Snow Play Area in Winter 2023. These data were compiled with previously published data by Cibola National Forest for the Las Huertas watershed and the surrounding Sandia Mountains (DeLay et al., 2021; Frus, 2016).

Sample locations were recorded using GPS. Water quality parameters were measured at each location, including pH, temperature (°C), specific conductance (μS/cm), and total dissolved solids (TDS reported in ppm) using an Oakton waterproof pH/CON 300 meter (Frus 2016, DeLay et al., 2021). The meter was calibrated daily using a three-point calibration for pH and 2 points for conductance. Syringes and bottles were pre-conditioned three times with sample water before collection. Two bottles were collected at each location – one unfiltered 125 mL sample with zero headspace (to avoid degassing affecting lab alkalinity measurements) for alkalinity, anion, and stable isotope analysis and one 60 ml aliquot filtered (0.45 μM) and acidified with ~1ml concentrated nitric acid with a pH of 2.0 for cation/metals analysis (Myers, 2006; Frus, 2016; DeLay et al. 2022). One snow sample was collected in the Capulin Snow Play Area in February 2023 for stable isotope analysis only. Samples were refrigerated until analysis.

Water Analysis

End Point Titration method with 0.02 N sulfuric acid (H_2SO_4) and an Oakton pH/CON 300 meter was used to determine alkalinity in the Diagenesis Laboratory at UNM in the Department of Earth and Planetary Sciences (EPS) at UNM (Baird et al. 2017). Samples with zero headspace are titrated as soon as possible after sampling with 10% duplicates for quality assurance. Ion chromatography (IC) and inductively coupled plasma-optical emission spectrometry (ICP-OES) in the Analytical Chemistry Laboratory at the UNM EPS are used to analyze anions and cations, respectively. Standard methods were used for IC (Jackson, 2000) and ICP-OES (Hou et al., 2000), comparable to EPA 300.0 and EPA 200.7, respectively. Samples were analyzed at various dilutions of up to 1:10, with ten percent duplicates run in addition to lab quality assurance standards and blanks during analysis. Ion charge balance from the chemical ICP-OES and IC analyses of the samples were routinely within 5% error. Total dissolved inorganic carbon (DIC) was calculated using the thermodynamic equilibrium speciation model PHREEQC (Parkhurst 1995) using pH, temperature, and measured alkalinity to estimate all DIC components, bicarbonate, carbonic acid, and carbonate. Geochemical modeling was performed with both PHREEQC and Geochemist's Workbench (Bethke, 2017).

Stable isotope analysis of hydrogen and oxygen was conducted using cavity ring-down spectroscopy (Picarro L 1102-I) in the Center for Stable Isotopes (CSI) at UNM to calculate the weighted mean values of the isotopologues of liquid water. Isotope values are reported in ratios of heavy to light isotopes, such as $^{18}O/^{16}O$ for oxygen and $^{2}H/H$ (D/H) for hydrogen. Both isotopes are reported with respect to the Vienna Standard Mean Ocean Water (VSMOW). A standard calculation used to report isotope composition in delta notation (Sharp, 2017) is expressed as

$$\delta^{18}O = \left(\frac{R_{sample}}{R_{standard}} - 1\right) \times 1000 \; where \; \frac{R_{sample}}{R_{standard}} = \frac{{}^{18}O/{}^{16}O}{{}^{18}O/{}^{16}O}$$

Stable isotope composition is reported in parts per thousand (‰ or per mil) deviation from the standard. Each sample was analyzed six times and then averaged. Results show each sample is routinely within 0.1 ‰ error for $\delta^{18}O$ and 2.0‰ for δD. Duplicates were run at a ten percent frequency and were within the reported margins of error.

Results

Field Parameters

Water quality parameters for sampled spring and stream locations were recorded for this study between Fall 2021 and Spring 2023 (Table 1). Water quality parameters were also compiled from previous studies (Frus, 2016; DeLay et al., 2021; Table 1). Field parameters measured for spring and stream samples from this study include temperature (°C), pH , conductance µS/cm, and alkalinities in mg/L as HCO_3^- .

Springs. Capulin Spring waters collected between 2012 and 2017 had an average TDS of 952 ppm, pH of 7.16, and 1,384 µS/cm conductivity; Capulin Spring waters collected between 2021 and 2023 had an average TDS of 1,269 ppm, average pH of 6.2, and average conductivity of 1,534 μS/cm. DeLay et al., 2021Las Huertas Spring waters collected in Fall 2021 temperature ranges from 7.8 to 8.4 ;pH ranges from 5.25 to 6.85; conductivity ranged from 681 μS/cm to 698 μS/cm ; TDS ranges from 508 ppm to 512 ppm .DeLay et al., 2021 DeLay et al., 2021DeLay et al., 2021Capulin Spring waters collected between 2012 and 2017 and then between 2021 and 2023 for this study have higher TDS than Las Huertas Spring waters (Table 1 and Figure 7).

Stream Samples. The temperature for Las Huertas stream waters collected for this study ranged from 0.4 °C to 15.0 °C, with a mean of 8.55 °C for 20 samples. The lowest recorded temperature for Las Huertas stream samples was 0.4 °C for N of Ditch Diversion in Fall 2022; the highest temperature was 15 °C measured at Canon Media at NM165. Las Huertas Stream waters for this study sit in a pH range from 4.92 (Capulin Canyon) to 8.13 (at Canon Media at NM165) with a mean pH of 7.02. Stream conductivity was lowest at 348 μS/cm (Las Huertas Picnic Area) and highest at 726 μS/cm (Capulin Canyon-1), with a mean conductivity of 540 μS/cm for Las Huertas Stream waters from this study. TDS calculated from major ion concentrations shows a mean TDS of 426 ppm for Las Huertas Stream waters, the lowest TDS at 285 ppm for (LHD) LH Downstream, and the highest TDS, of 519 ppm, at CC2 (Capulin Canyon-2).

Major Ions and Stable Isotopes

For this study, 26 samples from 13 unique locations within the Las Huertas watershed were analyzed (Figures 1 and 2; Tables 2 and 3). We compiled (63 samples) available water data from previous studies in the Las Huertas watershed and the surrounding Sandia Mountains (Frus, 2016; DeLay et al., 2021).

Calcium concentration, [Ca], for Las Huertas spring and stream and Capulin Spring waters collected between 2021 and 2023 range between 62 mg/L and 276 mg/L; alkalinity as HCO3- ranges from 160 mg/L to 472 mg/L; and chloride, [Cl], ranges between 25 mg/L to 504 mg/L. The lowest magnesium concentration [Mg] is 3 mg/L from November 2021 at LH Upper Reach, and the highest [Mg] was 7 mg/L from Capulin Spring in November 2022. Canon Media at NM 165 stream sample from May 2022 had the lowest concentrations of sodium, potassium, and bicarbonate at 17 mg/L, 0.74 mg/L, and 160 mg/L; Capulin Spring had the highest concentrations of these ions at 131 mg/L, 2 mg/L, and 472 mg/L respectively. Sulfate was lowest in stream waters collected from Las Huertas Picnic Area at 7 mg/L in November 2021; Sulfate was highest in waters collected from Capulin Spring in November 2022 at 27 mg/L. Piper diagrams compare the relative proportions among solute concentrations for a suite of waters (Piper, 1944; Drever, 1982). Analysis for collected geochemical was conducted by comparing the hydrochemical facies of these samples using Piper Diagrams. The charge balance for each sample major ion chemistry analysis was completed as part of QA/QC and is reported in Table 2. Major ion concentrations for Las Huertas springs and streams and Capulin Spring from 2012 through 2023 were plotted on a Piper diagram using Geochemist's Workbench (Figures 8, 9, and 10) (Bethke, 2008). Las Huertas waters from this study are calcium bicarbonate dominant, like those collected between 2012-2017, representative of deriving from a limestone aquifer (Drever, 1982; Frus, 2016; DeLay et al., 2021). Capulin Spring waters for this study collected between Fall 2021 and Spring 2023 had a mean [Cl] of 446 mg/L.

Stable Isotopes

Stable isotope geochemistry is utilized in this study to investigate potential recharge mechanisms, evaporation effects, and geochemistry of natural waters (Sharp, 2017). Stable isotope results are reported in Table 3. Values of δD and $\delta^{18}O$ from Las Huertas Springs and stream locations and previously collected data for Las Huertas and the surrounding Sandia Mountains were plotted with the Global Meteoric Water Line (GMWL) for reference (Figure 11). The GMWL ($\delta D = 8.0 * \delta^{18}O + 10$) describes the global average relationship between the measured values of stable isotopes of hydrogen and oxygen in meteoric waters worldwide. Variations from the GWML can be interpreted to be a result of mixing, water-rock alteration or evaporation, among other processes (Craig, 1961). Isotopologues from these studies, including this study and rain and snow isotopologues analyzed from the Sandia Mountains, are plotted to interpret possible variations with Las Huertas and Capulin waters. Isotopologues derived from rain samples have large variability. The δD and $\delta^{18}O$ values of rain are generally heavier (less negative), whereas snow is generally isotopically lighter than springs and surface waters (Frus, 2016). The physical mechanism for this trend is that the mass fraction of water is more pronounced at colder temperatures (Sharp, 2007).

δD values for Capulin Spring waters range between -87.2 to -84.1 permil; $\delta^{18}O$ values range between -12.7 to -12.4 permil, with means of -85.6 and -12.5 permil, respectively. Three Capulin Spring water samples were run for isotopic analysis between 2012 and 2017 with a mean $\delta^{18}O$ of -12.5 permil and δD of -85.4 permil. The heaviest δD value was recorded at -12.1 permil and the lightest at -12.6 permil. Capulin Spring waters for this study are about 0.2 permil ($\delta^{18}O$) and 0.5 permil (δD) lighter than water isotopologues for Capulin Spring waters collected from 2012 to 2017. The Las Huertas springs were visited in November 2021, and waters were collected as close to spring emergence as possible (within spring boxes with owner's permission). Camp Spring waters had a δD of -87.1 permil and $\delta^{18}O$ of -12.8 permil; Ellis Spring had a δD of -12.8 permil and $\delta^{18}O$ of -87.1 permil. Camp Spring and Ellis Spring water isotopologues vary slightly by 0.01 $\delta^{18}O$ permil and 0.02 δD permil (i.e., within analytical error). Camp Spring waters collected between 2012 and 2017 had a mean δD value of -86.6 and $\delta^{18}O$ of -12.5 permil; Ellis Spring waters had a mean δD of -86.4 permil and $\delta^{18}O$ of -12.4 permil.

Figure 2 highlights the Capulin Canyon and Las Huertas mainstem confluence and sampling cluster within the Las Huertas Picnic Area. Capulin Canyon encapsulates stream water samples collected from Capulin Canyon-1 and -2 located within the Las Huertas Picnic Site, accessible from NM165. Capulin Canyon-1 was identified southeast of the Las Huertas Picnic Area. Capulin Canyon-2 was identified next to the recreational area parking lot, southeast of Las Huertas Picnic Area, and water samples were collected for geochemical analysis in November 2022 and May 2023. Capulin Spring and Capulin Canyon-2 were both visited in May 2022. Waters from the stream sample are 0.05 δD permil and 0.6 $\delta^{18}O$ permil lighter than that of the Capulin Spring waters. In November 2022, Capulin Spring and both Capulin Canyon downstream locations were visited. Capulin Spring waters were 0.02 δD permil lighter and 0.44 permil $\delta^{18}O$ lighter than Capulin Canyon-1 and 0.1 permil δD and 0.8 permil $\delta^{18}O$ lighter than Capulin Canyon-2. Capulin Canyon downstream waters isotopically get lighter with distance from Capulin Spring, as would be expected with evaporation (Figure 12).

The upper reaches for Las Huertas encapsulate Camp Spring, Ellis Spring, and select locations along the downstream flow from these springs (Las Huertas Upper Reach, NE of House Spring, and Loop Trail). These waters are upstream from the confluence of Las Huertas and Capulin Canyon waters at the Las Huertas Picnic Site. Isotopologues of waters, for a total of five analyzed water samples, from the Upper Reach of Las Huertas. Looking at this cluster for Las Huertas waters, we can further observe variations among these waters (Figure 12). Water isotopologues for Las Huertas Stream water from the upper reaches of the stream range from -13.1 $\delta^{18}O$ permil (NE of House Spring) to -12.4 $\delta^{18}O$ permil (Loop Trail), and hydrogen isotopologues range from -89.1 δD permil (NE of House Spring) to -84.2 δD permil (Loop Trail). Las Huertas Stream waters from the upper reach are isotopically heavier than waters emerging from Las Huertas Springs.

Discussion and Interpretations

For comparison of major ion composition, Las Huertas spring and stream and Capulin Spring chemistries are plotted on a Piper Diagram with select springs from the surrounding Sandia Mountains (Figure 13). The geochemical analysis performed for this study indicates Las Huertas springs are influenced by the water-rock interaction of calcium carbonate from the lower Madera limestone aquifer, similar to previous interpretations (Frus, 2016; DeLay et al., 2021). Capulin Spring waters are geochemically distinct compared to Las Huertas springs and the surrounding Sandia Mountain springs, containing more chloride than Las Huertas springs (Figures 9 and 13). This suggests Capulin Spring waters flow through a different lithology than Las Huertas Springs, where

Capulin Spring recharge waters flow through the Lower Madera limestone and a more silica-rich lithology.

Capulin Spring is further differentiated from Las Huertas springs by significantly higher TDS (Figure 13). Waters from this spring have higher TDS in both the summer and fall months, with lower TDS values in the fall and spring and rising again in the summer months. Camp Spring and Ellis Spring waters are within the TDS range of waters previously collected from Sandia Mountain springs and Las Huertas waters (Frus, 2016; DeLay et al., 2021). Seasonal variations in TDS may indicate a mix of recharge mechanisms (snowmelt and monsoonal). High TDS recorded in the summer and Fall months may reflect summer monsoonal rain recharge infiltrating and causing a pulse within the aquifer feeding Capulin Spring resulting in a high TDS value of the emerging waters (Jacobson and Langmuir, 1974). In comparison, Tunnel Spring (TNS) and Osha Spring (OHS) within the Las Huertas watershed, and Cienega Spring (CNS) and Sulfur Spring (SLS) have similar Stiff geometries as Las Huertas springs (Figure 14), reflecting mainly the addition of calcium and bicarbonate from interaction with the limestone aquifer. Sulfur Spring, however, does have less calcium than the other modeled springs. Capulin Spring is further validated as significantly different from Las Huertas in this dataset with significantly higher TDS, calcium, and chloride.

Capulin Spring waters plot on a chloride-rich trend, representing the influence of a different hydrostratigraphic flow path for Capulin Spring compared to Las Huertas spring waters (Figure 15; Frus, 2016; DeLay et al., 2021). Sandia Mountain springs plot on a trend with less chloride and a higher amount of sodium, interpreted to represent silicate water-rock interactions (ie, more Na relative to chloride, reflecting Na inputs likely from feldspars rather than just small amounts of sedimentary-derived halite. Additionally, selected Sandia Mountain springs have higher sulfate concentrations- suggesting interaction with gypsum (Figure 16). In the springs inventory completed by Frus, 2016 and finalized by DeLay et al. 2022, Capulin Spring waters collected between 2012 and 2017 were reported as notable outliers. Capulin Spring waters collected for this study follow the shallow trend for Capulin Spring. This shallow trend indicates seasonal differences in spring water chemistry. Capulin Spring waters were collected for this study in May 2022 and May 2023, before the summer monsoonal season, and in November 2022, after the summer monsoonal season. Waters from Capulin Spring plot on a chloride-rich trend with increasing carbonate dissolution; however, Capulin Spring waters collected from this study have higher concentrations of Na and Cl than Capulin Spring waters from previous sampling seasons. Capulin Spring waters had lower [Na] in the spring months before the monsoonal summer season and higher [Na] after the monsoonal season. The Capulin Spring waters from this study and previous studies plot with a trend inferred to represent water-rock interactions with calcium carbonate as the groundwater flows through the Madera Limestone (DeLay et al., 2021, Frus, 2016). All Las Huertas springs, streams, and Capulin Spring samples have higher calcium concentrations than sulfate. Sulfate enrichment of the Las Huertas Spring and Capulin Spring waters is not evident (Figure 16). Capulin Spring waters between 2012 and 2023 have the highest calcium concentrations from the Las Huertas watershed. Spring samples from Las Huertas, Capulin, and Sandia Mountains show enrichment of bicarbonate in these waters. Capulin Spring has the highest calcium bicarbonate concentrations (Figure 17).

Sandia Mountain springs and Las Huertas springs and stream water samples plot generally centrally clustered between the rain and snow isotopologues range. Precipitation isotopologues can be used to investigate the timing of recharge events in which summer precipitation isotopologues are heavier than winter precipitation (Frus, 2016). Frus, 2016 and Sharp, 2017 utilized precipitation isotopologues for summer and winter precipitation events to develop an isotopic boundary for summer and winter recharge; these boundaries were applied to waters collected for this study (Figure 18). Las Huertas waters fall between these ranges, suggesting that the waters emerging from the headwater springs are a mix of winter and summer recharge. The variation in $\delta^{18}O$ isotopologues between Ellis Spring and Camp Spring may be due to the evaporation of spring waters within the spring box; Ellis Spring being slightly isotopically heavier than Camp Spring may also indicate waters emerging from Ellis Spring are subject to a more extended flow pathway than water emerging out of Camp Spring. However, the difference between Ellis Spring and Camp Spring isotopologues for this study varies minimally.

Chloride behaves conservatively and is used as a tracer to investigate potential flow pathways in aquifers, as it is typically unaffected by adsorption or other geochemical processes (Healy and Scanlon, 2010). Figure 19 shows δD (permil VSMOW) isotopologues versus [Cl]. Capulin Spring has some of the highest [Cl] between 333 mg/L and 504 mg/L, whereas the spring boxes and stream waters along the main stem range from 61 to 80 mg/L. Capulin Spring waters from this study and previous studies plots within the δD range for Las Huertas springs and stream; however, Capulin Spring is considered an outlier with the highest Cl concentrations. Las Huertas Stream and Capulin Spring waters collected in Spring 2022 were isotopically heavier than Las Huertas Stream waters and Capulin Spring waters collected in Fall 2022. Water isotopologues measured for Las Huertas Springs and Capulin Spring waters do not suggest an evaporation trend with Las Huertas mainstem waters or Capulin Spring, indicating that there may be cryptic groundwater inflow along the flow path. However, Capulin Spring is significantly saltier than Las Huertas springs; isotopologues allow us to rule out that evaporation effects are associated with the high [Cl] at Capulin Spring and suggest there may be other influences (different flow path) on the spring's salinity, and this is examined further below.

The regional aquifer, the Madera Formation, is classified into two sections, the Upper Madera and the Lower Madera. The Upper Madera is a well-cemented limestone interbedded with sandstone and mudstones. The lower Madera is described as massive and does not have these interbedded sandstones and mudstones like its upper counterpart. The Upper Madera has been eroded on the higher elevation regions of the Sandia Mountains, including the upper reaches of the Las Huertas watershed. The lower elevation regions of the Sandia Mountains, including near Cienega Spring and Sulfur Spring emergence to the south, and the lower reaches of the Las Huertas watershed to the north still contain the Upper Madera lithology and the Abo and Yeso formations that overlay the Upper Madera (see Figures 4, 20, and 21). These lithologies could supply components from gypsum (calcium and sulfate).

Spatially-Intermittent Travertine Occurrence. Las Huertas springs emerge within the upper reaches of Las Huertas, and travertine is visibly evident within the stream; geologic maps indicate these springs are located on colluvium and alluvium over the

Lower Madera limestone (Figure 20; Connell et al., 2000; Read et al., 2000). Downstream near NHS, where stream waters flow over the Sandia Formation, travertine step dams and pools are also evident. Capulin Spring, similar to Las Huertas springs, emerges in proximity to colluvium/alluvium on top of the Lower Madera; however, travertine was not observed near the spring. Further downstream, within the Las Huertas Picnic Area, travertine is not evident, and sample locations from this region flow over colluvium/alluvium over the Sandia granite. Near CNM and NDD sample locations, travertine is evident in the stream, and waters flow over the Madera Formation. Near our most downstream sample, LHD, travertine is not evident, and the stream flows over colluvium/alluvium sitting on top of the Abo Formation. The proximity of the Abo and Yeso formation suggests the Upper Madera limestone has been preserved.

Travertine-precipitating springs that feed the Las Huertas watershed emerge from the limestone aquifer with calcium carbonate-rich waters (Frus, 2016). The extensive travertine rimstone dams and pools encountered in these upper reaches of the Las Huertas drainage are unique in the Sandia mountains- only small amounts are noted to the south and north. Downstream from the springs, travertine deposits, forming dams and pools, are evident with intermittent occurrences along the Las Huertas Creek flow path. The following reaction represents calcite precipitation and the exsolution of carbon dioxide (Drever, 1982):

$$Ca^{2+} + 2HCO_3^- \leftrightarrow CaCO_3 + H_2O + CO_2\,(g)$$

The formation of travertine can be described as a three-step process consisting of acquiring solutes in groundwaters, followed by the transport of these dissolved solutes, and then the deposition of calcium carbonate as travertine (Crossey et al., 2006). The following equations describe the process of the acquisition of solutes through limestone/groundwater interactions, transport of solutes, and precipitation of travertine from calcite-rich waters (Crossey et al., 2006):

$$CO_{2(g,ext)} + H_2O + CaCO_{3\,(limestone)} \rightarrow Ca^{2+}_{(aq)} + 2HCO^{-}_{3\,(aq)} \; (Eqn\ 1)$$

$$Ca^{2+}_{(aq)} + 2HCO^{-}_{3\,(aq)} \rightarrow CO_{2\,(g)} + H_2O + CaCO_{3\,(travertine)} (Eqn\ 2)$$

Eqn. 1 represents CO_2-charged groundwaters dissolving carbonate from limestone, thus increasing calcium, magnesium, and alkalinity in the groundwaters (Crossey et al., 2006). Degassing described in Eqn. 2 favors carbonate precipitation (Crossey et al., 2006). If degassing is fast, such as in turbulent streams, spring waters can deposit travertine dams, such as the observed travertine dams and pools in the Las Huertas watershed, coatings, and drapes (Figure 3; Chafetz and Folk, 1984; Crossey et al., 2006).

The amount of $CaCO_3$ dissolved by water depends on the CO_2 present while $CaCO_3$ dissolves (Chafetz and Folk, 1984), often referred to as external CO_2 ($C_{g,ext}$; Crossey et al., 2009 and references therein). Ca^{2+} and HCO_3^- are the dominant solutes in karst aquifers- and are typically close to calcite equilibrium (Chafetz and Folk, 1984). Total dissolved solids (TDS) and Ca concentration depend on the initial P_{CO2} of the water, influenced by the soil atmosphere of the recharge zone (Drever, 1982) plus potential inputs of other CO_2 sources (Crossey et al., 2009). Degassing of CO_2, which may be caused by turbulence in the streamflow, occurs with the equilibration of CO_2 in the water from spring recharge water with lower atmospheric CO_2 levels, thus causing calcite precipitates on sediments and organic material in the spring channel (Drever 1982;

Chafetz and Folk, 1984; Crossey et al., 2009). Typically, springs precipitating travertine have waters with high concentrations of calcium carbonate and high TDS values compared to non-travertine precipitating springs (McCoy and Blanchard, 2008).

Rainwaters are in equilibrium with atmospheric CO_2 with a partial pressure of ~$10^{-3.5}$ atm, and soils may have up to $10^{-1.5}$ atm due to respiration and the decay of organic matter (Drever, 1982): the P_{CO2} increases (up to $10^{-1.5}$ atm) when water infiltrates into soils. The addition of CO_2 dramatically increases the amount of calcite in waters that can be dissolved (Drever, 1982); thus, the amount of $CaCO_3$ that can be dissolved in the recharge waters is dependent on the amount of CO_2 entering the system ($C_{g,ext}$ from Eqn. (1) above (Drever, 1982; Crossey et al., 2009). If CO_2 is not added from sources other than the atmospheric value, the amount of calcite that could be dissolved is limited (Drever, 1982). In an open system, like the Las Huertas stream, once the groundwater emerges to the surface, the P_{CO2} of water will equilibrate with the atmospheric value (constant), and if P_{CO2} of the groundwater is higher than the atmospheric value, CO_2 is transferred from the stream/groundwater to the atmosphere, raising the pH and facilitating the precipitation of $CaCO_3$ (Drever, 1982; Crossey et al., 2009). The amount of external CO_2 (initial atmospheric CO_2, plus any added from soil respiration and any other sources) will promote calcite dissolution initially, and more calcite will be dissolved into the water (Drever, 1982).

Springs monitored for this study have high dissolved inorganic carbon (DIC) in the form of HCO_3^- at pH >6.3 and < 10.3 (acid dissociation constants for carbonic acid and bicarbonate, respectively). Piper diagrams reflect that these spring waters are calcium bicarbonate dominant. Saturation indices for calcite, dolomite, gypsum, halite, quartz, amorphous silica, and the P_{CO2} for each water were computed using PHREEQC (Parkhurst, 1995). The computed saturation indices for each sample are shown in Table 4; Capulin Spring waters collected between 2021 and 2023 logP_{CO2} values range from -1.36 to +0.25; Capulin Spring waters collected between 2012 and 2017 logP_{CO2} values range from -2.71 to -1.15. PHREEQC-computed P_{CO2} indicates that emerging groundwaters show considerable excess P_{CO2} relative to the atmosphere, consistent with observed calcite precipitation. The modeled results indicate that in many cases, the P_{CO2} is orders of magnitude higher than expected for soil respiration.

A method of computing the amount of external carbon was shown by Crossey and others (2009). This method uses the modeled total DIC of each water, subtracting the portion of carbon contributed by calcite and gypsum dissolution by subtracting the mol/L of sulfate and calcium from the DIC. The values are shown in Table 5. These high values of external carbon exceed the range for soil contributions and are comparable to values reported in regional carbonic springs (Crossey et al., 2015; Crossey et al., 2009; 2016). The co-location of carbonic springs with regional faults indicates that some of this external CO_2 may be far traveled. In Edgewood, nearby in the eastern area downslope of the Sandia mountains, Edgewood Cavern has reported high CO_2 (Babb, R.G., 1974; Jenkins D., 1982) and further to the southeast of the Sandia mountains near Estancia, carbon dioxide was commercially produced in the 1930s and 40's (Broadhead, 1997).

The geochemical composition of water suggests these carbonic waters interact with any calcite in the soil matrix and the Madera limestone aquifer. Las Huertas springs waters collected in Fall 2021 were undersaturated with respect to calcite. Capulin Spring waters had variable saturation index with respect to calcite with time. Capulin Spring waters collected in Spring 2022 were supersaturated with calcite; in the following Fall and Spring, Capulin Spring waters were undersaturated with calcite. Capulin Canyon waters (CC1 and CC2) follow a similar pattern. Las Huertas stream waters near Las Huertas springs, NHS (North of House Spring) and LPT (Loop Trail), have similar saturation patterns. In the Spring 2022 and Spring 2023 sampling seasons, these surface waters were supersaturated with respect to calcite; Waters collected from LPT in Fall 2022 had a lower saturation index than waters collected in the Spring season and were undersaturated with respect to calcite. CNM (Canon Media and NM165), further downstream from CLH (Capulin Canyon and Las Huertas confluence), were supersaturated with respect to calcite for the Spring 2022, Fall 2022, and Spring 2023 sampling seasons. However, many of these waters also display P_{CO2} values well above atmospheric. This is discussed below, as this saturation state will dramatically change when the high-P_{CO2} groundwaters interact with the atmosphere. Saturation indices concerning dolomite were also calculated using PHREEQC for the waters collected for this study. It is important to note that the kinetics of dolomite are exceedingly slow at low temperatures; thus, it is not likely to lead to mineral precipitation (Drever, 1982). Our Piper diagrams show little magnesium, so we do not consider that much dolomite is present in the aquifer as that has been shown to yield Ca:Mg in approximated equimolar concentrations (Crossey et al., 2009). NHS waters collected in Spring 2022 and CNM waters collected in Fall 2022 were supersaturated with respect to dolomite. Gypsum saturation indices were also calculated; the waters collected for this study were all undersaturated with respect to gypsum.

A PHREEQC model was used to calculate how much calcite could be precipitated out of specific waters from the Las Huertas watershed. The model equilibrates waters with atmospheric P_{CO2} and calcite to determine how much calcite could be precipitated and reports the amount in mg/L (Table 5). Capulin Spring waters had the highest amount of calcite that could be precipitated, between 282 mg/L and 353 mg/L, almost double that of Camp Spring (188 mg/L) and Ellis Spring (193 mg/L). In comparison, Sulfur Spring waters, downgradient from our study area and within a different drainage basin, could precipitate about half; 90 mg/L of calcite. Camp Spring, Ellis Spring, and Capulin Spring emerge from colluvium and alluvium lithology, whereas Sulfur Spring is located on a colluvium/alluvium and Abo and Yeso Formation geologic contact. Cienega Spring, near Sulfur Spring, sits on contact between colluvium/alluvium, the Upper Madera Formation, and Abo and Yeso Formation contacts, which is reflected geochemically and could precipitate a large amount of calcite (220 mg/L). The Abo and Yeso Formations sit on top of the Madera Formation and have been eroded from the upper portions of the Sandia Mountains, including the upper reaches of the Las Huertas watershed. Stream samples from NHS, within the upper reaches of Las Huertas flowing over the Sandia Formation right on the fault, have lower calcite precipitation than the emerging springs (between 125 mg/L and 172 mg/L). At this location, massive travertine step pools are observed. Further downstream, CNM lies on the Madera Formation, and analysis shows waters collected from this location could precipitate calcite (between 81 mg/L and 130 mg/L). Like NHS, travertine is observed within the stream at CNM (See Figures 20, 22, 23, and 25).

Saturation indices indicate that Capulin Spring waters, Capulin Canyon surface waters, and surface waters downstream from the Capulin Canyon and Las Huertas confluence are saturated with respect to quartz (SiO_2). In comparison, Las Huertas spring waters and surface waters collected upstream from the confluence are undersaturated with respect to quartz. This, combined with major ion concentrations and Piper diagrams, further suggests that Capulin Spring recharge waters interacting with silica-rich geology such as the portions of the Upper Madera, the Sandia formation sandstones, or the basement rocks. Calcite saturation indices for Las Huertas watershed springs are variable for samples collected between 2012 and 2023. The Las Huertas spring waters collected in 2021 were undersaturated with respect to calcite; however, spring waters collected between 2012 and 2016 had three samples that were saturated with calcite. Capulin Spring waters collected in May 2022 were saturated with respect to calcite; Capulin Spring waters collected between 2012 and 2017 had variable calcite saturation, but the majority were saturated.

Measured parameters are plotted with respect to downstream site locations between Las Huertas springs (Ellis Spring and Camp Spring) and LHD (Las Huertas Downstream), and Capulin Spring (CPS) to observe changes along the Las Huertas flow path (Figures 26 and 27). We see an expected difference in temperature in that waters are cooler in the Fall months and warmer in the Spring months. For TDS, we see a general decrease in TDS downstream. In the Fall of 2021 and 2022, we see a slight increase in TDS at CLH and then decrease downstream. Although CLH was not visited in the spring seasons, we see a slight increase in TDS downstream from the confluence at LHP (Las Huertas Picnic Area). DIC is higher in the Fall than in the Spring. There is an increase in

DIC at CLH and LHP followed by a decrease in DIC downstream. In the Fall 2022 season, we see the previously mentioned trend but with a slight increase of DIC at NDD (North of Ditch Diversion). P_{CO2} was also plotted with respect to downstream locations. We see a similar trend as DIC with P_{CO2}, with higher values observed in the Fall months and lower in the Spring. For the samples collected in the fall, P_{CO2} is higher for the stream samples than the ESP spring waters, with the highest P_{CO2} at LHP. The higher P_{CO2} values, similar to the previously discussed parameters, are highest around CLH and LHP. With the Fall 2022 sample run, with our longest continuous downstream sampling, we see the increase of P_{CO2} at LHP followed by a decrease at NDD and then an increase at NDD. Similar to DIC and PCO2, C_{ext} follows seasonal and downstream trends. For all seasons sampled, we see an increase in external carbon downstream at CLH and LHP, followed by a decrease and an increase at NDD and LHD (see Figure 27). Calcite precipitation was also modeled and plotted with respect to the site locations downstream. We see the highest potential for calcite precipitation with the spring waters collected at ESP, followed by a decrease downstream. There is an increase of calcite precipitation between CLH and LHP followed by a decrease downstream.

Las Huertas springs and Capulin Spring waters geochemically reflect the primary hydrostratigraphic aquifer, the Madera limestone. Geochemical analysis indicates Capulin Spring waters are saturated with quartz, suggesting waters from Capulin Spring have also interacted with silicates in the Upper Madera, Sandia formation, or possibly from the thin Arroyo Peñasco Group. From this, we could infer that recharge water infiltrates from a higher elevation of Capulin Spring, near Sandia Crest, and can infiltrate into the Madera Group and the Sandia Formation, allowing silica incorporation into waters eventually emerging from Capulin Spring. Las Huertas springs emerge within a small fault-bound valley and geochemically differ from Capulin Spring to the south. The limited dataset from this study suggests a similar flow path for Las Huertas spring recharge waters as Capulin Spring, but these waters likely do not interact with a silica-rich lithology. Some downstream samples geochemically reflect the Madera group and are often saturated with calcite. Water samples collected during Spring 2023 geochemically reflect a high snowmelt Spring runoff from high snowpack during the 2022-2023 winter season. This may indicate a seep from the lower elevation Upper Madera group geology and suggest a near-surface karst terrain. Travertine near these lower reaches suggests high $CaCO_3$-rich waters interacting with the Las Huertas main stem, likely from seep due to this karst terrane.

Conclusions

The Las Huertas spring and stream system is unique to the East Mountain/Sandia Mountain region of New Mexico and significantly different than nearby Capulin Spring, and Madera dip-slope springs such as Cienega Spring and Sulfur Spring. The most significant difference is the carbonic nature of Las Huertas manifested by the dramatic travertine-depositing character. The use of multiple geochemical tracers (major ions and stable isotopes) shows that Las Huertas waters vary seasonally. Baseflow conditions observed in the Fall/post-monsoonal season have higher $CaCO_3$, dissolved solids, and salinity with stable isotopes more negative. Higher discharge from monsoons and snowmelt is characterized by lower TDS and less negative stable isotopes. In contrast, Capulin Spring, to the south, has a different chemistry that may reflect interaction with silica-rich lithology or basement rocks.

The interpretations of these data are that external CO_2 is added along the Las Huertas system, likely from deep sources, as groundwater is directed through the Madera karst aquifer system and along faults north towards Placitas. Our downstream analysis identifies additional geochemical input (high CO_2) in the wetland associated with the Las Huertas Picnic Area. In contrast, similar elevation recharge from Capulin Spring has a different geochemistry reflecting its flow path through the Sandia Formation Sandstone. Cienega Spring, also at nearly the same elevation, flows directly downslope and does not have the carbonic (travertine-depositing) character. This study indicates that high-elevation recharge on the east side of the Sandia Mountains has an important spatial and temporal variation that affects water quality. The water is essential to surrounding down-slope communities and should continue to be monitored for watershed resiliency and is a management priority for Cibola National Forest. Further investigation is needed to explore the larger implications for recharge to the eastern plains, where the highest part of the Sandia Crest recharge is diverted north along faults rather than down the Madera dip-slope.

Las Huertas waters are important to the Village of Placitas and are a management priority for Cibola National Forest. This study contributes toward a better understanding of this poorly connected karst system with the most robust evaluation of the upper reach to date, allowing us to assess the resiliency of this resource in a changing climate (Elias et al., 2021). Major ion and isotopic analysis indicated that Las Huertas watershed headsprings geochemically vary spatially. Capulin Spring has significantly higher salinity, and major ions suggest Capulin Spring waters are recharge from a mix of calcium carbonate-rich waters and sulfate-chloride-containing water, which may be coming from a flow path through a more silica-rich lithology such as the Sandia formation sandstone.

References

Babb II, Robert G., 1974. Cave Research Foundation, Edgewood Caverns, pp. 11-12.

Bailly-Comte, V., Jourde, H. and Pistre, S., 2009. Conceptualization and classification of groundwater-surface water hydrodynamic interactions in karst watersheds: Case of the karst watershed of the Coulazou River (Southern France). Journal of Hydrology, 376(3-4), pp.456-462

Bauer, P.W., 2003. Albuquerque: A Guide to Its Geology and Culture (No. 18). New Mexico Bureau of Geology & Mineral Resources.

Bethke, C. M. and S. Yeakel. 2017. The geochemist's workbench essentials guide, release 11. Aqueous Solutions, LLC, Champaign, Illinois.

Chafetz, H.S. and Folk, R.L., 1984. Travertines; depositional morphology and the bacterially constructed constituents. Journal of Sedimentary Research, 54(1), pp.289-316.

Connell, S.D., Cather, S.M., Ilg, B., Karlstrom, K.E., Menne, B., Picha, M., Andronicus, C., Read, A.S., Bauer, P.W. and Johnson, P.S., 2000. Geology of the Bernalillo and Placitas quadrangles. Sandoval County, New Mexico: New Mexico Bureau of Mines and Mineral Resources Open-File Geologic Map OF-GM, 2.

Craig, H., 1961. Standard for reporting concentrations of deuterium and oxygen-18 in natural waters. Science, 133(3467), pp.1833-1834.

Crossey, L.C., Karlstrom, K.E., Dorsey, R., Pearce, J., Wan, E., Beard, L.S., Asmerom, Y., Polyak, V., Crow, R.S., Cohen, A. and Bright, J., 2015. Importance of groundwater in propagating downward integration of the 6-5 Ma Colorado River system: Geochemistry of springs, travertines, and lacustrine carbonates of the Grand Canyon region over the past 12 Ma. Geosphere, 11(3), pp.660-682.

Crossey, L.J., Fischer, T.P., Patchett, P.J., Karlstrom, K.E., Hilton, D.R., Newell, D.L., Huntoon, P., Reynolds, A.C. and De Leeuw, G.A., 2006. Dissected hydrologic system at the Grand Canyon: Interaction between deeply derived fluids and plateau aquifer waters in modern springs and travertine. Geology, 34(1), pp.25-28.

Crossey, L.J., Karlstrom, K.E., Schmandt, B., Crow, R.R., Colman, D.R., Cron, B., Takacs-Vesbach, C.D., Dahm, C.N., Northup, D.E., Hilton, D.R. and Ricketts, J.W., 2016. Continental smokers couple mantle degassing and distinctive microbiology within continents. Earth and Planetary Science Letters, 435, pp.22-30.

Crossey, L.J., Karlstrom, K.E., Springer, A.E., Newell, D., Hilton, D.R. and Fischer, T., 2009. Degassing of mantle-derived CO2 and He from springs in the southern Colorado Plateau region-Neotectonic connections and implications for groundwater systems. Geological Society of America Bulletin, 121(7-8), pp.1034-1053.

DeLay, N., Crossey, L., Bixby, R., 2021. Cibola National Forest Spring Inventory Addendum: Hydrogeochemical and Biological Analysis of Spring Waters, Sandia and Manzano Mountains, New Mexico.

Drever, J.I., 1988. The geochemistry of natural waters (Vol. 437). Englewood Cliffs: Prentice hall.

Elias, E., James, D., Heimel, S., Steele, C., Steltzer, H. and Dott, C., 2021. Implications of observed changes in high mountain snow water storage, snowmelt timing and melt window. Journal of Hydrology: Regional Studies, 35, p.100799.

Frus, R. J. 2016. Multidisciplinary work to determine hydrology of arid land springs and how spring waters influence water quality and ecosystem health for desert environments. Ph.D. Dissertation, the University of New Mexico Digital Repository, Albuquerque, New Mexico.

Green, R.T., Painter, S.L., Sun, A. and Worthington, S.R., 2006. Groundwater contamination in karst terranes. Water, Air, & Soil Pollution: Focus, 6, pp.157-170.

Griego, B. (2023) Hydrogeochemical analysis of springs in the Sandia Mountains, New Mexico. Unpublished Undergraduate Thesis.

Healy, R.W., 2017. Chemical tracer methods.

Hou, X. and Jones, B.T., 2000. Inductively coupled plasma/optical emission spectrometry. Encyclopedia of analytical chemistry, 2000, pp.9468-9485.

Jackson, P.E., 2000. Ion chromatography in environmental analysis. Encyclopedia of analytical chemistry, 2779.

Jacobson, R.L. and Langmuir, D., 1974. Controls on the quality variations of some carbonate spring waters. Journal of Hydrology, 23(3-4), pp.247-265.

Johnson, P.S. and Campbell, A., 2002. Hydrogeology and water resources of the Placitas area, Sandoval County, New Mexico. New Mexico Bureau of Geology and Mineral Resources.

Karlstrom, K.E., Dallmeyer, R.D. and Grambling, J.A., 1997. 40Ar/39Ar evidence for 1.4 Ga regional metamorphism in New Mexico: Implications for thermal evolution of lithosphere in the southwestern USA. The Journal of Geology, 105(2), pp.205-224.

LeFevre, W. J. (1999). Geochemical characterization of geologically complex mountain front aquifers: Placitas, New Mexico (thesis). New Mexico Institute of Mining and Technology, Socorro, NM.

Lucas, S.G., Rowland, J.M., Kues, B.S., Estep, J.W. and Wilde, G.L., 1999. Uppermost Pennsylvanian and Permian stratigraphy and biostratigraphy at Placitas, New Mexico. Albuquerque geology: New Mexico Geological Society, Guidebook, 50, pp.281-292.

McCoy, K.J. and Blanchard, P.J., 2008. Precipitation, ground-water hydrology, and recharge along the eastern slopes of the Sandia Mountains, Bernalillo County, New Mexico. U. S. Geological Survey.

Myers, M.D., 2006. National field manual for the collection of water-quality data. US Geol. Surv. Tech. Water Resour. Investig. Book, 9.

National Oceanic and Atmospheric Administration. (2022). Large decline in snowpack across the U.S. West. https://www.climate.gov/news-features/understanding-climate/large-declines-snowpack-across-us-west.

New Mexico Geospatial Data Acquisition Coordination Committee (GDACC), State of New Mexico, 2018, Hagan 7.5 Minute Quad 35106, 10M Enhanced DEM, 2005, DEM GeoTIFF, raster digital data, accessed June 22, 2023, at URL https://rgis.unm.edu/rgis6/.

New Mexico Geospatial Data Acquisition Coordination Committee (GDACC), State of New Mexico, 2018, Placitas 7.5 Minute Quad 35106, 10M Enhanced DEM, 2005, DEM GeoTIFF, raster digital data, accessed May 29, 2023, at URL https://rgis.unm.edu/rgis6/ .

New Mexico Geospatial Data Acquisition Coordination Committee (GDACC), State of New Mexico, 2018, Sandia Crest 7.5 Minute Quad 35106, 10M Enhanced DEM, 2005, DEM GeoTIFF, raster digital data, accessed May 29, 2023, at URL https://rgis.unm.edu/rgis6/ .

New Mexico Geospatial Data Acquisition Coordination Committee (GDACC), State of New Mexico, 2018, Sandia Park 7.5 Minute Quad 35106, 10M Enhanced DEM, 2005, DEM GeoTIFF, raster digital data, accessed June 22, 2023, at URL https://rgis.unm.edu/rgis6/.

New Mexico Geospatial Data Acquisition Coordination Committee (GDACC), State of New Mexico, 2018, Sedillo 7.5 Minute Quad 35106, 10M Enhanced DEM, 2005, DEM GeoTIFF, raster digital data, accessed June 22, 2023, at URL https://rgis.unm.edu/rgis6/.

New Mexico Geospatial Data Acquisition Coordination Committee (GDACC), State of New Mexico, 2018, Tijeras 7.5 Minute Quad 35106, 10M Enhanced DEM, 2005, DEM GeoTIFF, raster digital data, accessed June 22, 2023, at URL https://rgis.unm.edu/rgis6/.

New Mexico Natural Resources Conservation Service State Office (NRCS), 2019, New Mexico HUC-8 Boundaries, vector digital data, accessed May 29, 2023, at URL https://rgis.unm.edu/rgis6/ .

Noe, W., B. Davis, K. Townsend, A. Porter, L. Rotche, C. Traft, N. Gayoso, M. Hanttula, R. Webb, B. Bixby (2021). UNM WR 573 Fall 2021 - Las Huertas data, HydroShare, https://doi.org/10.4211/hs.ae2dd1c92e1b4cd7b77d6115db1d8011

Parkhurst, D.L. and Appelo, C.A.J., 2013. Description of input and examples for PHREEQC version 3-a computer program for speciation, batch-reaction, onedimensional transport, and inverse geochemical calculations. US geological survey techniques and methods, 6(A43), p.497.

Piper, A.M. 1944. A graphical procedure in the geochemical interpretation of water analyses: Geophysical Union Transactions. Vol. 25. p. 914-923.

Quinn, J.J., Tomasko, D. and Kuiper, J.A., 2006. Modeling complex flow in a karst aquifer. Sedimentary Geology, 184(3-4), pp.343-351.

Read, A.S., Karlstrom, K.E., Connell, S., Kirby, E., Ferguson, C.A., Ilg, B., Osburn, G.R., Van Hart, D. and Pazzaglia, F.J., 2000. Geology of Sandia Crest quadrangle, Bernalillo and Sandoval Counties, New Mexico. New Mexico Bureau of Mines and Mineral Resources.

Rice, E.W., Bridgewater, L. and American Public Health Association eds., 2012. Standard methods for the examination of water and wastewater (Vol. 10). Washington, DC: American public health association.

Sharp, Z., 2017. Principles of stable isotope geochemistry.

Siirila-Woodburn, E.R., Rhoades, A.M., Hatchett, B.J., Huning, L.S., Szinai, J., Tague, C., Nico, P.S., Feldman, D.R., Jones, A.D., Collins, W.D. and Kaatz, L., 2021. A low-to-no snow future and its impacts on water resources in the western United States. Nature Reviews Earth & Environment, 2(11), pp.800-819.

Springer, K.B., Manker, C.R. and Pigati, J.S., 2015. Dynamic response of desert wetlands to abrupt climate change. Proceedings of the National Academy of Sciences, 112(47), pp.14522-14526.

Stevens, L.E., Schenk, E.R. and Springer, A.E., 2021. Springs ecosystem classification. Ecological Applications, 31(1), p.e2218.

United States Department of Agriculture, United States Forest Service. Las Huertas Picnic Site. https://www.fs.usda.gov/recarea/cibola/recarea/?recid=64220

United States Environmental Protection Agency. (2022, July). Climate Change Indicators: Snowpack. https://www.epa.gov/climate-indicators/climate-change-indicators-snowpack#ref1.

Williams, A.J., Crossey, L.J., Karlstrom, K.E., Newell, D., Person, M. and Woolsey, E., 2013. Hydrogeochemistry of the Middle Rio Grande aquifer system-Fluid mixing and salinization of the Rio Grande due to fault inputs. Chemical Geology, 351, pp.281-298.

Table 1. Sample locations and field parameters

Unique ID	Map Label	Site Name	Sample #	Location	Sample Date	Source	Latitude	Longitude	Temp °C	pH	Conduvitivity uS/cm
		Las Huertas Springs (2021)									
1	CSP	Camp Spring Box	LH Church Box	Camp Spring Box	11/6/2021	This Study	35.22665	-106.42069	7.8	5.25	681
2	ESP	Ellis Spring Box	LH Cooper Ellis	Ellis Spring Box	11/6/2021	This Study	35.22703	-106.42069	8.4	6.85	698
		Capulin Spring (2021-2023)									
5	CPS	Capulin Spring	KT22LHCPS	Capulin Spring	5/18/2022	This Study	35.21777702	-106.415145	12.2	6.91	1150
17	CPS	Capulin Spring	KT22FCPS	Capulin Spring	11/11/2022	This Study	35.21777702	-106.415145	6.7	6.47	1999
26	CPS	Capulin Spring	LH23CPS	Capulin Spring	5/11/2023	This Study	35.21777702	-106.415145	8.9	5.22	1454
		Las Huertas Stream (2021-2023)									
3	LHU	Las Huertas Upper Reach	LH Church Stream	LH at CDT	11/6/2021	This Study	35.22706602	-106.420613	7.9	6.05	681
4	LHP	Las Huertas Picnic Area	LH-3	Las Huertas Picnic Area	11/6/2021	This Study	35.23445098	-106.411718	8.7	6.01	614
6	CC2	At LHP Parking Area	KT22LHCPS2	Capulin Canyon-2	5/18/2022	This Study	35.23403498	-106.411381	11.5	7.74	603
7	NHS	NE of House Spring	KT22LH-1	NE of House Spring	5/18/2022	This Study	35.22934	-106.41435	11	8	684
8	LPT	Loop Trail	KT22LH-2	Loop Trail	5/18/2022	This Study	35.23377	-106.41198	11.9	7.88	586
9	LHP	Las Huertas Picnic Area	KT22LH-3	Las Huertas Picnic Area	5/18/2022	This Study	35.23462197	-106.411591	10.7	7.41	599
10	CNM	Canon Media at NM165	KT22LH-4	Canon Media at NM165	5/18/2022	This Study	35.25899202	-106.407119	15	7.87	529
18	CC1	Above LHP Parking Area	Capulin Canyon-1	Capulin Canyon-1	11/11/2022	This Study	35.234	-106.41141	7.7	6.28	726
19	CC2	At LHP Parking Area	Capulin Canyon-2	Capulin Canyon-2	11/11/2022	This Study	35.23403498	-106.411381	6.3	5.98	368
20	CLH	Confluence at LHP	KT22FCPS4	Confluence at LHP	11/11/2022	This Study	35.23421	-106.41167	6	6.46	364
21	LPT	Loop Trail	KT22FLH2	Loop Trail	11/11/2022	This Study	35.23375	-106.41199	4.9	7	599
22	LHP	Las Huertas Picnic Area	KT22FLH3	Las Huertas Picnic Area	11/11/2022	This Study	35.2349	-106.41177	5.5	6.08	348
23	CNM	Canon Media at NM165	KT22FLH4	Canon Media at NM165	11/11/2022	This Study	35.24275	-106.41231	2	8.13	608
24	NDD	N of Ditch Diversion	KT22FLH5	N of Ditch Diversion	11/11/2022	This Study	35.26051	-106.40706	0.4	7.5	593
27	NHS	NE of House Spring	KT23SLH1	NE of House Spring	5/11/2023	This Study	35.22975	-106.41408	9.6	7.84	508
28	LPT	Loop Trail	KT23SLH2	Loop Trail	5/11/2023	This Study	35.23386	-106.412	10.8	7.67	491
29	CC1	Above LHP Parking Area	Capulin Canyon-1	Above LHP Parking Area	5/11/2023	This Study	35.23331	-106.41122	9	4.92	545
30	LHP	Las Huertas Picnic Area	KT23SLH3	Las Huertas Picnic Area	5/11/2023	This Study	35.23445098	-106.411718	9.2	6.83	484
31	CNM	Canon Media at NM165	KT23SLH4	Canon Media at NM165	5/11/2023	This Study	35.24322	-106.41266	10.9	7.74	461
32	LHD	LH Downstream	KT23SLH6	LH Downstream	5/11/2023	This Study	35.28241	-106.41004	12	6.95	420

Table 1. Sample locations and field parameters

Unique ID	Map Label	Site Name	Sample #	Location	Sample Date	Source	Latitude	Longitude	Temp °C	pH	Conduvitivity uS/cm
		Capulin Spring (2012-2017)									
40	CPS	Capulin Spring	Capulin Spring	Capulin Spring	6/13/2012	(Frus, 2016; DeLay et al. 2022)	35.21770	-106.41513	n.r.	6.71	1670
41	CPS	Capulin Spring	Capulin Spring	Capulin Spring	6/8/2013	(Frus, 2016; DeLay et al. 2022)	35.21770	-106.41513	10.9	6.64	1810
42	CPS	Capulin Spring	Capulin Spring	Capulin Spring	8/27/2016	(Frus, 2016; DeLay et al. 2022)	35.21770	-106.41513	16.5	7.24	914
43	CPS	Capulin Spring	Capulin Spring	Capulin Spring	10/29/2016	(Frus, 2016; DeLay et al. 2022)	35.21770	-106.41513	10.6	8.20	1702
44	CPS	Capulin Spring	Capulin Spring	Capulin Spring	3/16/2017	(Frus, 2016; DeLay et al. 2022)	35.21770	-106.41513	11.0	7.30	1916
45	CPS	Capulin Spring	Capulin Spring	Capulin Spring	8/10/2017	(Frus, 2016; DeLay et al. 2022)	35.21770	-106.41513	n.r.	7.32	n.r.
54	CPS	Capulin Spring	Faulty Trail	Faulty Trail	6/13/2012	(Frus, 2016; DeLay et al. 2022)	35.21770	-106.41513	n.r.	6.88	1040
55	CPS	Capulin Spring	Faulty Trail	Faulty Trail	8/28/2016	(Frus, 2016; DeLay et al. 2022)	35.21770	-106.41513	12.5	6.58	1206
56	CPS	Capulin Spring	Faulty Trail	Faulty Trail	10/29/2016	(Frus, 2016; DeLay et al. 2022)	35.21770	-106.41513	11.44	7.76	1078
57	CPS	Capulin Spring	Faulty Trail	Faulty Trail	3/16/2017	(Frus, 2016; DeLay et al. 2022)	35.21770	-106.41513	9.1	6.92	1123
		Las Huertas Springs (2012-2017)									
53	ESP	Ellis Spring Box	Ellis Spring Box	Ellis Spring Box	6/1/2013	(Frus, 2016; DeLay et al. 2022)	35.22704	-106.42064	7.2	6.92	657
64	ESP	Ellis Spring Box	LH at Ellis Box	LH at Ellis Box	7/21/2012	(Frus, 2016; DeLay et al. 2022)	35.22704	-106.42064	7.4	7.47	623
65	ESP	Ellis Spring Box	LH at Ellis box	LH at Ellis box	7/13/2013	(Frus, 2016; DeLay et al. 2022)	35.22704	-106.42064	7.1	6.79	657
66	ESP	Ellis Spring Box	LH at Ellis box	LH at Ellis box	8/22/2013	(Frus, 2016; DeLay et al. 2022)	35.22704	-106.42064	7.3	7.29	691
67	ESP	Ellis Spring Box	LH at Ellis Box	LH at Ellis Box	5/21/2014	(Frus, 2016; DeLay et al. 2022)	35.22704	-106.42064	7.3	7.07	652
68	ESP	Ellis Spring Box	LH at Ellis Box	LH at Ellis Box	10/29/2016	(Frus, 2016; DeLay et al. 2022)	35.22704	-106.42064	7.3	8.33	615
69	CSP	Camp Spring Box	LH Camp Spr Box	LH Camp Spr Box	7/21/2012	(Frus, 2016; DeLay et al. 2022)	35.22676	-106.42075	7.0	7.36	644
70	CSP	Camp Spring Box	LH Camp Spr Box	LH Camp Spr Box	6/1/2013	(Frus, 2016; DeLay et al. 2022)	35.22676	-106.42075	10.7	7.20	668
71	CSP	Camp Spring Box	LH Camp Spr Box	LH Camp Spr Box	7/13/2013	(Frus, 2016; DeLay et al. 2022)	35.22676	-106.42075	8.7	6.82	654
72	CSP	Camp Spring Box	LH Camp Spr Box	LH Camp Spr Box	8/22/2013	(Frus, 2016; DeLay et al. 2022)	35.22676	-106.42075	8.5	7.29	688
73	CSP	Camp Spring Box	LH Camp Spr Box	LH Camp Spr Box	5/21/2014	(Frus, 2016; DeLay et al. 2022)	35.22676	-106.42075	7.2	6.68	618
74	CSP	Camp Spring Box	LH Camp Spr Box	LH Camp Spr Box	3/17/2017	(Frus, 2016; DeLay et al. 2022)	35.22676	-106.42075	7.8	7.42	1040
		Las Huertas Stream (2012-2017)									
60	LHU	Las Huertas Upper Reach	LH at CDT	LH at CDT	7/21/2012	(Frus, 2016; DeLay et al. 2022)	35.22753	-106.42070	9.8	7.45	606
61	LHU	Las Huertas Upper Reach	LH at CDT	LH at CDT	7/13/2013	(Frus, 2016; DeLay et al. 2022)	35.22753	-106.42070	11.3	7.90	629
62	LHU	Las Huertas Upper Reach	LH at CDT	LH at CDT	8/22/2013	(Frus, 2016; DeLay et al. 2022)	35.22753	-106.42070	10.2	8.15	659
63	LHU	Las Huertas Upper Reach	LH at CDT	LH at CDT	5/21/2014	(Frus, 2016; DeLay et al. 2022)	35.22753	-106.42070	7.4	7.61	631
75	LH1	LH Downstream #1	LH Downstream #1	LH Downstream #1	7/28/2012	(Frus, 2016; DeLay et al. 2022)	n.r.	n.r.	12.3	7.5	652
76	LH2	LH Downstream #2	LH Downstream #2	LH Downstream #2	7/28/2012	(Frus, 2016; DeLay et al. 2022)	n.r.	n.r.	9.2	7.2	682
77	LH3	LH Downstream #3	LH Downstream #3	LH Downstream #3	7/28/2012	(Frus, 2016; DeLay et al. 2022)	n.r.	n.r.	11.7	8.04	662
78	LH4	LH Downstream #4	LH Downstream #4	LH Downstream #4	7/28/2012	(Frus, 2016; DeLay et al. 2022)	n.r.	n.r.	11.3	7.7	638
79	LH5	LH Downstream #5	LH Downstream #5	LH Downstream #5	7/28/2012	(Frus, 2016; DeLay et al. 2022)	n.r.	n.r.	9.2	7.42	620
80	LH6	LH Downstream #6	LH Downstream #6	LH Downstream #6	7/28/2012	(Frus, 2016; DeLay et al. 2022)	n.r.	n.r.	9	7.9	696
81	LH7	LH Downstream #7	LH Downstream #7	LH Downstream #7	7/28/2012	(Frus, 2016; DeLay et al. 2022)	n.r.	n.r.	10	7.87	640
82	LH8	LH Downstream #8	LH Downstream #8	LH Downstream #8	7/28/2012	(Frus, 2016; DeLay et al. 2022)	n.r.	n.r.	11.9	8.11	626
83	LH9	LH Downstream	LH Downstream	LH Downstream	8/27/2016	(Frus, 2016; DeLay et al. 2022)	n.r.	n.r.	12.6	7.85	573
84	LHP	Las Huertas Picnic Area	Las Huertas Picnic Area	Las Huertas Picnic Area	6/1/2013	(Frus, 2016; DeLay et al. 2022)	35.23328	-106.41213	15	8.05	580

Table 1. Sample locations and field parameters

Unique ID	Map Label	Site Name	Sample #	Location	Sample Date	Source	Latitude	Longitude	Temp °C	pH	Conduvitivity uS/cm
		Sandia Mountain Springs (2012-2023)									
11	OHS	Osha Spring	Osha Spring	Osha Spring	8/24/2022	Spring Stewardship Institute 2022	35.24600	-106.43640	12.9	7.06	660
12	CCS	Canoncito Springs	Canoncito Springs	Canoncito Springs	8/26/2022	Spring Stewardship Institute 2022	35.14638	-106.38902	10.7	6.95	504
13	TS	Tree Spring	Tree Spring	Tree Spring	8/27/2022	Spring Stewardship Institute 2022	35.19351	-106.40278	11.7	6.77	1612
14	CNS	Cienega Spring	Cienega Spring	Cienega Spring	8/27/2022	Spring Stewardship Institute 2022	35.16959	-106.38503	10	6.85	526
15	SS	Sulfur Spring	Sulfur Spring	Sulfur Spring	8/25/2022	Spring Stewardship Institute 2022	35.17310	-106.37668	13.9	7.17	417
16	OS	Oso Spring	Oso Spring	Oso Spring	8/23/2022	Spring Stewardship Institute 2022	35.13095	-106.45268	12.7	6.96	410
33	ARS	Armijo Spring	Armijo Spring	Armijo Spring	4/23/2012	(Frus, 2016; DeLay et al. 2022)	35.15563	-106.38890	8.4	6.57	541
34	ARS	Armijo Spring	Armijo Spring	Armijo Spring	8/28/2016	(Frus, 2016; DeLay et al. 2022)	35.15563	-106.38890	10.3	7.38	709
35	ARS	Armijo Spring	Armijo Spring	Armijo Spring	10/30/2016	(Frus, 2016; DeLay et al. 2022)	35.15563	-106.38890	11.1	8.05	668
36	ARS	Armijo Spring	Armijo Spring	Armijo Spring	3/16/2017	(Frus, 2016; DeLay et al. 2022)	35.15563	-106.38890	8.4	7.21	618
37	BE	Border East	Border East	Border East	6/26/2012	(Frus, 2016; DeLay et al. 2022)	35.07933	-106.40116	17.9	7.32	1263
38	BW	Border West	Border West	Border West	6/19/2012	(Frus, 2016; DeLay et al. 2022)	35.07830	-106.40520	18.5	7.92	1371
39	CCS	Canoncito	Canoncito	Canoncito	7/11/2012	(Frus, 2016; DeLay et al. 2022)	35.14643	-106.38902	10.7	6.91	495
46	CNS	Cienga Spring	Cienga Spring	Cienga Spring	4/19/2012	(Frus, 2016; DeLay et al. 2022)	35.16942	-106.38464	10.0	6.63	564
47	CNS	Cienga Spring	Cienga Spring	Cienga Spring	7/5/2012	(Frus, 2016; DeLay et al. 2022)	35.16942	-106.38464	8.1	6.71	612
48	CNS	Cienga Spring	Cienga Spring	Cienga Spring	8/28/2016	(Frus, 2016; DeLay et al. 2022)	35.16942	-106.38464	10.9	6.86	615
49	CNS	Cienga Spring	Cienga Spring	Cienga Spring	10/29/2016	(Frus, 2016; DeLay et al. 2022)	35.16942	-106.38464	11.6	7.75	617
50	CNS	Cienga Spring	Cienga Spring	Cienga Spring	3/15/2017	(Frus, 2016; DeLay et al. 2022)	35.16942	-106.38464	10.1	7.02	548
51	COS	Cole Spring	Cole Spring	Cole Spring	5/21/2012	(Frus, 2016; DeLay et al. 2022)	35.13517	-106.38906	10.0	7.16	590
52	COS	Cole Spring	Cole Spring	Cole Spring	7/14/2017	(Frus, 2016; DeLay et al. 2022)	35.13517	-106.38906	11.1	7.02	597
58	GW	Grants West	Grants West	Grants West	6/19/2012	(Frus, 2016; DeLay et al. 2022)	35.07527	-106.40923	19.7	7.93	1203
59	HCS	Hobbies Central	Hobbies Central	Hobbies Central	6/26/2012	(Frus, 2016; DeLay et al. 2022)	35.09870	-106.38811	22.3	7.46	472
85	MUS	Mud Spring	Mud Spring	Mud Spring	6/5/2012	(Frus, 2016; DeLay et al. 2022)	35.12810	-106.38558	12.5	7.34	568
86	MUS	Mud Spring	Mud Spring	Mud Spring	9/11/2012	(Frus, 2016; DeLay et al. 2022)	35.12810	-106.38558	n.r.	7.49	n.r.
87	OSH	Oso Spring (High)	Oso Spring (High)	Oso Spring (High)	11/6/2016	(Frus, 2016; DeLay et al. 2022)	35.13211	-106.45756	9	8.01	593
88	OS	Oso Spring	Oso Spring	Oso Spring	3/18/2017	(Frus, 2016; DeLay et al. 2022)	35.13092	-106.45285	7.5	7.14	475
89	SS	Seven Springs	Seven Springs	Seven Springs	6/19/2012	(Frus, 2016; DeLay et al. 2022)	35.07681	-106.40903	18.8	8.01	1223
90	SLS	Sulphur Springs	Sulphur Springs	Sulphur Springs	5/21/2012	(Frus, 2016; DeLay et al. 2022)	35.17314	-106.37667	13.9	7.47	485
91	TGS	Three Gun Spring	Three Gun Spring	Three Gun Spring	11/6/2016	(Frus, 2016; DeLay et al. 2022)	35.09878	-106.43906	12.6	7.85	482
92	TGS	Three Gun Spring	Three Gun Spring	Three Gun Spring	3/17/2017	(Frus, 2016; DeLay et al. 2022)	35.09878	-106.43906	9.9	7.64	458
93	TRS	Torro Spring	Torro Spring	Torro Spring	7/21/2017	(Frus, 2016; DeLay et al. 2022)	35.15699	-106.39284	11.0	7.07	625
94	TVS	Travertine Falls	Travertine Falls	Travertine Falls	6/8/2013	(Frus, 2016; DeLay et al. 2022)	35.09538	-106.39375	12.4	7.09	1399
95	TVS	Travertine Falls	Travertine Falls	Travertine Falls	7/5/2012	(Frus, 2016; DeLay et al. 2022)	35.09538	-106.39375	13.1	7.14	615
96	TVS	Travertine Falls	Travertine Falls	Travertine Falls	8/27/2016	(Frus, 2016; DeLay et al. 2022)	35.09538	-106.39375	13.6	6.97	597
97	TVS	Travertine Falls	Travertine Falls	Travertine Falls	10/30/2016	(Frus, 2016; DeLay et al. 2022)	35.09538	-106.39375	13.6	8.08	552
98	TVS	Travertine Falls	Travertine Falls	Travertine Falls	3/17/2017	(Frus, 2016; DeLay et al. 2022)	35.09538	-106.39375	12.5	7.53	563
99	TNS	Tunnel Spring	Tunnel Spring	Tunnel Spring	6/1/2013	(Frus, 2016; DeLay et al. 2022)	35.29113	-106.43986	12.3	7.42	566
145	CNS	Cienega Spring	Cienega Spring	Cienega Spring	n.r.	(Frus, 2016; DeLay et al. 2022)	n.r.	n.r.	n.r.	n.r.	n.r.
146	CNS	Cienega Spring	Cienega Spring	Cienega Spring	n.r.	(Frus, 2016; DeLay et al. 2022)	n.r.	n.r.	n.r.	n.r.	n.r.
147	CNS	Cienega Spring	Cienega Spring	Cienega Spring	n.r.	(Frus, 2016; DeLay et al. 2022)	n.r.	n.r.	n.r.	n.r.	n.r.
148	CNS	Cienega Spring	Cienega Spring	Cienega Spring	n.r.	(Frus, 2016; DeLay et al. 2022)	n.r.	n.r.	n.r.	n.r.	n.r.

Table 1. Sample locations and field parameters

Unique ID	Map Label	Site Name	Sample #	Location	Sample Date	Source	Latitude	Longitude	Temp °C	pH	Conduvitivity uS/cm
149	CNS	Cienega Spring	Cienega Spring	Cienega Spring	n.r.	(Frus, 2016; DeLay et al. 2022)	n.r.	n.r.	n.r.	n.r.	n.r.
150	CNS	Cienega Spring	Cienega Spring	Cienega Spring	n.r.	(Frus, 2016; DeLay et al. 2022)	n.r.	n.r.	n.r.	n.r.	n.r.
151	CNS	Cienega Spring	Cienega Spring	Cienega Spring	n.r.	(Frus, 2016; DeLay et al. 2022)	n.r.	n.r.	n.r.	n.r.	n.r.
152	CNS	Cienega Spring	Cienega Spring	Cienega Spring	n.r.	(Frus, 2016; DeLay et al. 2022)	n.r.	n.r.	n.r.	n.r.	n.r.
153	CNS	Cienega Spring	Cienega Spring	Cienega Spring	n.r.	(Frus, 2016; DeLay et al. 2022)	n.r.	n.r.	n.r.	n.r.	n.r.
154	CNS	Cienega Spring	Cienega Spring	Cienega Spring	n.r.	(Frus, 2016; DeLay et al. 2022)	n.r.	n.r.	n.r.	n.r.	n.r.
155	CNS	Cienega Spring	Cienega Spring	Cienega Spring	n.r.	(Frus, 2016; DeLay et al. 2022)	n.r.	n.r.	n.r.	n.r.	n.r.
156	CNS	Cienega Spring	Cienega Spring	Cienega Spring	n.r.	(Frus, 2016; DeLay et al. 2022)	n.r.	n.r.	n.r.	n.r.	n.r.
157	CNS	Cienega Spring	Cienega Spring	Cienega Spring	n.r.	(Frus, 2016; DeLay et al. 2022)	n.r.	n.r.	n.r.	n.r.	n.r.
158	CNS	Cienega Spring	Cienega Spring	Cienega Spring	n.r.	(Frus, 2016; DeLay et al. 2022)	n.r.	n.r.	n.r.	n.r.	n.r.
159	CNS	Cienega Spring	Cienega Spring	Cienega Spring	n.r.	(Frus, 2016; DeLay et al. 2022)	n.r.	n.r.	n.r.	n.r.	n.r.
160	CNS	Cienega Spring	Cienega Spring	Cienega Spring	n.r.	(Frus, 2016; DeLay et al. 2022)	n.r.	n.r.	n.r.	n.r.	n.r.
161	CNS	Cienega Spring	Cienega Spring	Cienega Spring	n.r.	(Frus, 2016; DeLay et al. 2022)	n.r.	n.r.	n.r.	n.r.	n.r.
162	CNS	Cienega Spring	Cienega Spring	Cienega Spring	n.r.	(Frus, 2016; DeLay et al. 2022)	n.r.	n.r.	n.r.	n.r.	n.r.
163	CNS	Cienega Spring	Cienega Spring	Cienega Spring	n.r.	(Frus, 2016; DeLay et al. 2022)	n.r.	n.r.	n.r.	n.r.	n.r.
164	CNS	Cienega Spring	Cienega Spring	Cienega Spring	n.r.	(Frus, 2016; DeLay et al. 2022)	n.r.	n.r.	n.r.	n.r.	n.r.
165	CNS	Cienega Spring	Cienega Spring	Cienega Spring	n.r.	(Frus, 2016; DeLay et al. 2022)	n.r.	n.r.	n.r.	n.r.	n.r.
166	CNS	Cienega Spring	Cienega Spring	Cienega Spring	n.r.	(Frus, 2016; DeLay et al. 2022)	n.r.	n.r.	n.r.	n.r.	n.r.
167	CNS	Cienega Spring	Cienega Spring	Cienega Spring	n.r.	(Frus, 2016; DeLay et al. 2022)	n.r.	n.r.	n.r.	n.r.	n.r.
168	CNS	Cienega Spring	Cienega Spring	Cienega Spring	n.r.	(Frus, 2016; DeLay et al. 2022)	n.r.	n.r.	n.r.	n.r.	n.r.
169	CNS	Cienega Spring	Cienega Spring	Cienega Spring	n.r.	(Frus, 2016; DeLay et al. 2022)	n.r.	n.r.	n.r.	n.r.	n.r.
170	CNS	Cienega Spring	Cienega Spring	Cienega Spring	n.r.	(Frus, 2016; DeLay et al. 2022)	n.r.	n.r.	n.r.	n.r.	n.r.
171	CNS	Cienega Spring	Cienega Spring	Cienega Spring	n.r.	(Frus, 2016; DeLay et al. 2022)	n.r.	n.r.	n.r.	n.r.	n.r.
172	CNS	Cienega Spring	Cienega Spring	Cienega Spring	n.r.	(Frus, 2016; DeLay et al. 2022)	n.r.	n.r.	n.r.	n.r.	n.r.
173	CNS	Cienega Spring	Cienega Spring	Cienega Spring	n.r.	(Frus, 2016; DeLay et al. 2022)	n.r.	n.r.	n.r.	n.r.	n.r.
174	CNS	Cienega Spring	Cienega Spring	Cienega Spring	n.r.	(Frus, 2016; DeLay et al. 2022)	n.r.	n.r.	n.r.	n.r.	n.r.

Table 1. Sample locations and field parameters

Unique ID	Map Label	Site Name	Sample #	Location	Sample Date	Source	Latitude	Longitude	Temp °C	pH	Conduvitivity uS/cm
175	CNS	Cienega Spring	Cienega Spring	Cienega Spring	n.r.	(Frus, 2016; DeLay et al. 2022)	n.r.	n.r.	n.r.	n.r.	n.r.
176	CNS	Cienega Spring	Cienega Spring	Cienega Spring	n.r.	(Frus, 2016; DeLay et al. 2022)	n.r.	n.r.	n.r.	n.r.	n.r.
177	CNS	Cienega Spring	Cienega Spring	Cienega Spring	n.r.	(Frus, 2016; DeLay et al. 2022)	n.r.	n.r.	n.r.	n.r.	n.r.
178	CNS	Cienega Spring	Cienega Spring	Cienega Spring	n.r.	(Frus, 2016; DeLay et al. 2022)	n.r.	n.r.	n.r.	n.r.	n.r.
179	CNS	Cienega Spring	Cienega Spring	Cienega Spring	n.r.	(Frus, 2016; DeLay et al. 2022)	n.r.	n.r.	n.r.	n.r.	n.r.
180	CNS	Cienega Spring	Cienega Spring	Cienega Spring	n.r.	(Frus, 2016; DeLay et al. 2022)	n.r.	n.r.	n.r.	n.r.	n.r.
181	CNS	Cienega Spring	Cienega Spring	Cienega Spring	n.r.	(Frus, 2016; DeLay et al. 2022)	n.r.	n.r.	n.r.	n.r.	n.r.
182	CNS	Cienega Spring	Cienega Spring	Cienega Spring	n.r.	(Frus, 2016; DeLay et al. 2022)	n.r.	n.r.	n.r.	n.r.	n.r.
183	CNS	Cienega Spring CS1	Cienega Spring CS1	Cienega Spring CS1	n.r.	(Frus, 2016; DeLay et al. 2022)	n.r.	n.r.	n.r.	n.r.	n.r.
184	DLS	Doc Long Spring	Doc Long Spring	Doc Long Spring	n.r.	(Frus, 2016; DeLay et al. 2022)	n.r.	n.r.	n.r.	n.r.	n.r.
185	DLS	Doc Long Spring	Doc Long Spring	Doc Long Spring	n.r.	(Frus, 2016; DeLay et al. 2022)	n.r.	n.r.	n.r.	n.r.	n.r.
186	DLS	Doc Long Spring	Doc Long Spring	Doc Long Spring	n.r.	(Frus, 2016; DeLay et al. 2022)	n.r.	n.r.	n.r.	n.r.	n.r.
187	DLS	Doc Long Spring	Doc Long Spring	Doc Long Spring	n.r.	(Frus, 2016; DeLay et al. 2022)	n.r.	n.r.	n.r.	n.r.	n.r.
230	CRS	Carlito Spring	Carlito Spring	Carlito Spring	5/11/2023	This Study	35.08804	-106.39999	15.8	6.94	437
231	CNS	Cienega Spring	Cienega Spring	Cienega Spring	5/11/2023	This Study	35.16958	-106.38503	11.4	8.82	561

n.r. - not reported

Unique ID	Number assigned from Master spreadsheet
Spring Name	Site name assigned based on location
Sample #	Sample number assigned during collection
Location	Geographic name for location
Map Label	code assigned by site location for map labels
Sample Date	Date of sample location (M/DD/YYYY)
Source	Indicates where data was compiled from.
Latitude	GPS site using a Garmin
Longitude	GPS site using a Garmin
Temp °C	Temperature of water sample
pH	pH of sample measured with probe
Conduvitivity uS/cm	measured conductivity in uS/cm with probe

Table 2. Major Ions

Unique ID	Sample #	Site Name	Sample Date	Ca	Mg	Na	K	Alkalinity	Cl	SO4	% Error
		Las Huertas Springs (2021)									
1	Camp Spring	Camp Spring Box	11/6/2021	117.9	3.2	17.1	1.0	292.9	66.1	9.9	0.3
2	Ellis Spring	Ellis Spring Box	11/6/2021	121.1	3.2	17.4	0.9	297.8	63.0	10.0	1.6
		Capulin Spring (2021-2023)									
5	KT22LHCPS	Capulin Spring	5/18/2022	275.7	6.7	127.9	1.3	472.3	504.1	20.6	-5.9
17	KT22FCPS	Capulin Spring	11/11/2022	262.7	7.0	130.8	1.7	429.6	501.3	27.1	-5.6
26	LH23CPS	Capulin Spring	5/11/2023	202.9	5.2	88.3	1.2	391.7	333.3	14.8	-5.6
		Las Huertas Stream (2021-2023)									
3	LH Church Stream	Las Huertas Upper Reach	11/6/2021	116.0	3.1	17.2	1.0	292.9	60.5	9.9	0.8
4	LH-3	Las Huertas Picnic Area	11/6/2021	100.5	4.0	17.1	0.8	301.4	62.2	7.2	-5.7
6	KT22LHCPS2	Capulin Canyon-2	5/18/2022	101.9	4.0	17.3	0.8	262.4	63.0	10.1	-0.8
7	KT22LH-1	NE of House Spring	5/18/2022	109.5	3.5	25.4	1.0	272.1	80.5	10.3	-0.5
8	KT22LH-2	Loop Trail	5/18/2022	92.0	3.7	23.0	0.8	220.9	77.9	10.6	-1.0
9	KT22LH-3	Las Huertas Picnic Area	5/18/2022	91.4	3.8	20.8	0.8	228.2	76.0	10.3	-2.5
10	KT22LH-4	Canon Media at NM165	5/18/2022	67.7	4.2	16.9	0.7	159.9	68.7	10.5	-3.3
18	Capulin Canyon-1	Capulin Canyon-1	11/11/2022	114.5	4.2	24.1	1.3	291.7	64.6	16.0	1.5
19	Capulin Canyon-2	Capulin Canyon-2	11/11/2022	108.6	4.6	22.4	1.3	302.6	63.2	16.2	-2.0
20	KT22FCPS4	CC and LH Confluence	11/11/2022	99.7	4.2	24.2	1.3	269.7	72.1	16.2	-2.9
21	KT22FLH2	Loop Trail	11/11/2022	96.1	3.8	27.2	1.3	236.7	66.4	18.0	1.6
22	KT22FLH3	Las Huertas Picnic Area	11/11/2022	99.8	4.0	26.2	1.3	250.2	68.7	18.0	0.6
23	KT22FLH4	Canon Media at NM165	11/11/2022	90.6	4.2	24.3	1.3	238.0	69.9	16.4	-2.1
24	KT22FLH5	N of Ditch Diversion	11/11/2022	90.5	4.7	24.9	1.3	220.9	72.7	16.7	0.0
27	KT23SLH1	NE of House Spring	5/11/2023	71.4	2.9	10.3	0.9	238.0	28.7	9.0	-6.8
28	KT23SLH2	Loop Trail	5/11/2023	69.1	3.0	10.4	0.9	225.8	26.3	9.4	-5.3
29	Capulin Canyon-1	Capulin Canyon-1	5/11/2023	71.4	3.5	15.0	0.9	262.4	35.4	9.9	-9.8
30	KT23SLH3	Las Huertas Picnic Area	5/11/2023	70.4	3.1	11.1	1.0	234.3	25.3	8.8	-5.1
31	KT23SLH4	Canon Media at NM165	5/11/2023	66.0	2.9	10.2	0.9	212.3	27.7	9.1	-5.4
32	KT23SLH6	LH Downstream	5/11/2023	61.6	3.1	11.0	0.9	185.5	29.0	9.6	-2.9

Table 2. Major Ions

Unique ID	Sample #	Site Name	Sample Date	Ca	Mg	Na	K	Alkalinity	Cl	SO4	% Error
		Capulin Spring (2012-2017)									
40	Capulin Spring	Capulin Spring	6/13/2012	204.2	5.4	86.3	1.0	401.5	262.2	7.7	0.9
41	Capulin Spring	Capulin Spring	6/8/2013	232.4	5.8	85.2	1.3	405.2	274.3	9.7	4.1
42	Capulin Spring	Capulin Spring	8/27/2016	233.9	6.2	99.7	1.3	419.2	350.8	14.0	-1.5
44	Capulin Spring	Capulin Spring	3/16/2017	237.2	7.0	94.4	2.7	417.4	279.7	11.4	5.1
45	Capulin Spring	Capulin Spring	8/10/2017	265.1	6.5	121.3	1.3	430.8	366.7	14.0	3.7
54	Faulty Trail	Capulin Spring	6/13/2012	143.9	11.0	31.4	1.5	417.4	92.4	39.2	-3.9
55	Faulty Trail	Capulin Spring	8/28/2016	170.1	13.0	34.3	1.3	396.6	114.6	58.5	0.6
56	Faulty Trail	Capulin Spring	10/29/2016	147.2	11.5	33.7	1.3	406.6	119.7	47.4	-5.9
57	Faulty Trail	Capulin Spring	3/16/2017	172.6	14.5	35.0	1.3	402.7	99.7	45.7	4.6
		Las Huertas Springs (2012-2017)									
53	Ellis Spring	Ellis Spring	6/1/2013	111.4	3.4	14.1	1.0	274.1	48.7	9.5	3.3
64	Ellis Spring	Ellis Spring	7/21/2012	104.7	3.0	11.3	0.9	273.4	35.3	9.9	2.6
65	Ellis Spring	Ellis Spring	7/13/2013	105.3	3.1	11.9	0.9	282.9	54.7	9.6	-2.6
66	Ellis Spring	Ellis Spring	8/22/2013	111.8	3.2	17.5	b.d.*	289.6	65.0	9.7	-1.2
67	Ellis Spring	Ellis Spring	5/21/2014	105.8	2.9	17.3	0.6	303.9	42.6	7.8	-0.4
68	Ellis Spring	Ellis Spring	10/29/2016	101.9	3.2	12.1	0.8	308.7	45.6	9.4	-5.2
69	LH Camp Spr Box	Camp Spring	7/21/2012	103.0	2.9	23.0	0.8	294.5	36.7	9.8	2.7
70	LH Camp Spr Box	Camp Spring	6/1/2013	101.7	3.2	13.5	1.0	289.6	49.3	9.5	-3.1
71	LH Camp Spr Box	Camp Spring	7/13/2013	101.6	3.2	12.2	0.9	285.9	47.3	9.5	-2.8
72	LH Camp Spr Box	Camp Spring	8/22/2013	112.2	3.2	18.2	0.5	289.3	66.4	9.7	-1.1
73	LH Camp Spr Box	Camp Spring	5/21/2014	104.4	2.7	13.5	0.9	300.8	36.8	7.5	-0.7
74	LH Camp Spr Box	Camp Spring	3/17/2017	146.6	4.6	44.4	1.2	295.3	108.1	9.1	8.9

Table 2. Major Ions

Unique ID	Sample #	Site Name	Sample Date	Ca	Mg	Na	K	Alkalinity	Cl	SO4	% Error
		Las Huertas Stream (2012-2017)									
60	LH at CDT	Las Huertas Upper Reach	7/21/2012	97.4	3.0	11.3	0.8	302.8	36.8	9.6	-4.9
61	LH at CDT	Las Huertas Upper Reach	7/13/2013	106.4	3.1	12.4	1.0	275.7	49.7	9.7	0.1
62	LH at CDT	Las Huertas Upper Reach	8/22/2013	109.8	3.2	18.3	b.d.	271.2	66.3	9.7	0.3
63	LH at CDT	Las Huertas Upper Reach	5/21/2014	103.4	2.8	14.7	0.6	303.9	39.7	7.6	-1.7
75	LH Downstream #1	LH Downstream #1	7/28/2012	101.5	3.0	11.6	0.7	288.7	39.9	9.1	-1.8
76	LH Downstream #2	LH Downstream #2	7/28/2012	99.5	3.2	12.5	0.8	287.4	40.1	9.1	-2.1
77	LH Downstream #3	LH Downstream #3	7/28/2012	99.1	3.2	12.4	0.8	287.4	40.2	9.2	-2.2
78	LH Downstream #4	LH Downstream #4	7/28/2012	93.2	3.3	13.4	0.8	261.8	41.0	8.9	-1.0
79	LH Downstream #5	LH Downstream #5	7/28/2012	102.0	3.9	8.2	0.9	284.0	29.6	9.9	0.8
80	LH Downstream #6	LH Downstream #6	7/28/2012	101.6	3.6	13.9	0.9	285.6	46.5	9.5	-1.6
81	LH Downstream #7	LH Downstream #7	7/28/2012	95.5	3.6	11.3	0.8	276.4	36.8	9.6	-1.7
82	LH Downstream #8	LH Downstream #8	7/28/2012	94.2	3.6	11.9	0.8	257.9	37.8	9.6	0.3
83	LH Downstream	LH Downstream	8/27/2016	87.7	3.8	13.1	0.7	244.1	38.4	10.2	-0.2
84	LH Picnic	Las Huertas Picnic Area	6/1/2013	89.9	3.9	13.0	1.0	255.4	43.1	10.3	-2.0
		Sandia Mountain Springs (2012-2023)									
33	Armijo Spring	Armijo Spring	4/23/2012	98.7	4.3	2.7	0.6	346.6	1.8	8.0	-4.4
34	Armijo Spring	Armijo Spring	8/28/2016	126.8	5.9	2.5	0.7	427.1	2.5	10.9	-2.5
35	Armijo Spring	Armijo Spring	10/30/2016	128.7	6.0	2.7	0.7	425.3	2.7	11.1	-1.6
36	Armijo Spring	Armijo Spring	3/16/2017	128.0	6.0	2.6	0.6	388.1	1.8	8.9	3.1
37	Border East	Border East	6/26/2012	149.3	30.0	60.1	3.6	365.5	156.2	166.3	-4.7
38	Border West	Border West	6/19/2012	123.4	32.2	61.3	3.2	318.1	143.2	148.6	-3.3
39	Canoncito	Canoncito	7/11/2012	107.7	4.0	4.0	0.9	328.3	2.5	15.6	1.0
12	Canoncito Springs	Canoncito Springs	8/26/2022	104.9	4.3	3.8	1.7	314.8	11.3	20.5	-0.9
230	Carlito Spring	Carlito Spring	5/11/2023	87.6	5.8	4.9	4.3	246.5	10.8	23.0	3.5
231	Cienega Spring	Cienega Spring	5/11/2023	121.2	5.6	5.5	4.1	333.2	16.8	10.3	5.4
183	Cienega Spring CS1	Cienega Spring CS2		**n.r	n.r	n.r	n.r	n.r	n.r	n.r	n.r
46	Cienga Spring	Cienga Spring	4/19/2012	98.6	4.5	6.8	0.8	336.8	13.0	10.3	-4.2
47	Cienga Spring	Cienga Spring	7/5/2012	109.2	4.8	6.9	0.8	315.5	17.3	13.1	1.9
48	Cienga Spring	Cienga Spring	8/28/2016	104.8	4.9	6.5	0.8	320.9	16.9	13.8	-0.8
49	Cienga Spring	Cienga Spring	10/29/2016	90.3	5.0	6.2	0.8	320.7	14.4	13.9	-6.7
50	Cienga Spring	Cienga Spring	3/15/2017	104.6	5.2	5.9	0.8	329.5	9.3	9.9	0.4

Table 2. Major Ions

Unique ID	Sample #	Site Name	Sample Date	Ca	Mg	Na	K	Alkalinity	Cl	SO4	% Error
51	Cole Spring	Cole Spring	5/21/2012	106.9	4.6	3.9	0.8	357.0	2.5	15.9	-2.9
52	Cole Spring	Cole Spring	7/14/2017	115.6	4.9	3.5	0.7	356.6	2.7	16.0	0.7
58	Grants West	Grants West	6/19/2012	114.9	26.5	45.2	2.5	286.8	113.3	137.1	-3.9
59	Hobbies Central	Hobbies Central	6/26/2012	79.2	11.5	7.3	0.9	295.0	11.2	18.2	-2.7
85	Mud Spring	Mud Spring	6/5/2012	104.2	9.0	10.9	1.6	398.4	5.1	4.7	-2.4
86	Mud Spring	Mud Spring	9/11/2012	92.5	8.9	12.5	2.1	372.5	6.4	12.6	-4.8
11	Osha Spring	Osha Spring	8/24/2022	154.0	4.5	2.6	1.9	424.7	12.3	22.0	2.8
16	Oso Spring	Oso Spring		64.7	15.8	17.1	3.9	238.0	15.0	46.9	0.7
88	Oso Spring	Oso Spring	3/18/2017	62.6	16.7	14.5	2.9	234.3	4.7	40.8	3.8
87	Oso Spring (High)	Oso Spring (High)	11/6/2016	69.1	18.0	20.5	3.5	301.4	8.4	63.8	-4.8
89	Seven Springs	Seven Springs	6/19/2012	113.9	29.9	46.0	2.6	291.2	118.0	138.0	-3.6
15	Sulfur Spring	Sulfur Spring	8/25/2022	45.9	6.5	43.3	2.4	242.8	14.0	33.4	-3.1
90	Sulphur Springs	Sulphur Springs	5/21/2012	44.0	6.5	44.5	1.8	242.9	5.5	25.4	0.5
91	Three Gun Spring	Three Gun Spring	11/6/2016	49.9	14.3	14.3	4.8	227.6	6.1	49.4	-5.6
92	Three Gun Spring	Three Gun Spring	3/17/2017	60.9	18.1	13.0	2.3	236.7	5.5	44.6	1.9
93	Torro Spring	Torro Spring	7/21/2017	123.5	4.2	1.8	0.6	379.0	2.6	9.8	0.9

Table 2. Major Ions

Unique ID	Sample #	Site Name	Sample Date	Ca	Mg	Na	K	Alkalinity	Cl	SO4	% Error
94	Travertine Falls	Travertine Falls	6/8/2013	107.9	8.6	4.8	1.0	352.1	2.5	19.9	0.6
95	Travertine Falls	Travertine Falls	7/5/2012	108.2	8.4	4.8	0.9	339.6	3.1	17.9	2.4
96	Travertine Falls	Travertine Falls	8/27/2016	102.9	8.7	4.2	0.9	337.4	2.3	18.9	0.6
97	Travertine Falls	Travertine Falls	10/30/2016	90.1	8.7	4.8	1.6	341.1	3.3	22.1	-5.9
98	Travertine Falls	Travertine Falls	3/17/2017	96.7	9.4	4.0	0.9	334.4	4.0	16.3	-1.2
99	Tunnel Spring	Tunnel Spring	6/1/2013	102.8	5.6	5.2	1.1	304.2	2.8	25.5	2.2
14	Cienega Spring	Cienega Spring	8/27/2022	100.0	5.6	7.3	1.7	302.6	19.3	18.9	-0.7
13	Tree Spring	Tree Spring	8/27/2022	131.9	16.0	131.7	3.0	347.8	256.9	26.7	0.7
	*b.d.= below detection	**n.r.=not reported									

Unique ID	Number assigned from Master spreadsheet
Sample #	Sample number assigned during collection
Site Name	Site name assigned based on location
Ca	total calcium in mg/l
Mg	total magnesium in mg/l
Na	total sodium in mg/l
K	total potassium in mg/l
Alkalinity	alkanility as bicarbonate in mg/l
Cl	total Cl in mg/l
SO4	total SO4 in mg/l
% Error	percent error calculated from mass balance

Table 3. Stable Isotopes and Minor Elements

Unique ID	Sample #	Site Name	Sample Date	δ18O	δD	SI as ppm SiO2	NO3	F	Br	Fe	Ba	Li	Sr
		Las Huertas Springs (2021)											
1	Camp Spring	Camp Spring Box	11/6/2021	-12.82	-87.10	5.41	3.96	0.20	0.96	b.d.	0.12	b.d.	0.16
2	Ellis Spring	Ellis Spring Box	11/6/2021	-12.81	-87.12	5.45	3.82	0.20	0.92	b.d.	0.12	b.d.	0.16
		Capulin Spring (2021-2023)											
5	KT22LHCPS	Capulin Spring	5/18/2022	-12.74	-87.16	10.26	2.97	0.51	1.01	b.d.	0.16	0.10	0.52
17	KT22FCPS	Capulin Spring	11/11/2022	-12.53	-85.42	9.82	4.46	0.75	1.61	b.d.	0.20	b.d.	0.54
26	LH23CPS	Capulin Spring	5/11/2023	-12.36	-84.11	9.66	b.d.	b.d.	b.d.	0.66	0.22	0.22	0.52
		Las Huertas Stream (2021-2023)											
3	LH Church Stream	Las Huertas Upper Reach	11/6/2021	-12.81	-87.13	5.42	3.98	0.24	1.03	b.d.	0.12	b.d.	0.15
4	LH-3	Las Huertas Picnic Area	11/6/2021	-12.68	-86.72	8.57	1.67	0.25	0.90	b.d.	0.11	b.d.	0.18
6	KT22LHCPS2	Capulin Canyon-2	5/18/2022	-12.80	-87.75	10.20	1.68	0.66	0.61	b.d.	0.13	0.06	0.21
7	KT22LH-1	NE of House Spring	5/18/2022	-13.06	-89.06	6.79	3.51	0.51	0.60	b.d.	0.13	0.07	0.18
8	KT22LH-2	Loop Trail	5/18/2022	-12.93	-88.52	7.69	2.24	0.54	0.59	b.d.	0.12	0.06	0.20
9	KT22LH-3	Las Huertas Picnic Area	5/18/2022	-12.89	-88.18	8.45	1.73	0.52	0.60	b.d.	0.12	0.06	0.20
10	KT22LH-4	Canon Media at NM165	5/18/2022	-12.41	-86.13	9.89	0.66	0.62	0.59	b.d.	0.12	0.05	0.21
18	Capulin Canyon-1	Capulin Canyon-1	11/11/2022	-12.51	-84.98	8.64	3.07	0.93	1.05	b.d.	0.18	b.d.	0.26
19	Capulin Canyon-2	Capulin Canyon-2	11/11/2022	-12.45	-84.63	9.91	2.31	0.88	1.00	b.d.	0.19	b.d.	0.28
20	KT22FCPS4	Confluence at LHP	11/11/2022	-12.47	-84.93	8.11	2.71	0.89	1.02	b.d.	0.17	b.d.	0.25
21	KT22FLH2	Loop Trail	11/11/2022	-12.37	-84.24	6.32	3.34	0.88	1.03	b.d.	0.16	b.d.	0.23
22	KT22FLH3	Las Huertas Picnic Area	11/11/2022	-12.42	-84.42	7.15	3.09	0.83	1.04	b.d.	0.17	b.d.	0.24
23	KT22FLH4	Canon Media at NM165	11/11/2022	-12.35	-84.02	8.09	2.64	0.92	1.04	b.d.	0.16	b.d.	0.24
24	KT22FLH5	N of Ditch Diversion	11/11/2022	-12.28	-83.54	9.46	2.69	0.93	1.10	b.d.	0.17	b.d.	0.26
27	KT23SLH1	NE of House Spring	5/11/2023	-12.30	-83.47	6.55	b.d.	b.d.	b.d.	0.64	0.19	0.20	0.26
28	KT23SLH2	Loop Trail	5/11/2023	-12.27	-83.22	6.94	b.d.	b.d.	b.d.	0.71	0.19	0.19	0.26
29	Capulin Canyon-1	Capulin Canyon-1	5/11/2023	-12.30	-83.67	9.33	b.d.	b.d.	b.d.	0.67	0.22	0.20	0.28
30	KT23SLH3	Las Huertas Picnic Area	5/11/2023	-12.35	-83.67	7.28	b.d.	b.d.	b.d.	0.64	0.20	0.20	0.27
31	KT23SLH4	Canon Media at NM165	5/11/2023	-12.29	-83.38	6.99	b.d.	b.d.	b.d.	0.65	0.19	0.19	0.25
32	KT23SLH6	LH Downstream	5/11/2023	-12.19	-83.10	7.58	b.d.	b.d.	b.d.	0.64	0.19	0.19	0.26
		Capulin Snow Play Area (Winter 2023)											
25	KTCSPA SNOW	Capulin Snow Play Area	2/2/2023	-12.87	-90.60	n.r.	n.r.	n.r.	n.r.	n.r.	n.r.	n.r.	n.r.

Table 3. Stable Isotopes and Minor Elements

Unique ID	Sample #	Site Name	Sample Date	δ18O	δD	SI as ppm SiO2	NO3	F	Br	Fe	Ba	Li	Sr
		Capulin Spring (2012-2017)											
40	Capulin Spring	Capulin Spring	6/13/2012	-12.60	-87.30	8.69	b.d.	0.51	0.32	b.d.	n.r.	n.r.	n.r.
41	Capulin Spring	Capulin Spring	6/8/2013	-12.60	-86.60	7.12	n.r.	0.61	b.d.	b.d.	n.r.	n.r.	n.r.
42	Capulin Spring	Capulin Spring	8/27/2016	*n.r.	n.r.	10.79	n.r.	0.15	2.82	b.d.	n.r.	n.r.	n.r.
43	Capulin Spring	Capulin Spring	10/29/2016	n.r.	n.r.	10.96	n.r.	n.a.	n.a.	b.d.	n.r.	n.r.	n.r.
44	Capulin Spring	Capulin Spring	3/16/2017	n.r.	n.r.	9.06	n.r.	0.59	0.60	b.d.	n.r.	n.r.	n.r.
45	Capulin Spring	Capulin Spring	8/10/2017	-12.07	-82.31	10.69	n.r.	1.71	0.78	b.d.	n.r.	n.r.	n.r.
54	Faulty Trail	Capulin Spring	6/13/2012	n.r.	n.r.	13.20	n.r.	0.72	0.35	b.d.	n.r.	n.r.	n.r.
55	Faulty Trail	Capulin Spring	8/28/2016	n.r.	n.r.	15.31	n.r.	0.38	1.42	0.65	n.r.	n.r.	n.r.
56	Faulty Trail	Capulin Spring	10/29/2016	n.r.	n.r.	16.47	n.r.	n.a.	n.a.	0.27	n.r.	n.r.	n.r.
57	Faulty Trail	Capulin Spring	3/16/2017	n.r.	n.r.	14.26	n.r.	0.72	0.61	b.d.	n.r.	n.r.	n.r.
		Las Huertas Springs (2012-2017)											
53	Ellis Spring Box	Ellis Spring Box	6/1/2013	-12.60	-87.90	4.69	n.r.	0.67	b.d.	b.d.	n.r.	n.r.	n.r.
64	LH at Ellis Box	Ellis Spring Box	7/21/2012	-12.70	-86.10	5.54	n.r.	0.43	b.d.	b.d.	n.r.	n.r.	n.r.
65	LH at Ellis box	Ellis Spring Box	7/13/2013	-11.70	-85.10	4.09	n.r.	0.60	b.d.	b.d.	n.r.	n.r.	n.r.
66	LH at Ellis box	Ellis Spring Box	8/22/2013	-12.70	-87.30	6.31	n.r.	0.42	b.d.	b.d.	n.r.	n.r.	n.r.
67	LH at Ellis Box	Ellis Spring Box	5/21/2014	-12.40	-85.70	5.69	n.r.	0.66	0.09	b.d.	n.r.	n.r.	n.r.
68	LH at Ellis Box	Ellis Spring Box	10/29/2016	n.r.	n.r.	6.87	n.r.	n.a.	3.51	b.d.	n.r.	n.r.	n.r.
69	LH Camp Spr Box	Camp Spring Box	7/21/2012	-12.50	-87.00	5.54	n.r.	0.44	b.d.	b.d.	n.r.	n.r.	n.r.
70	LH Camp Spr Box	Camp Spring Box	6/1/2013	-12.50	-87.80	4.47	n.r.	0.70	b.d.	b.d.	n.r.	n.r.	n.r.
71	LH Camp Spr Box	Camp Spring Box	7/13/2013	-12.60	-86.70	4.11	n.r.	0.69	b.d.	b.d.	n.r.	n.r.	n.r.
72	LH Camp Spr Box	Camp Spring Box	8/22/2013	-12.90	-85.50	6.29	n.r.	0.43	0.08	b.d.	n.r.	n.r.	n.r.
73	LH Camp Spr Box	Camp Spring Box	5/21/2014	-12.10	-86.20	5.76	n.r.	0.63	0.04	b.d.	n.r.	n.r.	n.r.
74	LH Camp Spr Box	Camp Spring Box	3/17/2017	n.r.	n.r.	5.56	n.r.	0.62	0.47	b.d.	n.r.	n.r.	n.r.
		Las Huertas Stream (2012-2017)											
60	LH at CDT	Las Huertas Upper Reach	7/21/2012	n.r.	n.r.	6.05	n.r.	0.41	b.d.	b.d.	n.r.	n.r.	n.r.
75	LH at CDT	Las Huertas Upper Reach	7/13/2013	n.r.	n.r.	4.15	n.r.	0.92	0.65	b.d.	n.r.	n.r.	n.r.
76	LH at CDT	Las Huertas Upper Reach	8/22/2013	n.r.	n.r.	6.38	n.r.	0.39	0.07	b.d.	n.r.	n.r.	n.r.
77	LH at CDT	Las Huertas Upper Reach	5/21/2014	n.r.	n.r.	5.67	n.r.	0.61	b.d.	b.d.	n.r.	n.r.	n.r.
78	LH Downstream #1	LH Downstream #1	7/28/2012	n.r.	n.r.	6.46	n.r.	0.59	b.d.	b.d.	n.r.	n.r.	n.r.
79	LH Downstream #2	LH Downstream #2	7/28/2012	n.r.	n.r.	6.50	n.r.	0.61	b.d.	b.d.	n.r.	n.r.	n.r.
80	LH Downstream #3	LH Downstream #3	7/28/2012	n.r.	n.r.	6.89	n.r.	0.60	b.d.	b.d.	n.r.	n.r.	n.r.
81	LH Downstream #4	LH Downstream #4	7/28/2012	n.r.	n.r.	7.32	n.r.	0.66	b.d.	b.d.	n.r.	n.r.	n.r.
82	LH Downstream #5	LH Downstream #5	7/28/2012	n.r.	n.r.	7.38	n.r.	0.67	b.d.	b.d.	n.r.	n.r.	n.r.
84	LH Downstream #6	LH Downstream #6	7/28/2012	n.r.	n.r.	6.50	n.r.	0.65	0.13	b.d.	n.r.	n.r.	n.r.
61	LH Downstream #7	LH Downstream #7	7/28/2012	n.r.	n.r.	7.34	n.r.	0.63	b.d.	b.d.	n.r.	n.r.	n.r.
62	LH Downstream #8	LH Downstream #8	7/28/2012	n.r.	n.r.	7.38	n.r.	0.60	b.d.	b.d.	n.r.	n.r.	n.r.
63	LH Downstream	LH Downstream	8/27/2016	n.r.	n.r.	8.76	n.r.	0.38	0.59	-0.03	n.r.	n.r.	n.r.
83	LH Picnic	Las Huertas Picnic Area	6/1/2013	n.r.	n.r.	5.99	n.r.	0.78	b.d.	b.d.	n.r.	n.r.	n.r.

Table 3. Stable Isotopes and Minor Elements

Unique ID	Sample #	Site Name	Sample Date	δ18O	δD	SI as ppm SiO2	NO3	F	Br	Fe	Ba	Li	Sr
		Sandia Mountain Springs (2012-2023)											
33	Armijo Spring	Armijo Spring	4/23/2012	-12.80	-86.60	9.80	n.r.	0.81	0.20	b.d.	n.r.	n.r.	n.r.
34	Armijo Spring	Armijo Spring	8/28/2016	-12.20	-86.30	11.96	n.r.	0.37	0.29	b.d.	n.r.	n.r.	n.r.
35	Armijo Spring	Armijo Spring	10/30/2016	-12.50	-84.90	12.76	n.r.	0.57	1.33	b.d.	n.r.	n.r.	n.r.
36	Armijo Spring	Armijo Spring	3/16/2017	-12.40	-86.00	10.54	n.r.	0.62	0.45	b.d.	n.r.	n.r.	n.r.
37	Border East	Border East	6/26/2012	-12.60	-86.90	15.62	n.r.	0.63	0.51	b.d.	n.r.	n.r.	n.r.
38	Border West	Border West	6/19/2012	-12.60	-85.70	15.32	n.r.	0.65	0.47	b.d.	n.r.	n.r.	n.r.
39	Canoncito	Canoncito	7/11/2012	-12.80	-86.00	9.59	n.r.	0.70	b.d.	b.d.	n.r.	n.r.	n.r.
12	Canoncito Springs	Canoncito Springs	8/26/2022	-12.50	-86.30	10.29	1.89	0.95	n.a.	b.d.	0.15	b.d.	0.24
182	Cienega Spring	Cienega Spring	n.r.	-13.10	-87.30	n.r.	n.r.	n.r.	n.r.	b.d.	n.r.	n.r.	n.r.
183	Cienega Spring CS1	Cienega Spring CS2	n.r.	-12.30	-86.50	n.r.	n.r.	n.r.	n.r.	b.d.	n.r.	n.r.	n.r.
46	Cienga Spring	Cienga Spring	4/19/2012	-12.60	-87.40	n.r.	n.r.	n.r.	n.r.	b.d.	n.r.	n.r.	n.r.
47	Cienga Spring	Cienga Spring	7/5/2012	n.r.	n.r.	9.86	n.r.	0.74	b.d.	b.d.	n.r.	n.r.	n.r.
48	Cienga Spring	Cienga Spring	8/28/2016	-12.30	-87.30	10.42	n.r.	0.70	b.d.	b.d.	n.r.	n.r.	n.r.
49	Cienga Spring	Cienga Spring	10/29/2016	n.r.	n.r.	11.10	n.r.	0.44	0.26	b.d.	n.r.	n.r.	n.r.
50	Cienga Spring	Cienga Spring	3/15/2017	n.r.	n.r.	11.77	n.r.	n.a.	n.a.	b.d.	n.r.	n.r.	n.r.
51	Cole Spring	Cole Spring	5/21/2012	-12.50	-88.20	10.04	n.r.	0.68	0.44	b.d.	n.r.	n.r.	n.r.
52	Cole Spring	Cole Spring	7/14/2017	-12.66	-88.05	10.51	n.r.	0.73	b.d.	b.d.	n.r.	n.r.	n.r.
58	Grants West	Grants West	6/19/2012	-10.80	-79.00	11.76	n.r.	1.65	n.a.	0.00	n.r.	n.r.	n.r.
59	Hobbies Central	Hobbies Central	6/26/2012	-12.20	-86.60	15.45	n.r.	0.60	0.50	b.d.	n.r.	n.r.	n.r.
85	Mud Spring	Mud Spring	6/5/2012	-12.40	-87.30	16.62	n.r.	0.59	0.41	b.d.	n.r.	n.r.	n.r.
86	Mud Spring	Mud Spring	9/11/2012	-12.50	-88.10	26.87	n.r.	0.63	0.42	0.22	n.r.	n.r.	n.r.
11	Osha Spring	Osha Spring	8/24/2022	-12.28	-83.80	22.83	n.r.	1.21	1.14	0.72	n.r.	n.r.	n.r.
88	Oso Spring	Oso Spring	8/23/2022	-12.30	-85.19	10.48	1.43	0.88	n.a.	b.d.	0.21	b.d.	0.40
16	Oso Spring	Oso Spring	3/18/2017	n.r.	n.r.	28.89	n.r.	1.63	0.76	b.d.	n.r.	n.r.	n.r.
87	Oso Spring (High)	Oso Spring (High)	11/6/2016	n.r.	n.r.	30.19	0.98	1.68	7.37	b.d.	0.09	b.d.	0.23
89	Seven Springs	Seven Springs	6/19/2012	-11.00	-79.70	33.19	n.r.	1.52	n.a.	0.12	n.r.	n.r.	n.r.
15	Sulfur Spring	Sulfur Spring	8/25/2022	-12.09	-82.35	15.60	n.r.	0.72	0.43	b.d.	n.r.	n.r.	n.r.
90	Sulphur Springs	Sulphur Springs	5/21/2012	-11.80	-83.40	31.88	0.79	3.65	n.a.	0.02	0.12	b.d.	0.40
91	Three Gun Spring	Three Gun Spring	11/6/2016	n.r.	n.r.	24.13	n.r.	3.57	b.d.	0.18	n.r.	n.r.	n.r.
92	Three Gun Spring	Three Gun Spring	3/17/2017	n.r.	n.r.	22.30	n.r.	1.83	n.a.	0.69	n.r.	n.r.	n.r.
93	Torro Spring	Torro Spring	7/21/2017	-12.30	-84.36	20.57	n.r.	1.64	0.52	b.d.	n.r.	n.r.	n.r.
95	Travertine Falls	Travertine Falls	6/8/2013	-12.60	-88.80	8.77	n.r.	1.76	0.19	b.d.	n.r.	n.r.	n.r.
94	Travertine Falls	Travertine Falls	7/5/2012	-12.20	-88.00	10.59	n.r.	0.69	0.34	b.d.	n.r.	n.r.	n.r.
96	Travertine Falls	Travertine Falls	8/27/2016	n.r.	n.r.	7.23	n.r.	0.64	b.d.	b.d.	n.r.	n.r.	n.r.
97	Travertine Falls	Travertine Falls	10/30/2016	n.r.	n.r.	11.26	n.r.	0.37	0.30	b.d.	n.r.	n.r.	n.r.
98	Travertine Falls	Travertine Falls	3/17/2017	n.r.	n.r.	11.61	n.r.	0.58	0.97	b.d.	n.r.	n.r.	n.r.
99	Tunnel Spring	Tunnel Spring	6/1/2013	-12.50	-86.40	10.38	n.r.	0.64	0.47	b.d.	n.r.	n.r.	n.r.
14	Cienega Spring	Cienega Spring	8/27/2022	-12.70	-86.60	7.75	n.r.	1.02	0.08	b.d.	n.r.	n.r.	n.r.
13	Tree Spring	Tree Spring	8/27/2022	-11.42	-77.46	12.33	1.45	0.89	n.a.	b.d.	0.32	b.d.	0.44
230	Carlito Spring	Carlito Spring	5/11/2023	-12.74	-87.92	10.25	6.96	n.r.	n.r.	0.65	0.19	0.20	0.25
231	Cienega Spring	Cienega Spring	5/11/2023	-12.07	-81.83	9.48	7.19	n.r.	n.r.	0.64	0.20	0.20	0.31

Table 3. Stable Isotopes and Minor Elements

Unique ID	Sample #	Site Name	Sample Date	δ18O	δD	SI as ppm SiO2	NO3	F	Br	Fe	Ba	Li	Sr
		Sandia Mountain Stream											
131	Cienega Stream	Cienega Stream	n.r.	-13.03	-86.20	n.r.	n.r.	n.r.	n.r.	n.r.	n.r.	n.r.	n.r.
132	Cienega Stream	Cienega Stream	n.r.	-12.70	-84.30	n.r.	n.r.	n.r.	n.r.	n.r.	n.r.	n.r.	n.r.
144	cstream080616	Cienega Stream	n.r.	-11.83	-83.55	n.r.	n.r.	n.r.	n.r.	n.r.	n.r.	n.r.	n.r.
130	Cienega PG	Cienega Stream	n.r.	-12.79	-88.23	n.r.	n.r.	n.r.	n.r.	n.r.	n.r.	n.r.	n.r.
133	Cienega Wetland CW1	Cienega Stream	n.r.	-12.71	-88.18	n.r.	n.r.	n.r.	n.r.	n.r.	n.r.	n.r.	n.r.
134	CM011016	Cienega Stream	n.r.	-13.05	-86.87	n.r.	n.r.	n.r.	n.r.	n.r.	n.r.	n.r.	n.r.
135	UNK08131601	Cienega Stream	n.r.	-13.19	-86.06	n.r.	n.r.	n.r.	n.r.	n.r.	n.r.	n.r.	n.r.
136	UNK08131602	Cienega Stream	n.r.	-13.26	-87.76	n.r.	n.r.	n.r.	n.r.	n.r.	n.r.	n.r.	n.r.
137	080416-A	Cienega Stream	n.r.	-6.27	-51.24	n.r.	n.r.	n.r.	n.r.	n.r.	n.r.	n.r.	n.r.
138	UCS091916	Cienega Stream	n.r.	-12.54	-85.35	n.r.	n.r.	n.r.	n.r.	n.r.	n.r.	n.r.	n.r.
139	UCS100216	Cienega Stream	n.r.	-12.62	-85.44	n.r.	n.r.	n.r.	n.r.	n.r.	n.r.	n.r.	n.r.
140	UCS090716	Cienega Stream	n.r.	-12.51	-84.66	n.r.	n.r.	n.r.	n.r.	n.r.	n.r.	n.r.	n.r.
141	UCS01816	Cienega Stream	n.r.	-12.63	-85.85	n.r.	n.r.	n.r.	n.r.	n.r.	n.r.	n.r.	n.r.
142	unk081316-01	Cienega Stream	n.r.	-12.33	-86.28	n.r.	n.r.	n.r.	n.r.	n.r.	n.r.	n.r.	n.r.
143	cm011016	Cienega Stream	n.r.	-12.21	-85.16	n.r.	n.r.	n.r.	n.r.	n.r.	n.r.	n.r.	n.r.

n.r.=not reported　　b.d.=below detection

Sample #	Sample number assigned during collection
Site Name	Site name assigned based on location
δ18O	D18o isotope value with repsect to VSMOW
δD	dD, hydrogen isotope with respect to VSMOW
SI as ppm SiO2	total SI as SIO2 in parts per million
NO3	total nitrate in mg/l
F	total flouride in mg/l
Br	total bromide in mg/l
Fe	total iron in mg/l
Ba	total barium in mg/l
Li	total lithium in mg/l
Sr	total strontium in mg/l

Table 4. Saturation Indices

Unique ID		si_Calcite	si_CO2(g)	si_Dolomite	si_Gypsum	si_Halite	si_Quartz	si_SiO2(a)
	2021-2023							
1	Camp Spring Box	-1.95	0.10	-5.19	-2.35	-7.50	-0.12	-1.51
2	Ellis Spring Box	-0.33	-1.49	-1.95	-2.34	-7.51	-0.13	-1.52
5	**Capulin Spring**	0.23	-1.36	-0.86	-1.91	-5.80	0.08	-1.27
17	**Capulin Spring**	-0.35	-0.98	-1.99	-1.78	-5.78	0.15	-1.24
26	**Capulin Spring**	-1.66	0.25	-4.63	-2.07	-6.53	0.11	-1.27
3	LH at CDT	-1.15	-0.70	-3.59	-2.36	-7.54	-0.13	-1.51
4	*Las Huertas Picnic Area*	-1.23	-0.64	-3.57	-2.54	-7.53	0.06	-1.32
6	**At LHP Parking Area**	0.49	-2.42	-0.14	-2.40	-7.52	0.09	-1.27
7	NE of House Spring	0.77	-2.67	0.35	-2.37	-7.25	-0.08	-1.45
8	Loop Trail	0.52	-2.63	-0.06	-2.41	-7.30	-0.04	-1.40
9	*Las Huertas Picnic Area*	0.05	-2.15	-0.99	-2.42	-7.35	0.02	-1.35
10	*Canon Media at NM165*	0.30	-2.74	-0.29	-2.50	-7.48	0.02	-1.32
18	**Above LHP Parking Area**	-0.94	-0.93	-3.03	-2.16	-7.36	0.08	-1.31
19	**At LHP Parking Area**	-1.26	-0.62	-3.63	-2.16	-7.40	0.16	-1.24
20	**Confluence at LHP**	-0.87	-1.15	-2.84	-2.19	-7.31	0.08	-1.32
21	Loop Trail	-0.41	-1.75	-1.95	-2.14	-7.29	-0.01	-1.42
22	*Las Huertas Picnic Area*	-1.29	-0.80	-3.70	-2.13	-7.29	0.03	-1.37
23	*Canon Media at NM165*	0.64	-2.90	0.21	-2.19	-7.31	0.14	-1.29
24	*N of Ditch Diversion*	-0.03	-2.30	-1.10	-2.17	-7.28	0.24	-1.20
27	NE of House Spring	0.39	-2.56	-0.32	-2.54	-8.07	-0.07	-1.45
28	Loop Trail	0.21	-2.41	-0.66	-2.53	-8.10	-0.07	-1.43
29	**Above LHP Parking Area**	-2.50	0.40	-6.02	-2.50	-7.82	0.09	-1.29
30	*Las Huertas Picnic Area*	-0.63	-1.56	-2.33	-2.55	-8.09	-0.02	-1.40
31	*Canon Media at NM165*	0.23	-2.50	-0.60	-2.56	-8.09	-0.07	-1.43
32	*LH Downstream*	-0.62	-1.76	-2.24	-2.56	-8.04	-0.05	-1.41

Table 4. Saturation Indices

Unique ID		si_Calcite	si_CO2(g)	si_Dolomite	si_Gypsum	si_Halite	si_Quartz	si_SiO2(a)
	2012-2017							
40	Capulin Spring	0.06	-1.15	-1.11	-2.41	-6.25	-0.19	-1.46
41	Capulin Spring	-0.16	-1.15	-1.63	-2.24	-6.22	-0.06	-1.42
42	**Capulin Spring**	0.52	-1.71	-0.21	-2.11	-6.06	0.04	-1.29
44	**Capulin Spring**	0.51	-1.80	-0.21	-2.17	-6.17	0.05	-1.32
45	Capulin Spring	0.78	-1.74	0.30	-2.10	-5.96	-0.10	-1.37
54	Faulty Trail	0.13	-1.29	-0.52	-1.79	-7.12	-0.01	-1.28
55	**Faulty Trail**	-0.32	-1.08	-1.46	-1.54	-6.98	0.25	-1.10
56	**Faulty Trail**	0.79	-2.26	0.78	-1.67	-6.97	0.30	-1.06
57	**Faulty Trail**	-0.02	-1.44	-0.82	-1.63	-7.03	0.27	-1.10
53	**Ellis Spring Box**	-0.34	-1.60	-1.91	-2.38	-7.71	0.11	-1.28
64	LH at Ellis Box	0.19	-2.15	-0.88	-2.38	-7.95	-0.11	-1.50
65	LH at Ellis box	-0.48	-1.45	-2.20	-2.39	-7.74	-0.24	-1.63
66	LH at Ellis box	0.06	-1.94	-1.15	-2.37	-7.50	-0.05	-1.44
67	LH at Ellis Box	-0.16	-1.70	-1.60	-2.48	-7.68	-0.10	-1.49
68	LH at Ellis Box	1.06	-2.97	0.91	-2.42	-7.81	-0.02	-1.41
69	LH Camp Spr Box	0.10	-2.01	-1.07	-2.39	-7.62	-0.10	-1.50
70	LH Camp Spr Box	-0.02	-1.84	-1.25	-2.42	-7.73	-0.26	-1.62
71	LH Camp Spr Box	-0.43	-1.47	-2.08	-2.41	-7.79	-0.26	-1.64
72	LH Camp Spr Box	0.07	-1.94	-1.11	-2.38	-7.47	-0.07	-1.45
73	LH Camp Spr Box	-0.56	-1.32	-2.43	-2.50	-7.85	-0.09	-1.48
74	LH Camp Spr Box	0.29	-2.07	-0.64	-2.34	-6.88	-0.11	-1.50

Table 4. Saturation Indices

Unique ID		si_Calcite	si_CO2(g)	si_Dolomite	si_Gypsum	si_Halite	si_Quartz	si_SiO2(a)
60	LH at CDT	0.22	-2.07	-0.78	-2.42	-7.93	-0.11	-1.48
61	LH at CDT	0.68	-2.56	0.13	-2.40	-7.76	-0.30	-1.66
62	LH at CDT	0.91	-2.83	0.58	-2.39	-7.47	-0.10	-1.47
63	LH at CDT	0.37	-2.24	-0.55	-2.50	-7.78	-0.10	-1.49
75	LH Downstream #1	0.30	-2.13	-0.62	-2.44	-7.89	-0.12	-1.48
76	LH Downstream #2	-0.05	-1.85	-1.31	-2.44	-7.85	-0.07	-1.45
77	LH Downstream #3	0.81	-2.68	0.44	-2.45	-7.85	-0.09	-1.45
78	LH Downstream #4	0.41	-2.38	-0.33	-2.47	-7.81	-0.05	-1.42
79	LH Downstream #5	0.18	-2.07	-0.78	-2.39	-8.16	-0.01	-1.39
80	LH Downstream #6	0.64	-2.56	0.13	-2.41	-7.74	-0.07	-1.45
81	LH Downstream #7	0.59	-2.53	0.06	-2.43	-7.93	-0.03	-1.40
82	LH Downstream #8	0.82	-2.80	0.52	-2.44	-7.90	-0.06	-1.42
83	**LH Downstream**	0.53	-2.55	-0.01	-2.44	-7.85	0.00	-1.35
84	LH Picnic	0.78	-2.73	0.52	-2.43	-7.80	-0.20	-1.54

Table 5. Geochemical Modeling

Unique ID	Label	Name	Location	Map Lithology	Sample Date	si_Calcite	si_CO2(g)	pH	pCO2	logPCO2	Cc ppt mol/l	Cc ppt mmol/l	Cc ppt mg/L	C(4) (mol/l)	C(4) mmol/l	DIC mol/L	CaToT mpl/L	MgToT mol/L	SulfateToT mol/L	Ca-GypCorr	Ccarb mol/L	Cext mol/L	%Cext	Csoil at PCO2 10^-1.5 mol/L	Min Estimate of Endogenic	%Cext that is Endogenic
1	CSP	Camp Spring Box	Camp Spring Box	Colluvium and alluvium over Lower Madera	11/6/2021	-1.95	0.10	8.21	1.27E+00	0.10	1.86E-03	1.86	188	0.07862	78.615	7.86E-02	2.94E-03	1.30E-04	1.03E-04	2.84E-03	2.97E-03	7.56E-02	96.2	1.10E-03	7.45E-02	98.5
2	ESP	Ellis Spring Box	Ellis Spring Box	Colluvium and alluvium over Lower Madera	11/6/2021	-0.33	-1.49	8.21	3.25E-02	-1.49	1.91E-03	1.91	193	0.00672	6.7236	6.72E-03	3.02E-03	1.31E-04	1.04E-04	2.92E-03	3.05E-03	3.67E-03	54.6	1.10E-03	2.57E-03	70.1
5	CPS	Capulin Spring	Capulin Spring	Colluvium and alluvium over Lower Madera	11/11/2022	-0.35	-0.98	8.02	1.04E-01	-0.98	3.15E-03	3.15	318	0.01328	13.284	1.33E-02	6.56E-03	2.89E-04	2.83E-04	6.28E-03	6.57E-03	6.71E-03	50.5	1.10E-03	5.61E-03	83.6
17	CPS	Capulin Spring	Capulin Spring	Colluvium and alluvium over Lower Madera	5/11/2023	-1.68	0.25	8.08	1.77E+00	0.25	2.80E-03	2.80	282	0.10492	104.92	1.05E-01	5.07E-03	2.16E-04	1.54E-04	4.91E-03	5.13E-03	9.98E-02	95.1	1.10E-03	9.87E-02	98.9
26	EPS	Ellis Spring Box	Ellis Spring Box	Colluvium and alluvium over Lower Madera	11/6/2021	-0.33	-1.49	8.21	3.25E-02	-1.49	1.91E-03	1.91	193	0.00672	6.7236	6.72E-03	3.02E-03	1.31E-04	1.04E-04	2.92E-03	3.05E-03	3.67E-03	54.6	1.10E-03	2.57E-03	70.1
4	LHP	Las Huertas Picnic Area	Las Huertas Picnic Area	Colluvium and alluvium over Sandia granite	11/6/2021	-1.23	-0.64	8.30	2.31E-01	-0.64	1.81E-03	1.81	183	0.01789	17.886	1.79E-02	2.51E-03	1.63E-04	7.47E-05	2.43E-03	2.60E-03	1.53E-02	85.5	1.10E-03	1.42E-02	92.8
7	NHS	NE of House Spring	NE of House Spring	Sandia Formation	5/18/2022	0.77	-2.67	8.21	2.13E-03	-2.67	1.71E-03	1.71	172	0.00452	4.5191	4.52E-03	2.73E-03	1.45E-04	1.07E-04	2.63E-03	2.77E-03	1.75E-03	38.7	1.10E-03	6.49E-04	37.1
8	LPT	Loop Trail	Loop Trail	Colluvium and alluvium over Sandia granite	5/18/2022	0.52	-2.63	8.21	2.33E-03	-2.63	1.29E-03	1.29	130	0.00371	3.7072	3.71E-03	2.30E-03	1.53E-04	1.11E-04	2.19E-03	2.34E-03	1.37E-03	36.9	1.10E-03	2.70E-04	19.7
9	LHP	Las Huertas Picnic Area	Las Huertas Picnic Area	Colluvium and alluvium over Sandia granite	5/18/2022	0.05	-2.15	8.23	7.10E-03	-2.15	1.33E-03	1.33	134	0.0041	4.1025	4.10E-03	2.28E-03	1.57E-04	1.07E-04	2.17E-03	2.33E-03	1.77E-03	43.2	1.10E-03	6.72E-04	37.9
10	CNM	Canon Media at NM165	Canon Media at NM166	Madera Formation	5/18/2022	0.30	-2.74	8.22	1.82E-03	-2.74	8.02E-04	0.80	81	0.00268	2.6812	2.68E-03	1.69E-03	1.73E-04	1.10E-04	1.58E-03	1.75E-03	9.31E-04	34.7	1.10E-03	0.00E+00	0.0
21	LPT	Loop Trail	Loop Trail	Colluvium and alluvium over Sandia granite	11/11/2022	-0.41	-1.75	8.24	1.78E-02	-1.75	1.34E-03	1.34	136	0.00502	5.0234	5.02E-03	2.40E-03	1.58E-04	1.87E-04	2.21E-03	2.37E-03	2.65E-03	52.8	1.10E-03	1.55E-03	58.5
20	CLH	Confluence at LHP	Confluence at LHP	Colluvium and alluvium over Sandia granite	11/11/2022	-0.87	-1.15	8.27	7.10E-02	-1.15	1.59E-03	1.59	160	0.00881	8.8103	8.81E-03	2.49E-03	1.74E-04	1.68E-04	2.32E-03	2.49E-03	6.32E-03	71.7	1.10E-03	5.22E-03	82.6
22	LHP	Las Huertas Picnic Area	Las Huertas Picnic Area	Colluvium and alluvium over Sandia granite	11/11/2022	-1.29	-0.80	8.24	1.57E-01	-0.80	1.46E-03	1.46	147	0.01401	14.01	1.40E-02	2.49E-03	1.65E-04	1.88E-04	2.30E-03	2.47E-03	1.15E-02	82.4	1.10E-03	1.04E-02	90.5
23	CNM	Canon Media at NM165	Canon Media at NM166	Madera Formation	11/11/2022	0.64	-2.90	8.27	1.27E-03	-2.90	1.29E-03	1.29	130	0.00395	3.9495	3.95E-03	2.26E-03	1.74E-04	1.70E-04	2.09E-03	2.26E-03	1.69E-03	42.7	1.10E-03	5.86E-04	34.8
24	NDD	N of Ditch Diversion	N of Ditch Diversion	Madera Formation	11/11/2022	-0.0343	-2.2991	8.26	5.02E-03	-2.30	1.16E-03	1.16	117	0.004	3.9968	4.00E-03	2.26E-03	1.94E-04	1.74E-04	2.09E-03	2.28E-03	1.72E-03	42.9	1.10E-03	6.17E-04	35.9
27	NHS	NE of House Spring	NE of House Spring	Sandia Formation	5/11/2023	0.3883	-2.5639	8.35	2.73E-03	-2.56	1.24E-03	1.24	125	0.00402	4.0246	4.03E-03	1.78E-03	1.21E-04	9.33E-05	1.69E-03	1.81E-03	2.22E-03	55.1	1.10E-03	1.12E-03	50.4
28	LPT	Loop Trail	Loop Trail	Colluvium and alluvium over Sandia granite	5/11/2023	0.2052	-2.4084	8.34	3.90E-03	-2.41	1.17E-03	1.17	118	0.00389	3.8883	3.89E-03	1.73E-03	1.23E-04	9.79E-05	1.63E-03	1.75E-03	2.14E-03	55.0	1.10E-03	1.04E-03	48.6
30	LHP	Las Huertas Picnic Area	Las Huertas Picnic Area	Colluvium and alluvium over Sandia granite	5/11/2023	-0.6315	-1.5574	8.35	2.77E-02	-1.56	1.21E-03	1.21	122	0.00537	5.3684	5.37E-03	1.76E-03	1.29E-04	9.11E-05	1.67E-03	1.79E-03	3.57E-03	66.6	1.10E-03	2.47E-03	69.2
31	CNM	Canon Media at NM165	Canon Media at NM166	Madera Formation	5/11/2023	0.2332	-2.5043	8.33	3.13E-03	-2.50	1.07E-03	1.07	108	0.00363	3.6258	3.63E-03	1.65E-03	1.19E-04	9.50E-05	1.55E-03	1.67E-03	1.96E-03	53.9	1.10E-03	8.55E-04	43.7
32	LHD	LH Downstream	LH Downstream	Madera Formation	5/11/2023	-0.6176	-1.7625	8.30	1.73E-02	-1.76	8.97E-04	0.90	90	0.00391	3.9055	3.91E-03	1.54E-03	1.27E-04	9.97E-05	1.44E-03	1.56E-03	2.34E-03	59.9	1.10E-03	1.24E-03	53.0

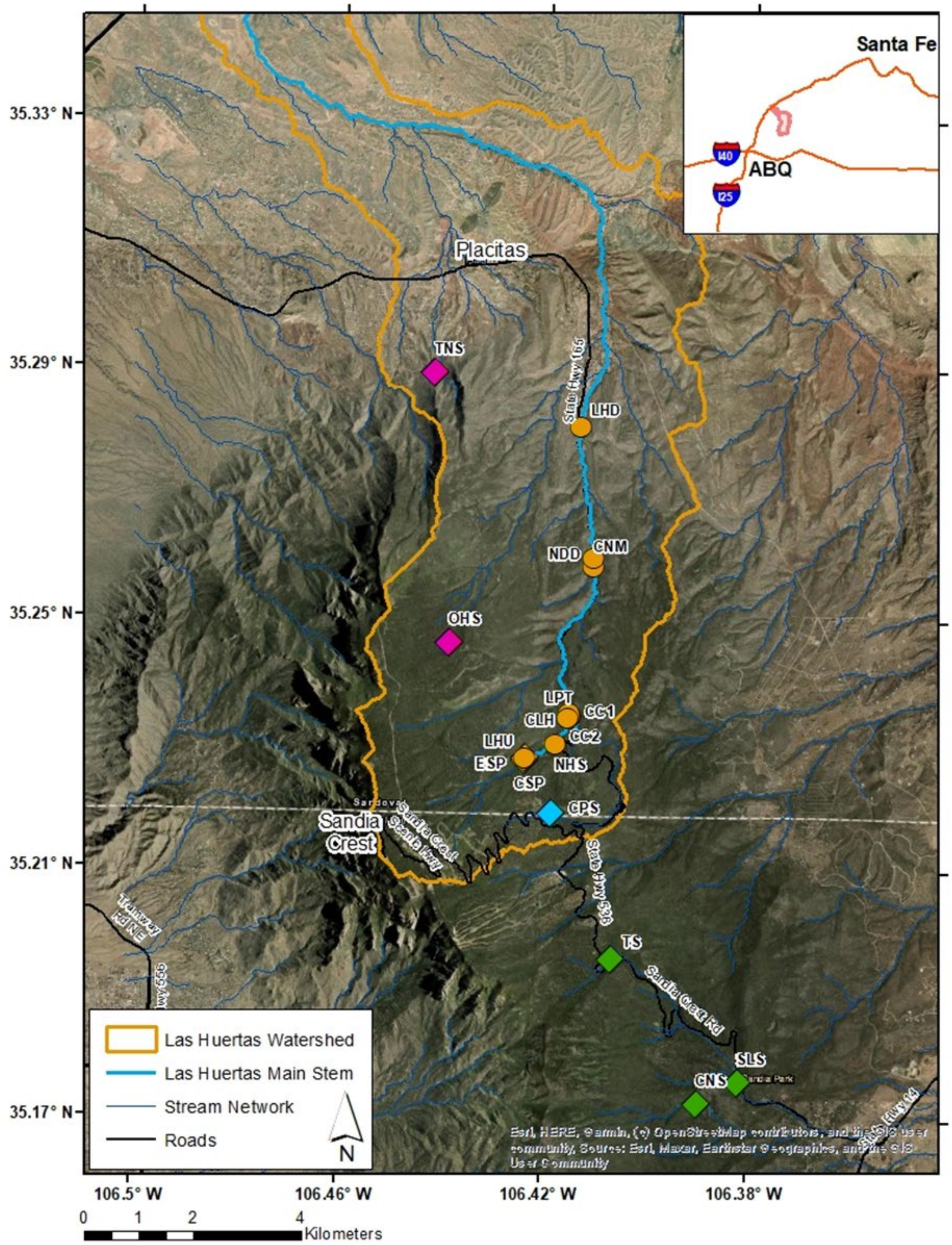

Figure 1 - Satellite imagery, including the general Sandia Mountain range, the Las Huertas watershed (orange outline), drainage flow lines, and sample locations from this study and previous studies. The watershed of interest is in the northern portion of the Sandia Mountains and into Placitas.

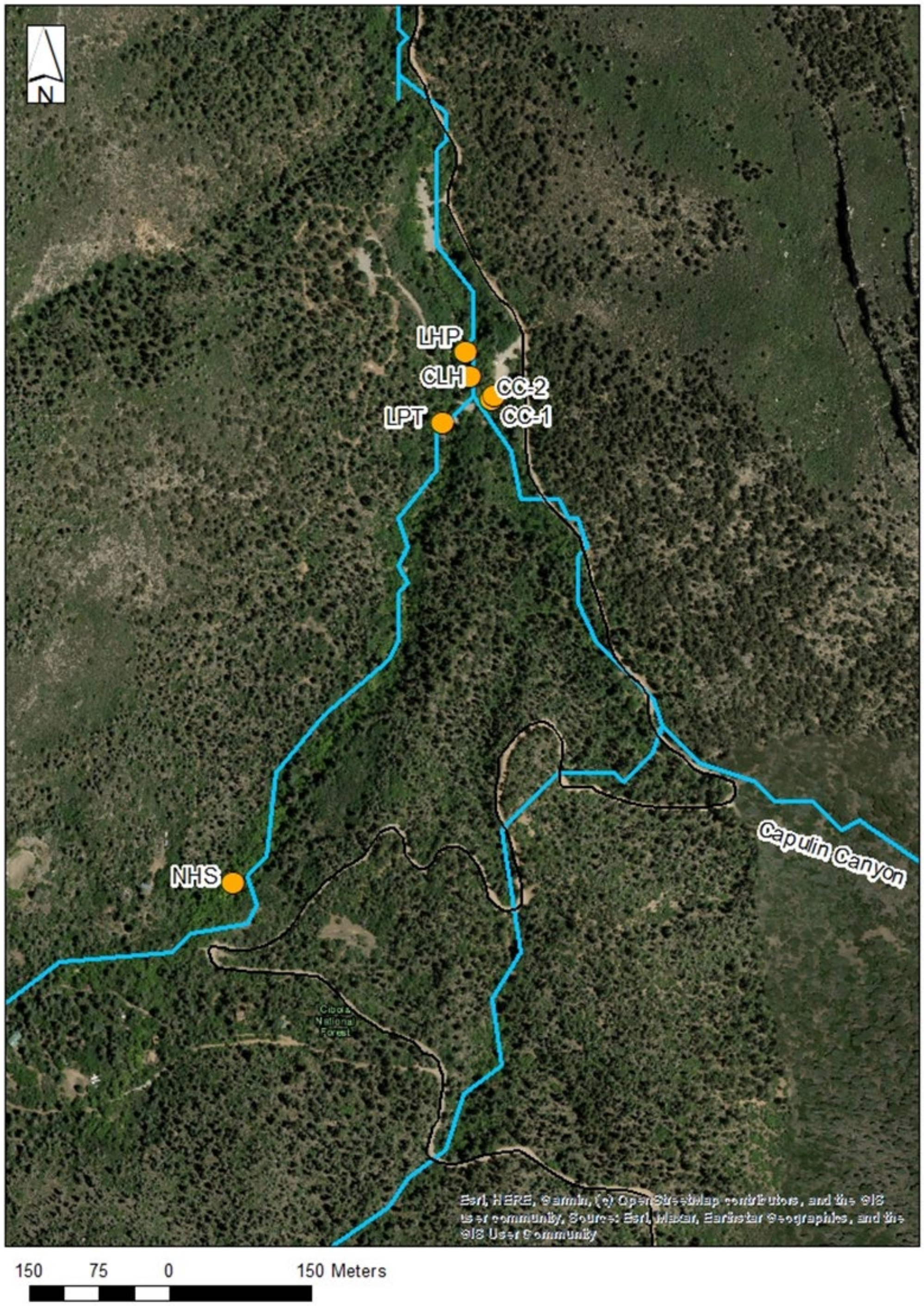

Figure 2 - ESRI image showing a detailed view of the sampling cluster near Las Huertas Picnic Area.

Figure 3 - Travertine step dams and pools observed in the Las Huertas stream channel. Photography by Dr. Laura J. Crossey.

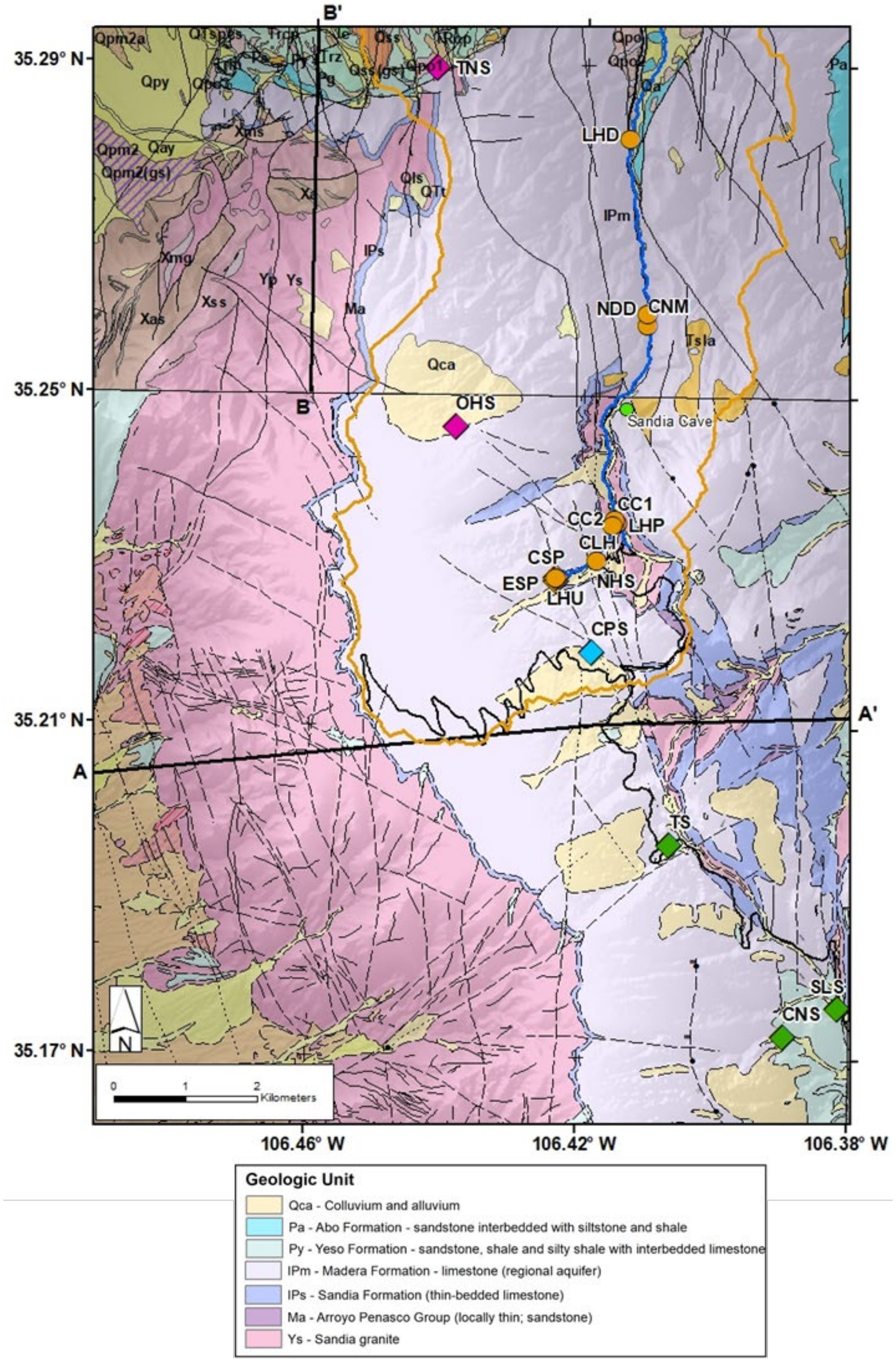

Figure 4 - Geologic map of the study region over digital elevation model (DEM). The Madera limestone operates as the primary regional aquifer, greatly influencing the water chemistry of spring and stream waters in the Las Huertas watershed. Las Huertas sample locations for this study are depicted in orange diamonds, circles, and blue squares. Site map adapted from Connell et al., 2000 (Cross section A-A') and Read et al., 2000 (Cross section B-B').

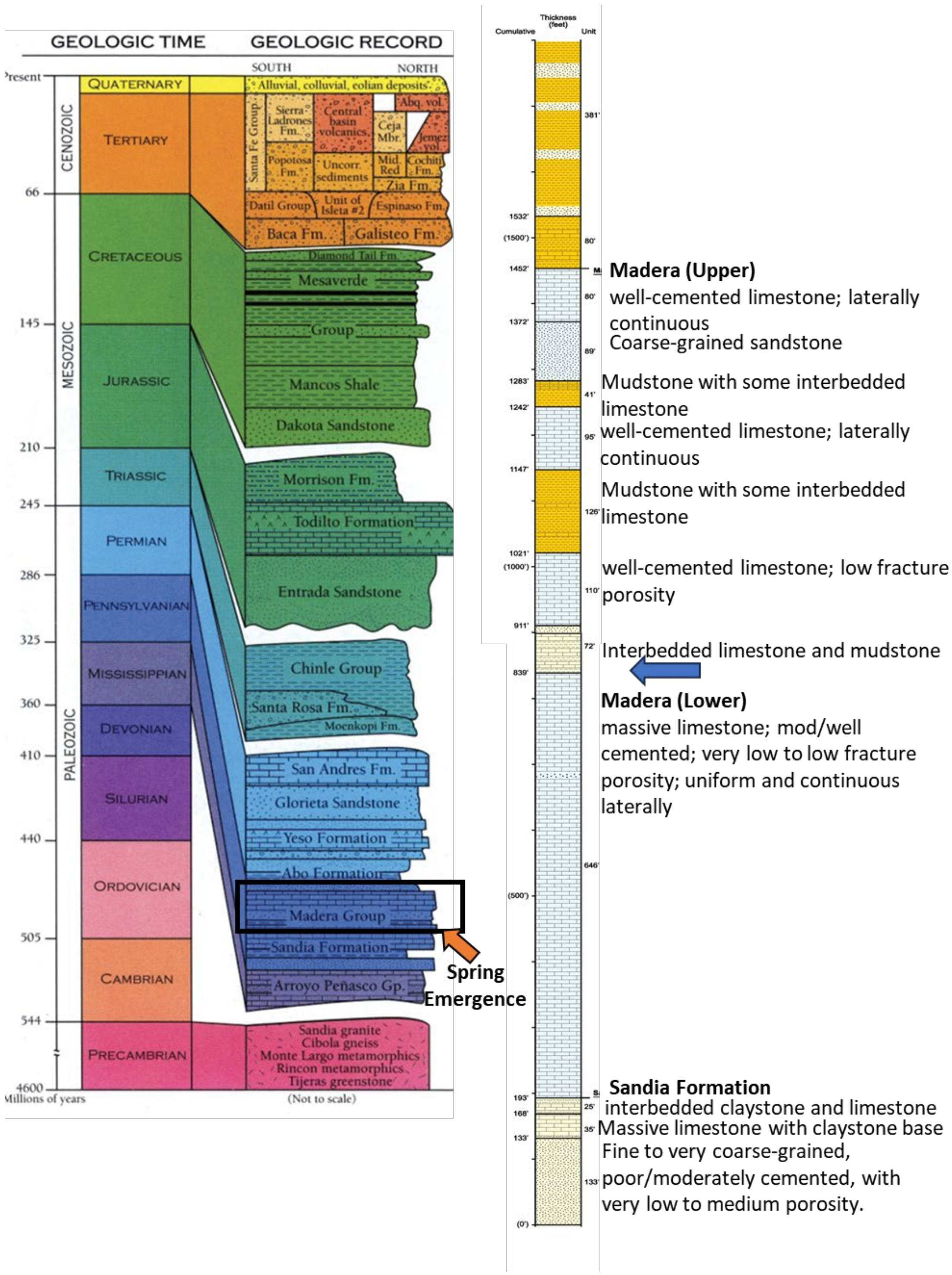

Figure 5 - (Left) Generalized stratigraphy of the Sandia Mountains. The regional aquifer is highlighted in black (Bauer et al., 2003). Capulin Spring and Las Huertas springs emerge from the Madera group (orange arrow). (Right) Detailed lithology and thickness of the Madera Group from Johnson and Campbell, 2002). Blue Arrow indicates the level of erosion at the Sandia Crest.

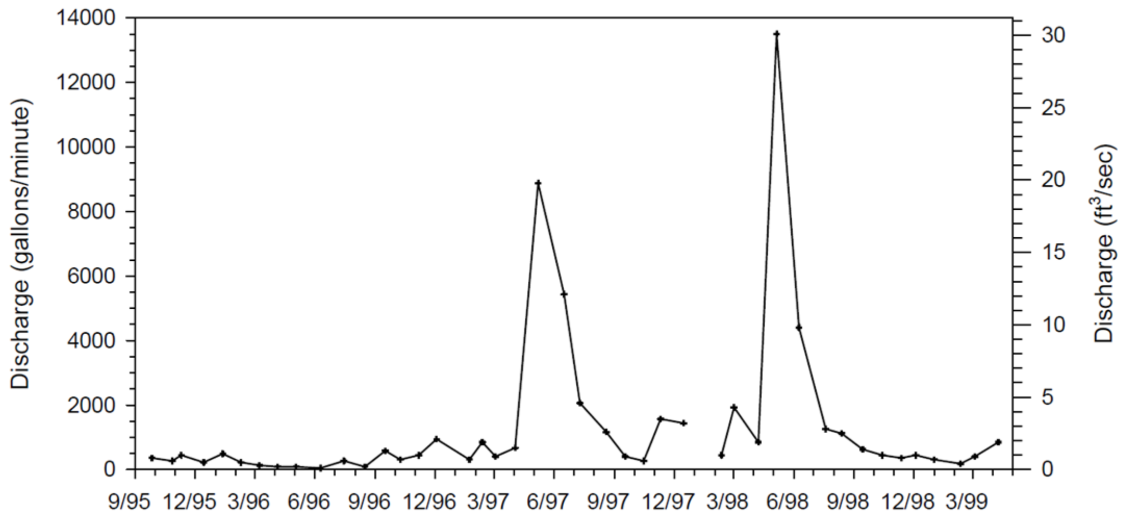

Figure 6 - Stream hydrograph from Johnson and Campbell’s 2002 study near Sandia Cave. Peak discharge was recorded in mid to late summer 1997 and 1998 (during the summer monsoonal season). Las Huertas stream receives bimodal precipitation, including summer monsoonal precipitation.

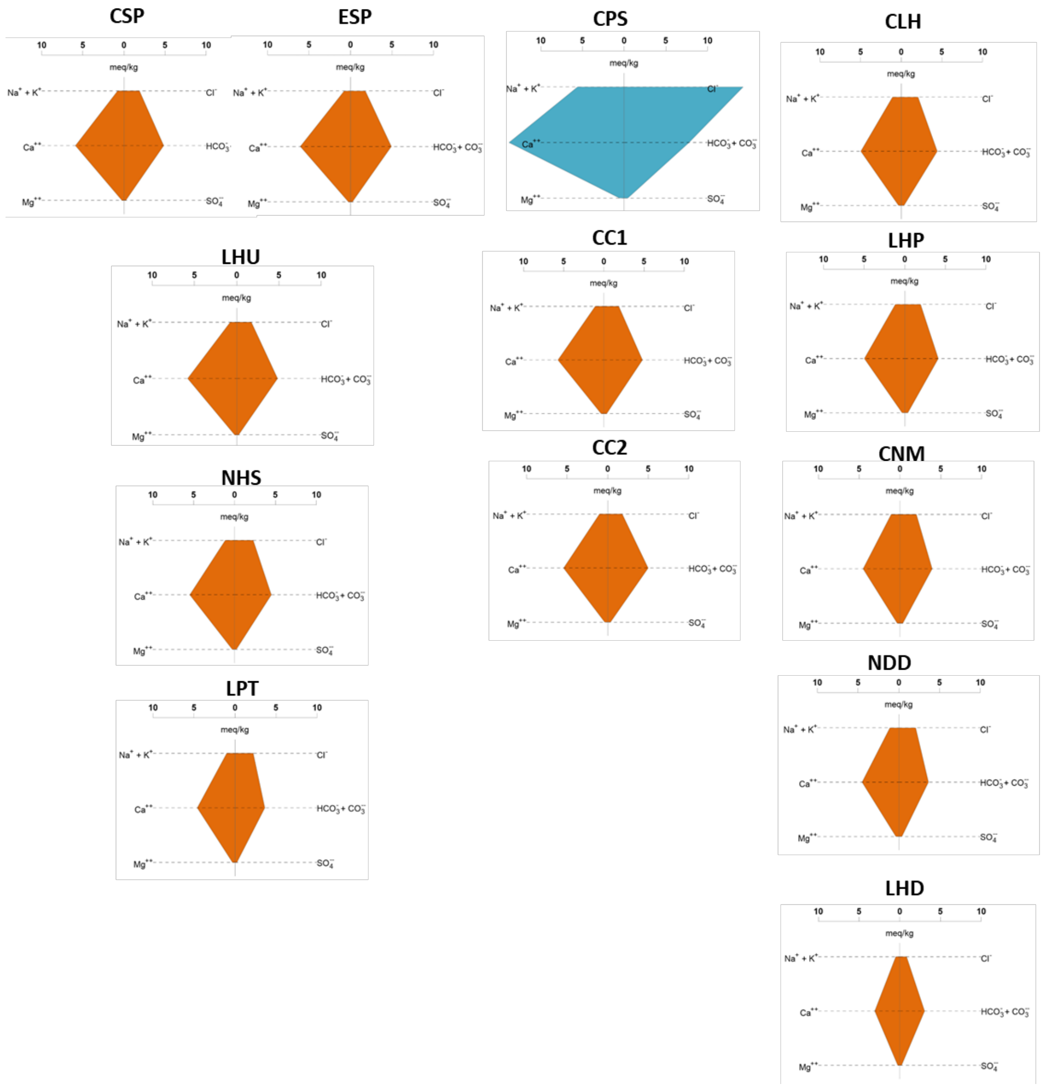

Figure 7 - Stiff diagrams portray the geometry of waters from Las Huertas spring (CSP and ESP) and Capulin Spring (blue) and downstream Las Huertas stream samples (orange). Las Huertas spring and stream waters have significantly lower TDS than Capulin Spring.

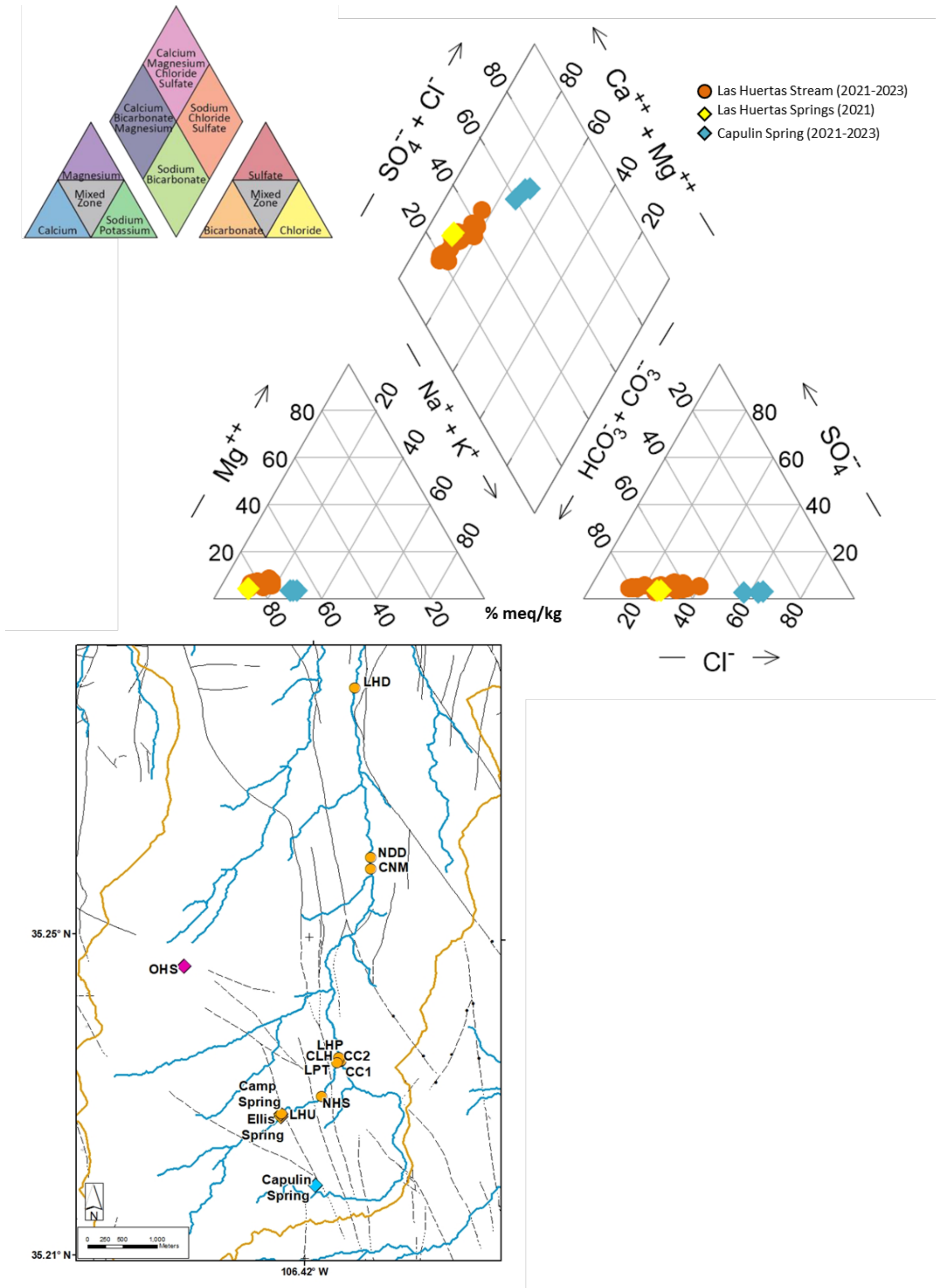

Figure 8 - (Center) Piper diagram showing major ion concentrations of waters from the Las Huertas watershed. Piper diagram shows waters are calcium bicarbonate dominated. Capulin Spring (blue boxes) has higher Cl and SO4 than Las Huertas spring and stream waters. The upper parallelogram indicates the Las Huertas spring and stream waters are within the Ca_Mg_HCO3 hydrochemical facies; Capulin Spring waters lie within the Ca_Mg_Cl_SO4 hydrochemical facies. (Upper Left) Piper diagram key from Frus, 2016. (Bottom Right) Simplified site map with sample points, faults and watershed boundaries for reference.

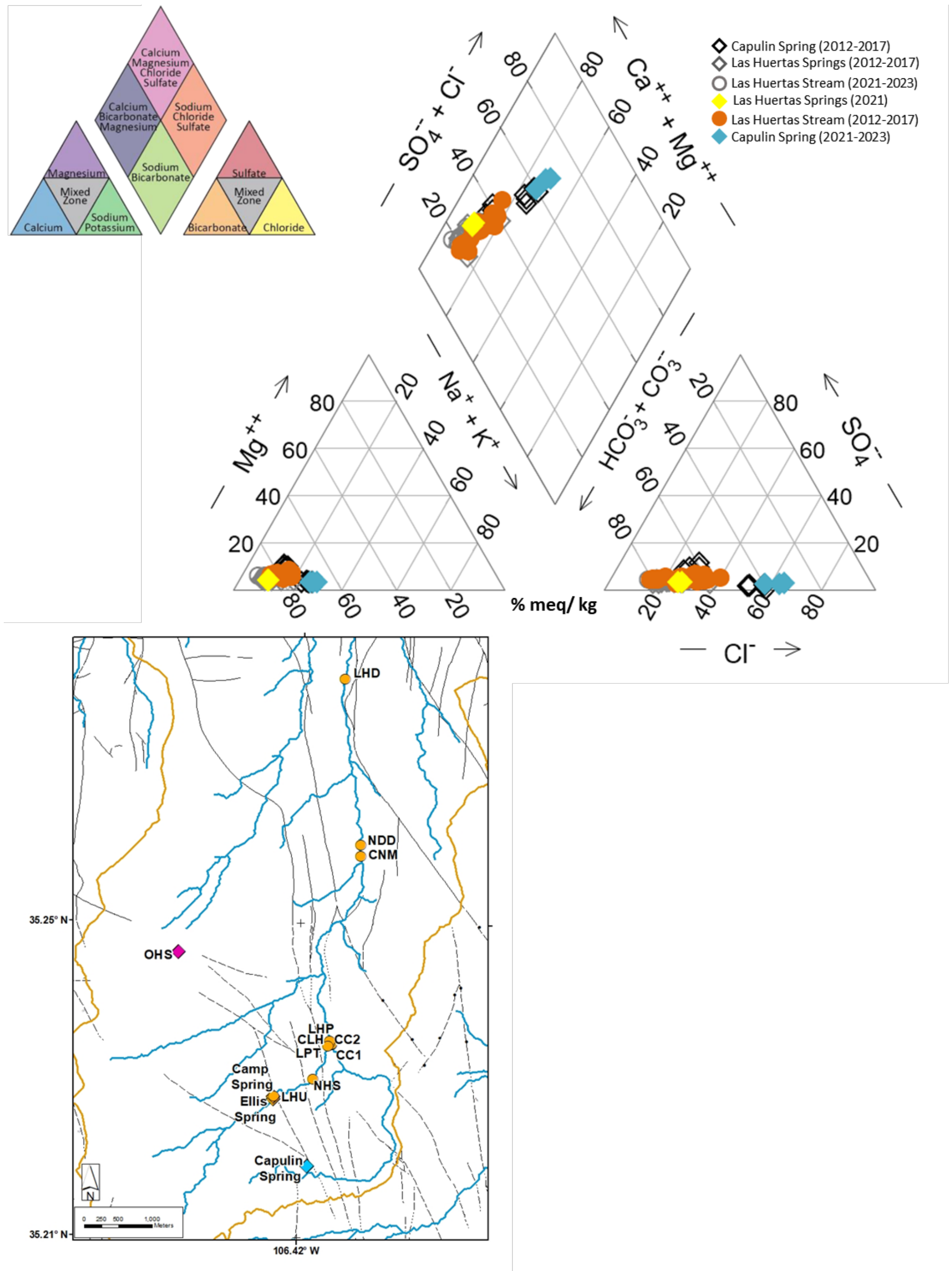

Figure 9 - Piper diagram showing hydrochemical facies of spring and stream waters from the Las Huertas watershed from this study (2021-2023) and previous studies (2012-2017) for comparison. Las Huertas spring and stream waters from this study and previous studies plot within the Ca_Mg_HCO3 hydrochemical facies. Capulin Spring waters collected for this study and previous studies plot within the Ca_Mg_HCO3 and the Ca_Mg_Cl_SO4 hydrochemical facies. (Right) Piper diagram key from Frus, 2016. (Bottom) Simplified site map with sample points and watershed boundaries for reference.

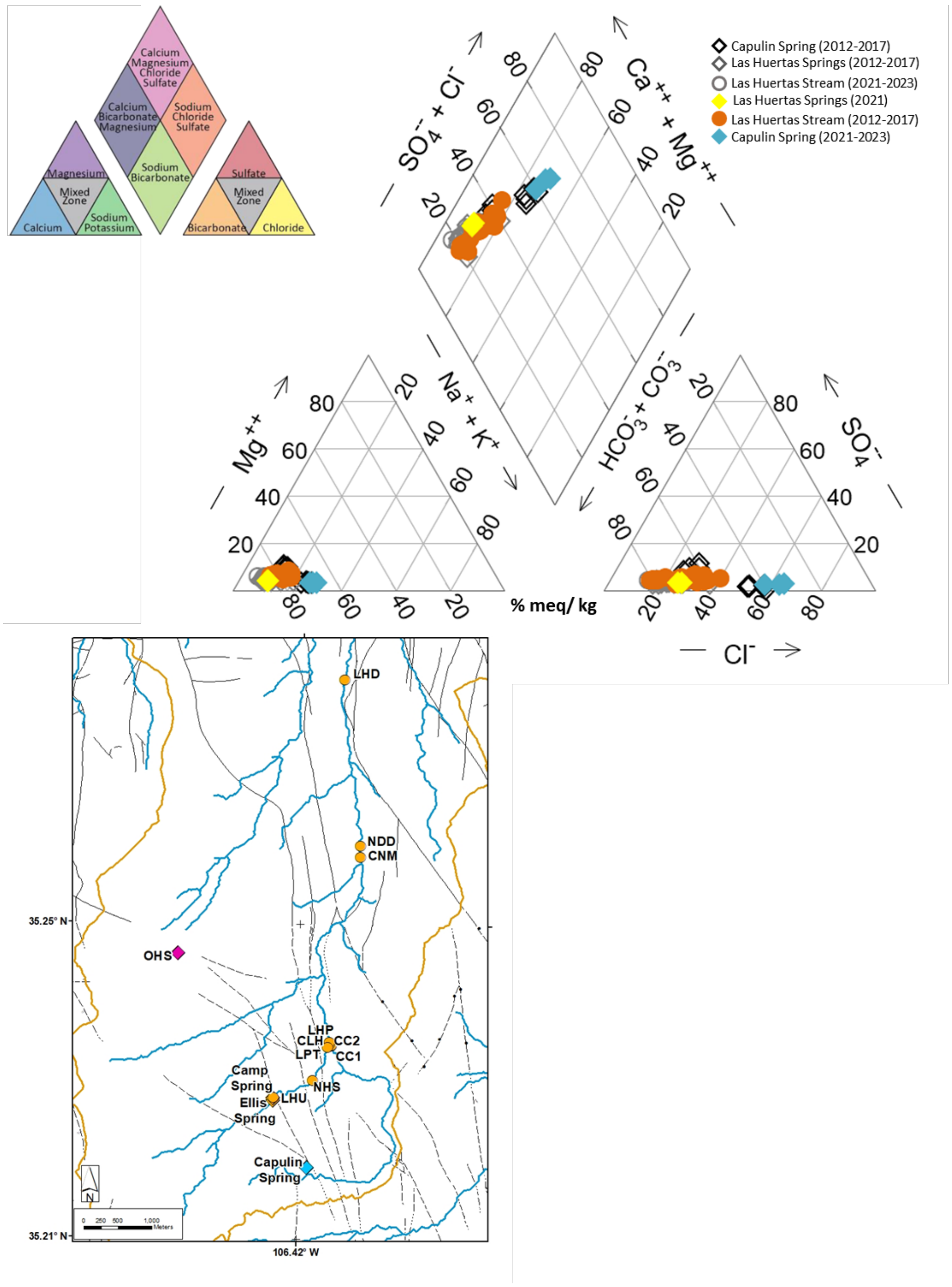

Figure 10 - Piper diagram including waters collected from the Las Huertas watershed from previous studies, this study, and Sandia Mountain Springs from previous studies and this study (Frus, 2016; DeLay et al., 2022). The upper parallelogram shows the Sandia Mountain springs plot primarily within the Ca_Mg_HCO3 hydrochemical facies, like Las Huertas springs, and into the sodium bicarbonate hydrochemical facies.

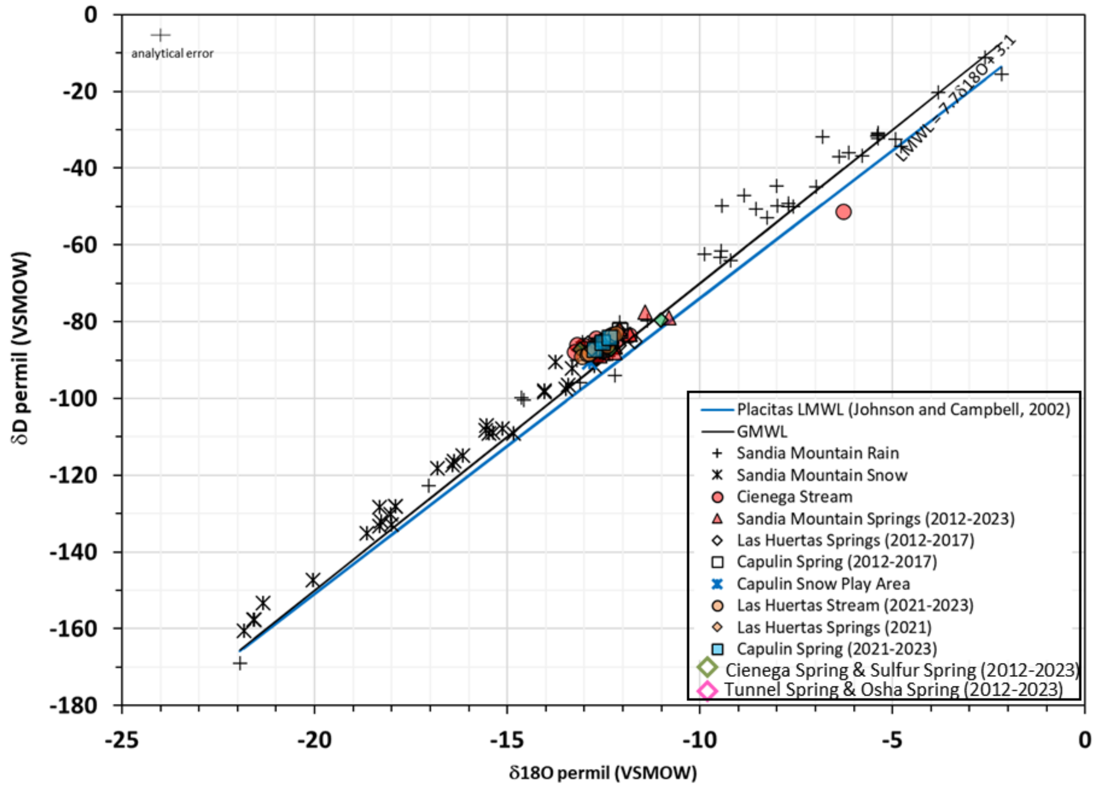

Figure 11 - Stable isotope values of dD and d18O for Las Huertas watershed waters from this study and previous studies and the surrounding Sandia Mountain Springs plotted relative to the Global Meteoric Water Line (GMWL)m showing the linear relation with a slope of 8 of global surface waters (Craig, 1961; Frus, 2016; DeLay et al., 2021). The blue line depicts the Placitas Local MWL (LMWL) plotted with a slope of 7.7 (Johnson and Campbell, 2002). Snow is generally lighter, while rain is heavier. Isotopologues from the Sandia Mountain and Las Huertas watershed waters generally cluster within the middle of the precipitation range.

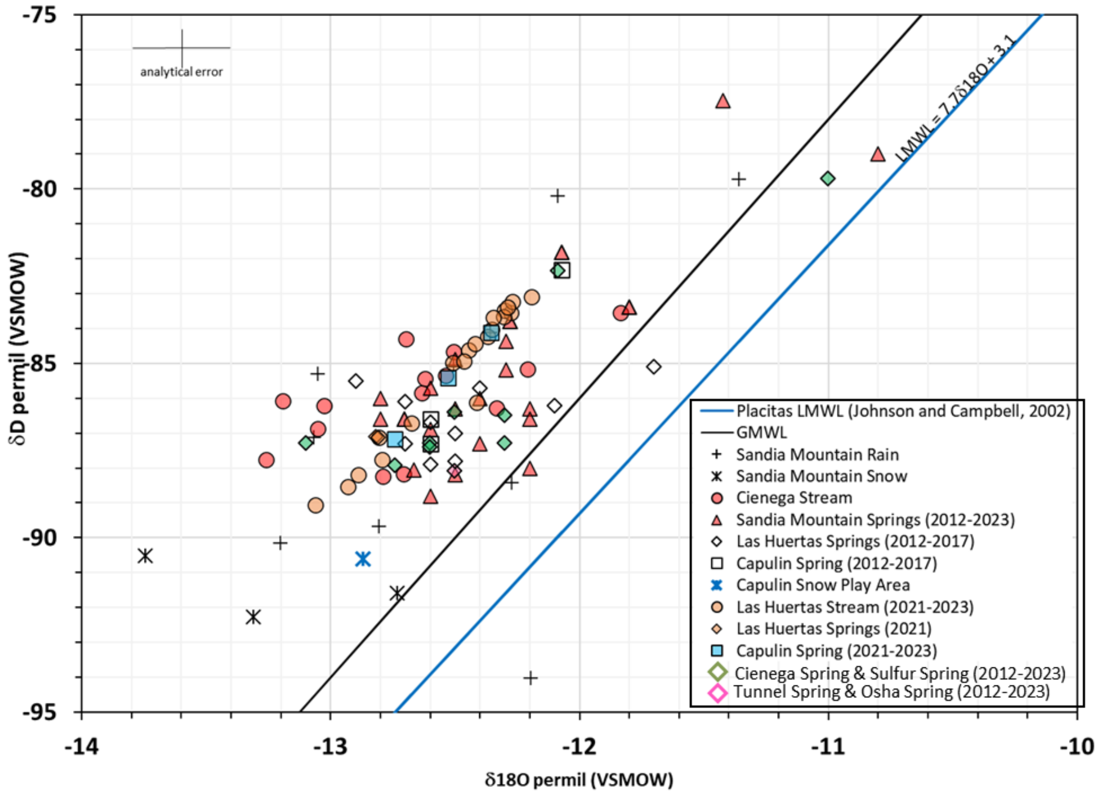

Figure 12 - Plot showing a detailed view of water isotopologues from the Las Huertas watershed and the surrounding Sandia Mountains. Stream samples from the upper reaches of Las Huertas are generally lighter than downstream samples, which are progressively heavier downstream. Waters collected between Fall 2021 and Spring 2022 and generally lighter than waters collected during Fall 2022 and Spring 2023.

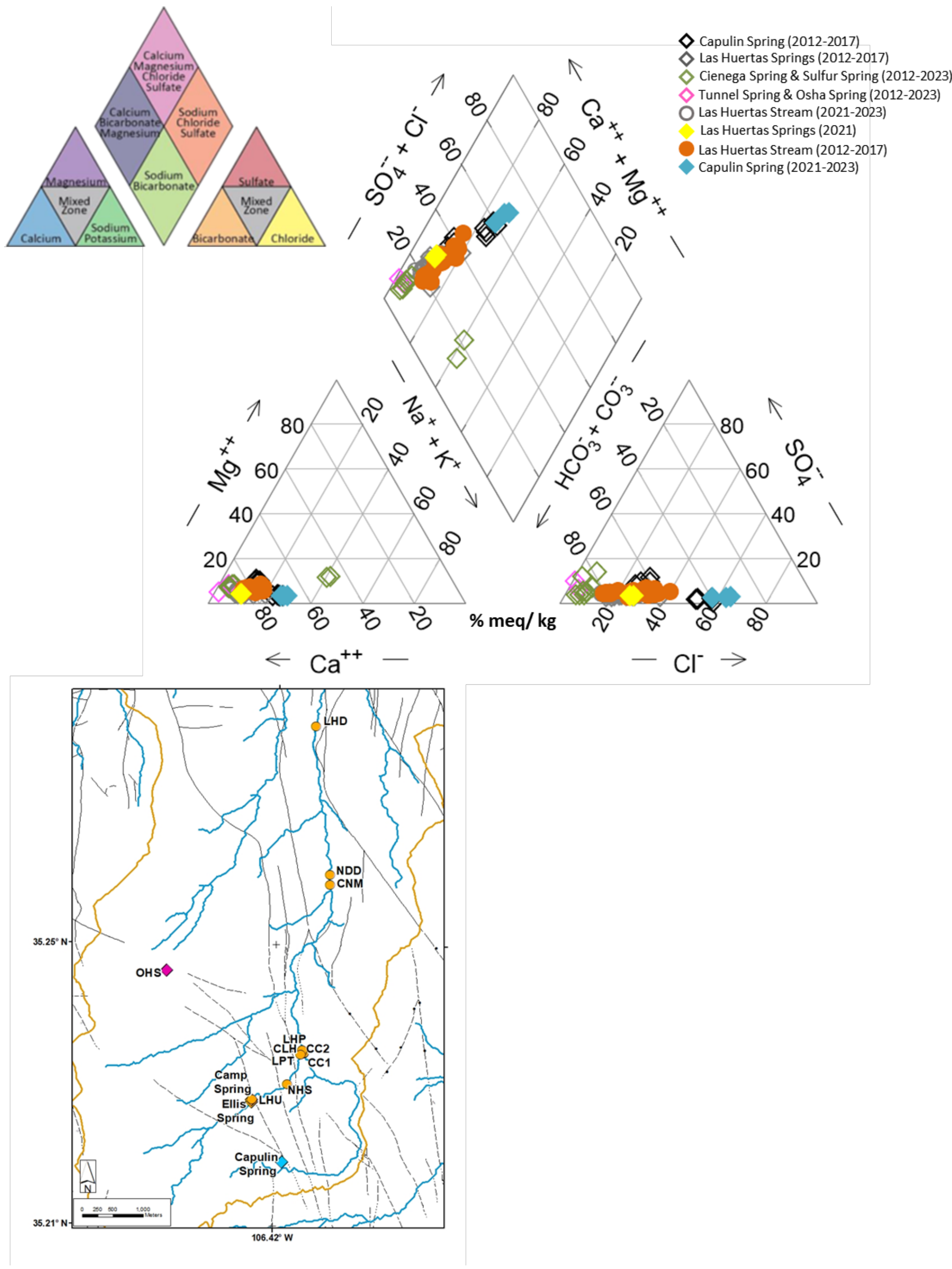

Figure 13 - Piper diagram depicting hydrochemical facies of waters collected within the Las Huertas watershed and select springs from the surrounding Sandia Mountains. Las Huertas springs, Cienega Spring, and Tunnel Spring plot similarly within the Ca_Mg_HCO3 hydrochemical facies, suggesting recharge waters for these waters are interacting with the regional limestone aquifer. Capulin Spring waters plot distinctly different from the latter, with higher Cl and SO4, suggesting these waters have an alternative flow path to the surrounding springs, likely with longer residence time and interacting with a sulfate-rich lithology such as the Sandia formation sandstone.

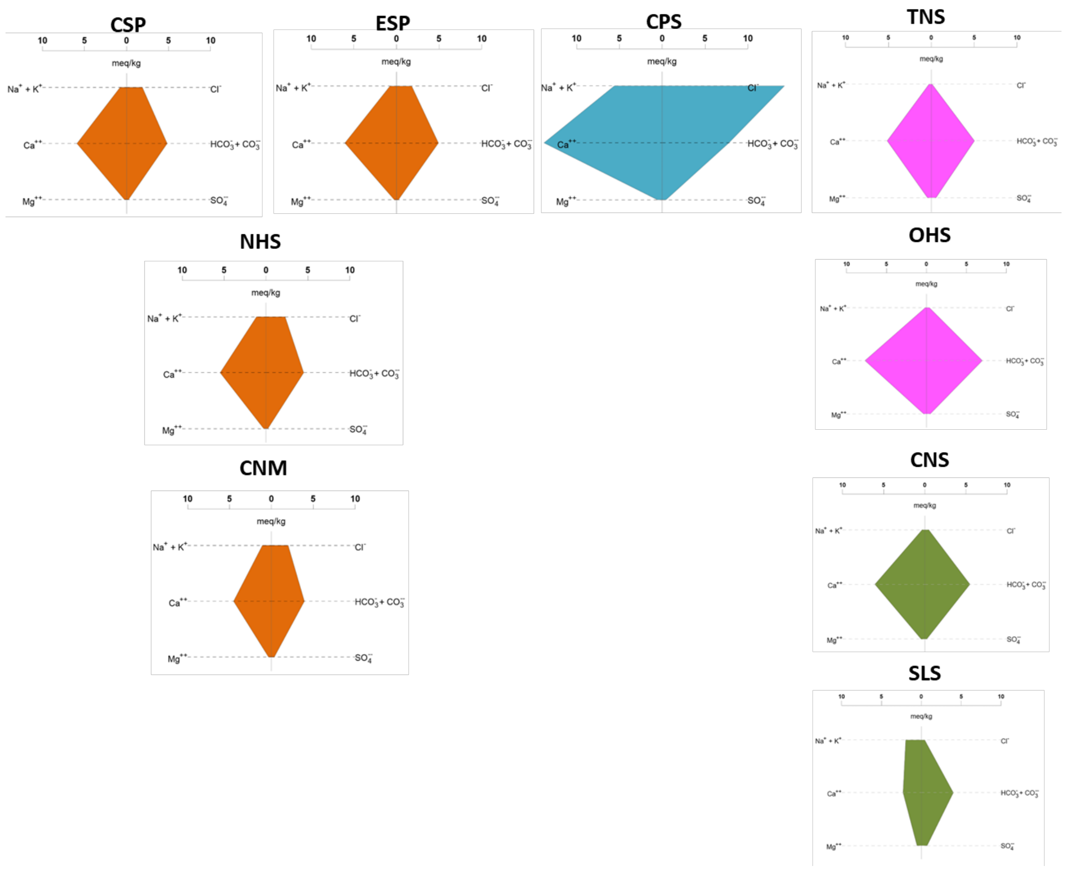

Figure 14 - Stiff diagrams showing Las Huertas Springs (orange; CSP and ESP) and downstream samples (orange; NHS and CNM) from above and below the Las Huertas confluence with Capulin Canyon waters, respectively. Capulin Spring (blue) Stiff geometry significantly differs from the other springs modeled for this study. This is inferred to be due to different flow paths of recharge waters between Las Huertas springs, Capulin Spring, and springs from the surrounding Sandia Mountains (pink and green; Tunnel Spring (TNS), Osha Springs (OHS), Cienega Spring (CNS), and Sulphur Spring (SLS)); likely also due to recharge waters for Capulin Spring having longer residence time and flowing through differing lithology from Las Huertas springs.

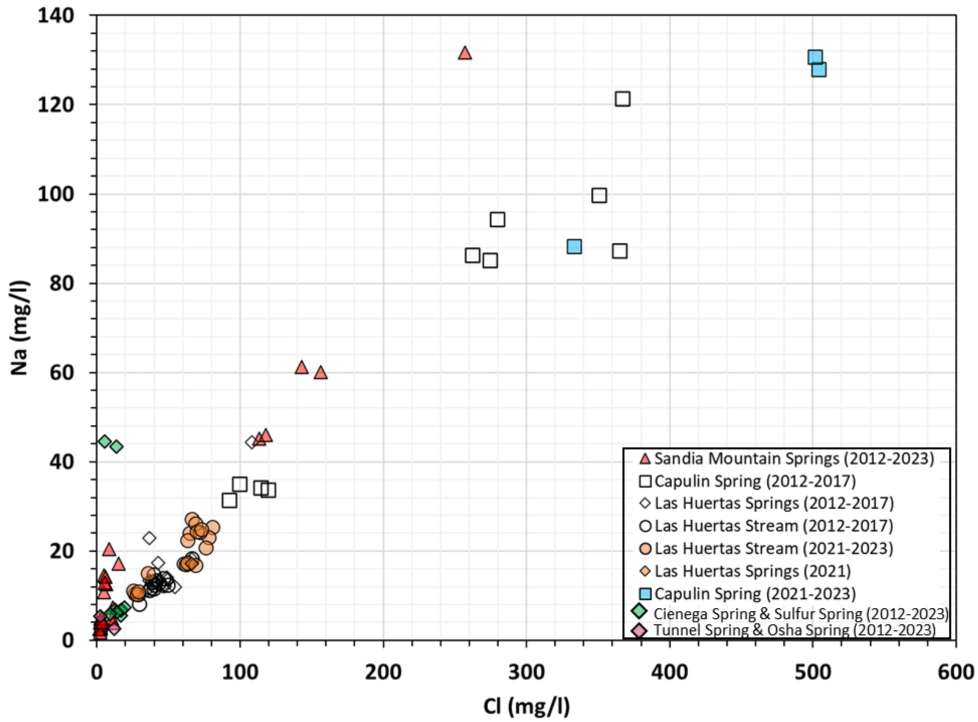

Figure 15 - NaCl cross plot for Las Huertas watershed waters collected from this study, previous studies, and Sandia Mountain Springs. Select Sandia Mountain springs (Osha, Sulfur, Tunnel, and Cienega) are painted pink and green squares. Capulin Spring (light blue boxes) has significantly higher NaCl than the remaining waters. Capulin Spring waters plot on a chloride-rich trend with increasing carbonate dissolution; however, NaCl values for Capulin Spring from this study are within the range of Capulin Spring waters from previous studies. The increasing chloride-rich trend has been inferred to represent water-rock interactions with calcium carbonate as groundwater flows through the Madera limestone (Frus, 2016; De Lay et al., 2022)

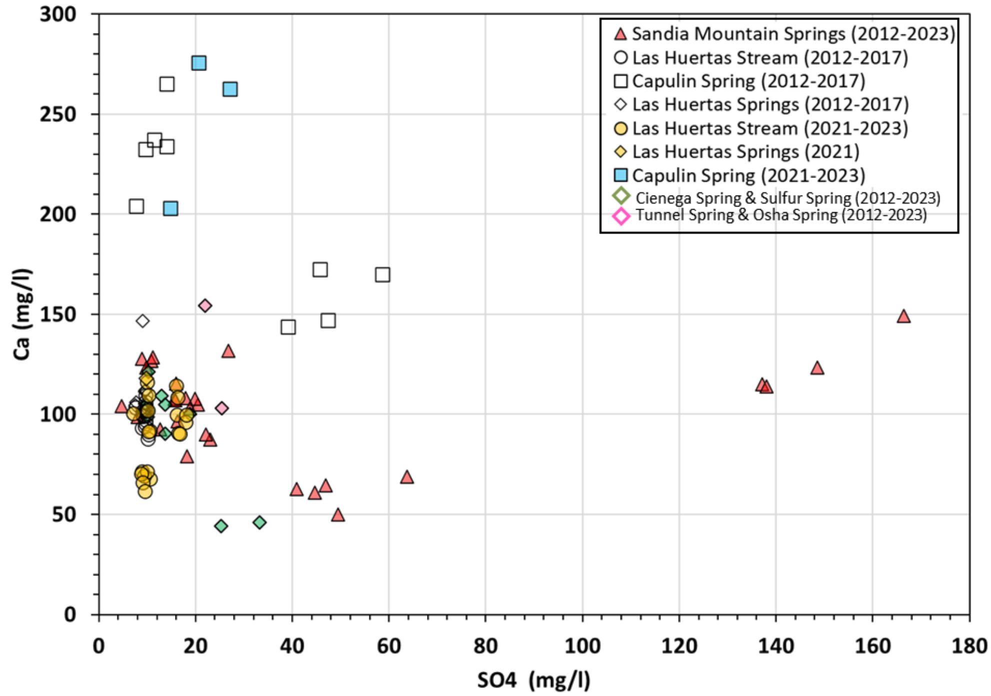

Figure 16 - All Las Huertas Springs and Streams and Capulin Spring samples have higher calcium concentrations than sulfate. An enrichment of sulfate of the Las Huertas Spring and Capulin Spring waters is not evident. Capulin Spring waters between 2012 and 2023 have the highest calcium concentrations from the Las Huertas watershed.

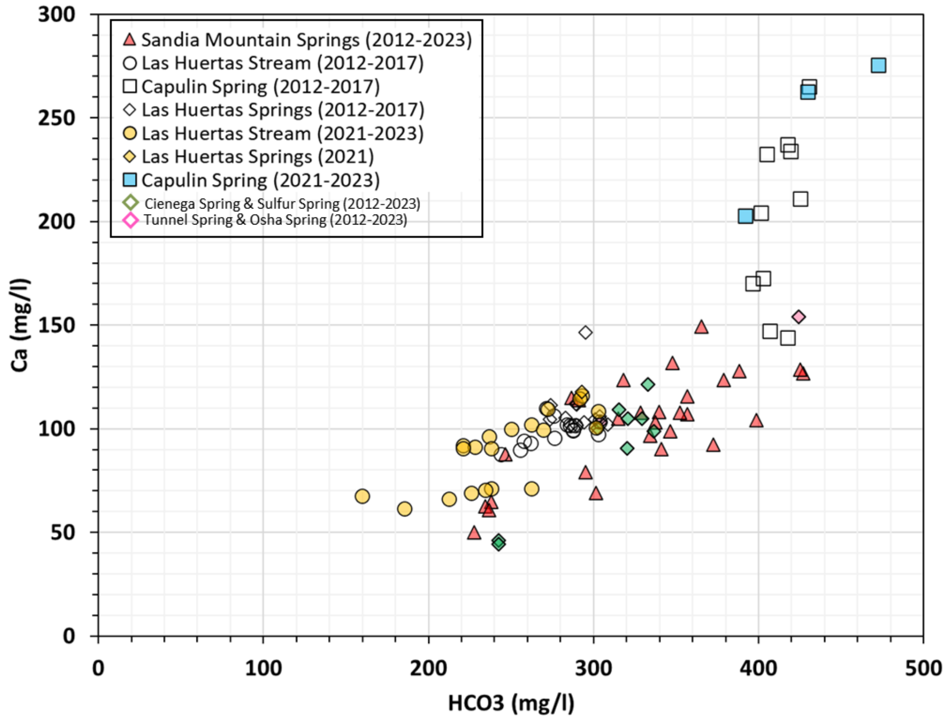

Figure 17 - Calcium concentrations and alkalinity (HCO_3^-) for Huertas Springs and Stream, Capulin Spring, and Sandia Mountain Spring samples between 2012 and 2023. Spring samples from Las Huertas, Capulin, and Sandia Mountains show enrichment of bicarbonate in these waters. Capulin Spring has some of the highest calcium bicarbonate concentrations.

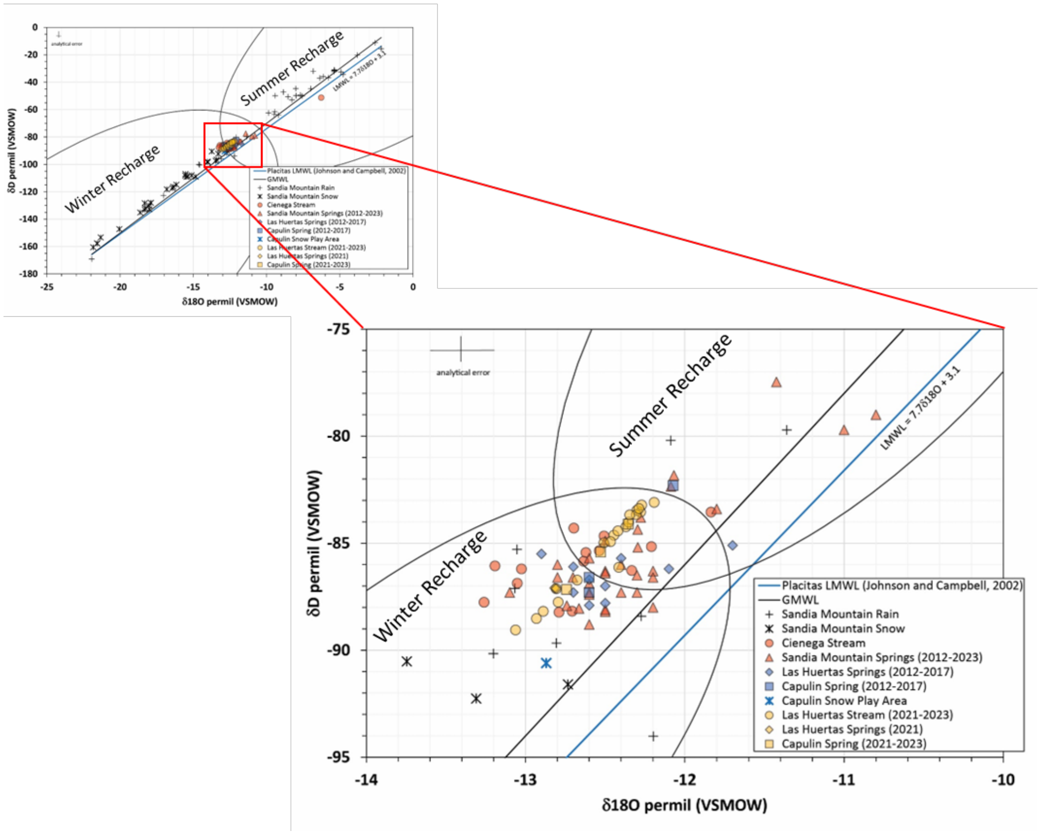

Figure 18 - XY plot of stable isotopes (dD and d18O) of waters from the Las Huertas watershed and Sandia Mountains, as well as local precipitation events, plotted relative to the GMWL and Placitas LMWL (Craig, 1961; Johnson and Campbell 2002; Frus, 2016; DeLay et al., 2021). Combining the seasonal variability of Las Huertas and Sandia Mountain waters with precipitation seasonality creates a picture of hydrologic recharge that takes shape with winter and summer recharge zones somewhat overlapping (seasonal zones are modified from Frus, 2016 and Sharp, 2017).

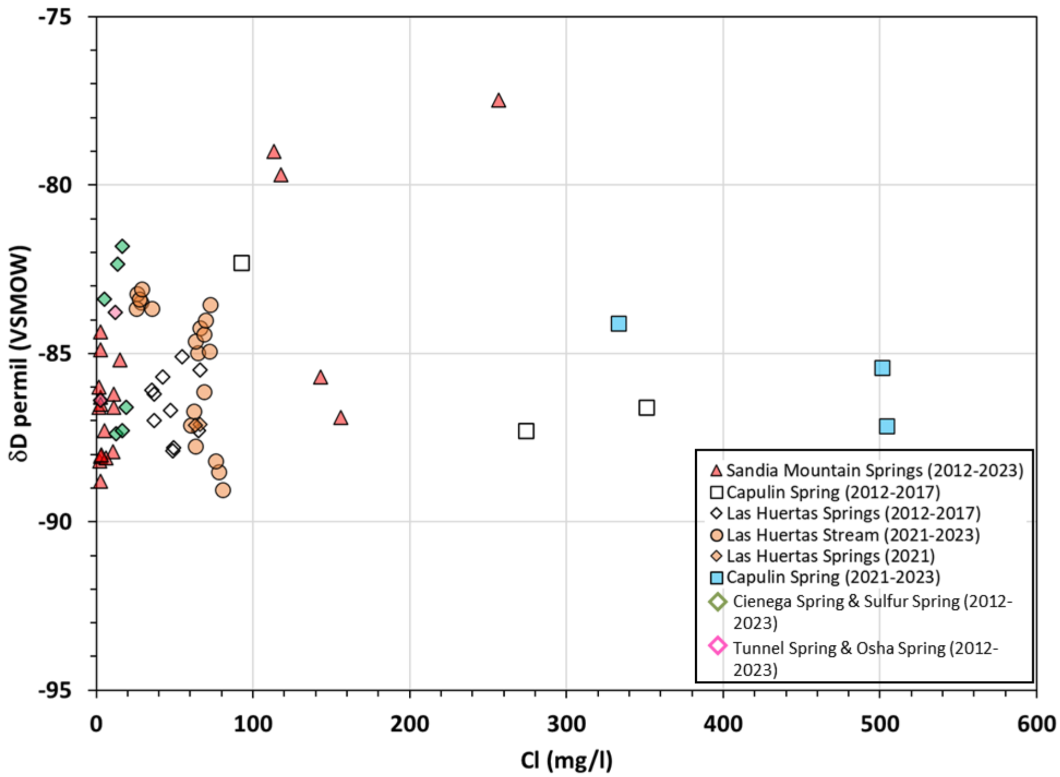

Figure 19 - Cross plot showing dD values and Cl- concentration of waters in the Sandia Mountains, including the Las Huertas watershed waters, inferred to be meteoric waters interacting with the regional aquifer. Stable isotopes allow us to determine if these waters have been subjected to alteration from geothermal processes or evaporation. An increase in heavier dD values would reflect evaporation effects. Variations in dD and Cl- are not due to evaporation.

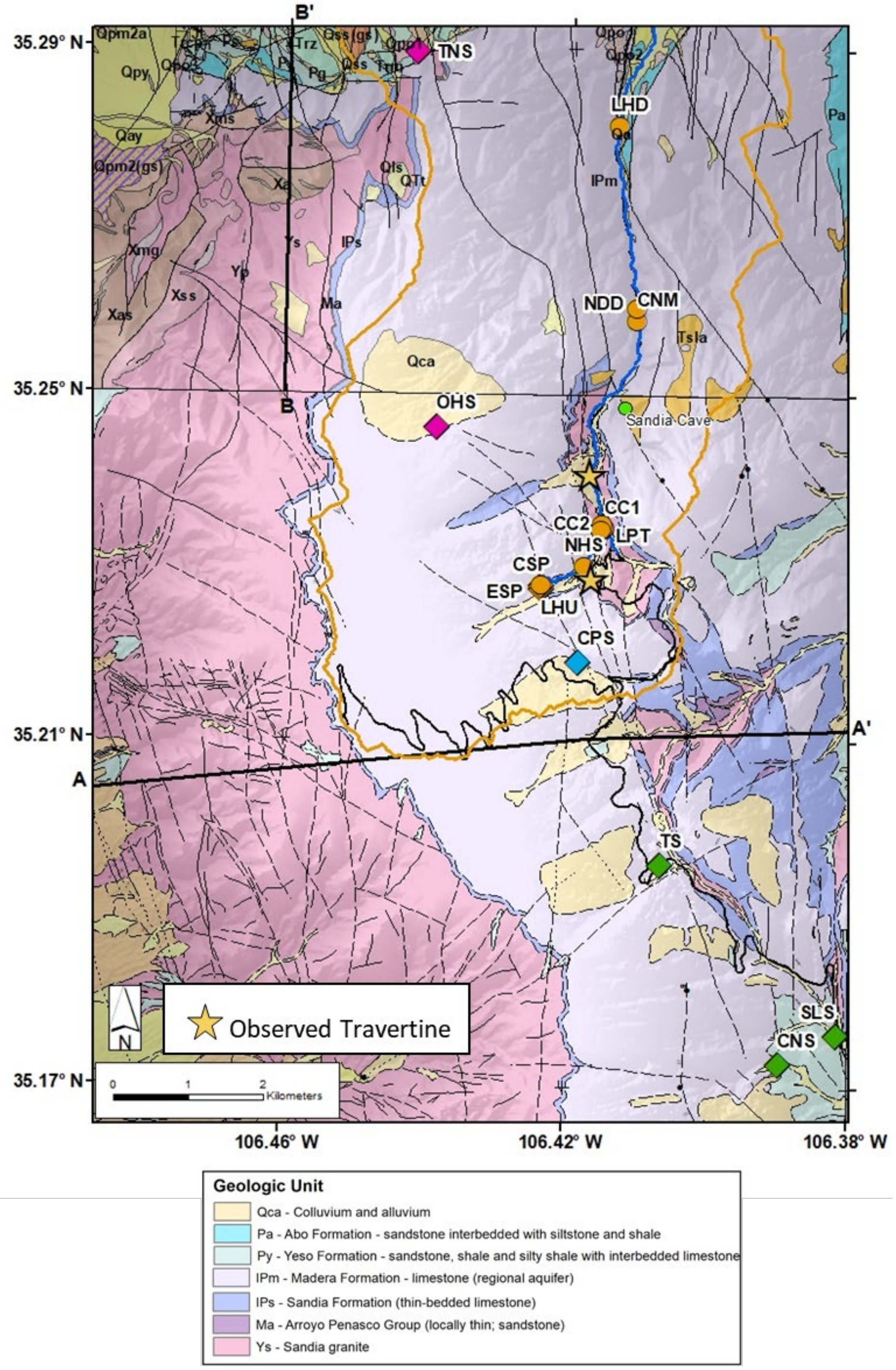

Figure 20 - Geologic map of the study region. Pennsylvanian Madera Limestone operates as the primary regional aquifer of the Las Huertas watershed, greatly influencing the water chemistry of Las Huertas spring and stream water. Springs and stream sample locations are depicted as triangles and circles, respectively. Orange stars represent observed travertine along the stream. Site map adapted from Connell et al., 2000 (Cross section A-A'); Read et al., 2000 (Cross section B-B').

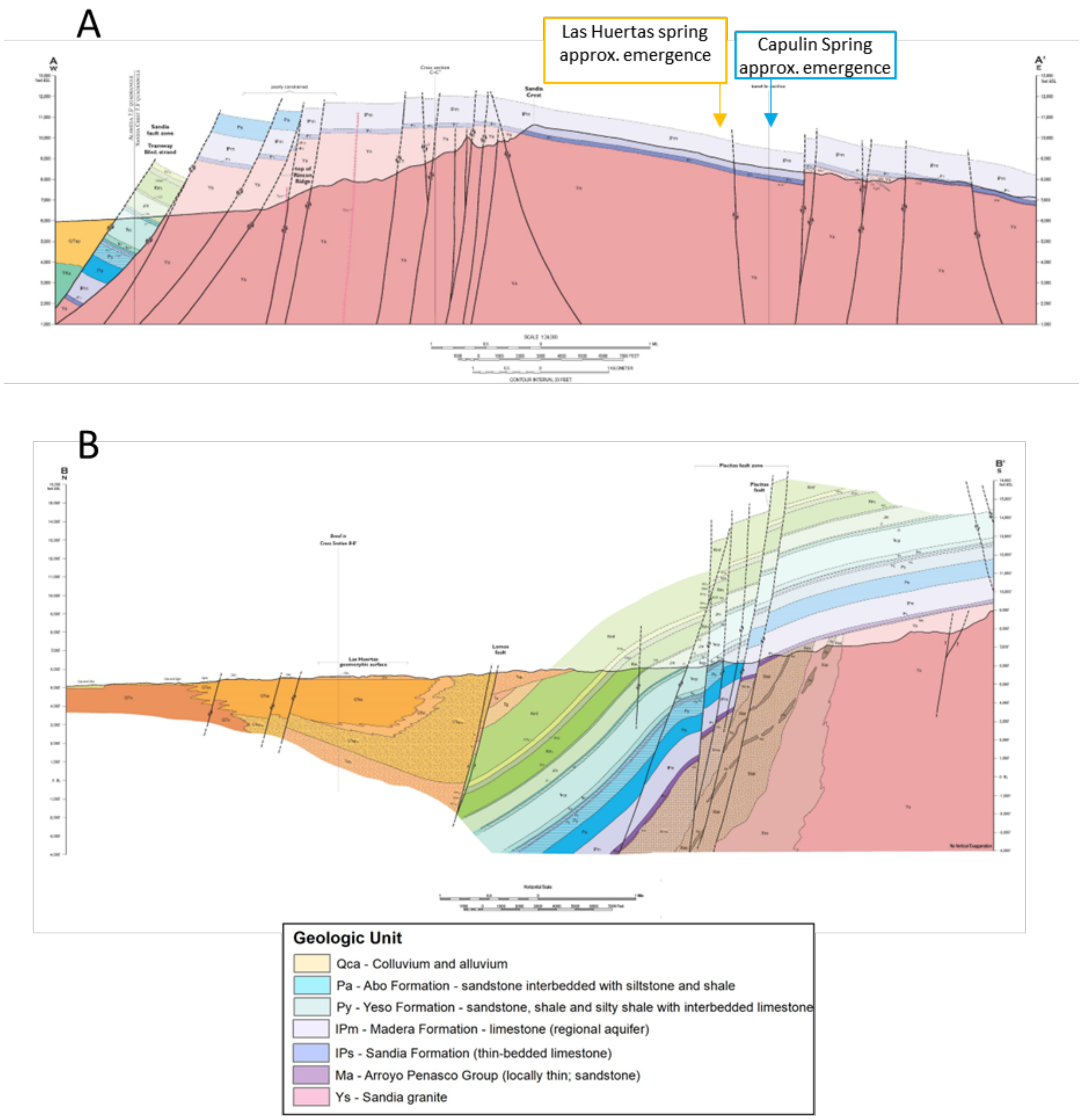

Figure 21 - A) Latitude cross section showing Sandia Crest and dip slope of the east portion of the Sandia Mountains. Las Huertas springs and Capulin Spring emerge alone on the limestone dip slope (Connell et al., 2000). B) Latitudinal cross section showing geology like the downstream section of Las Huertas (Read et al., 2000).

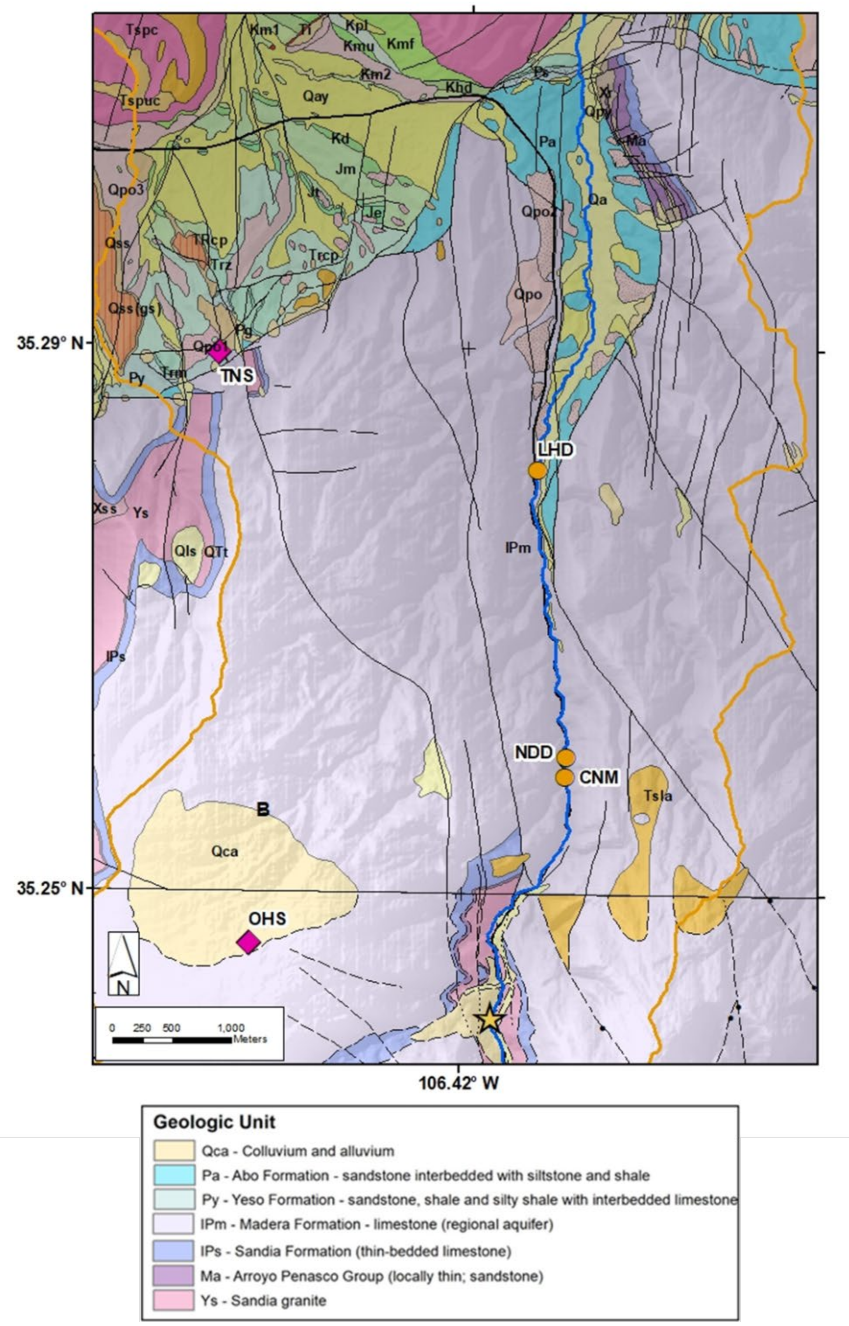

Figure 22 - Northern portion of the Las Huertas watershed showing furthest downstream locations from this study. Stream waters at North of Ditch Diversion (NDD) and Canon Media at NM165 (CNM) flow over the Madera Limestone unit (Ipm in light purple). Map adapted from Read et al., 2000.

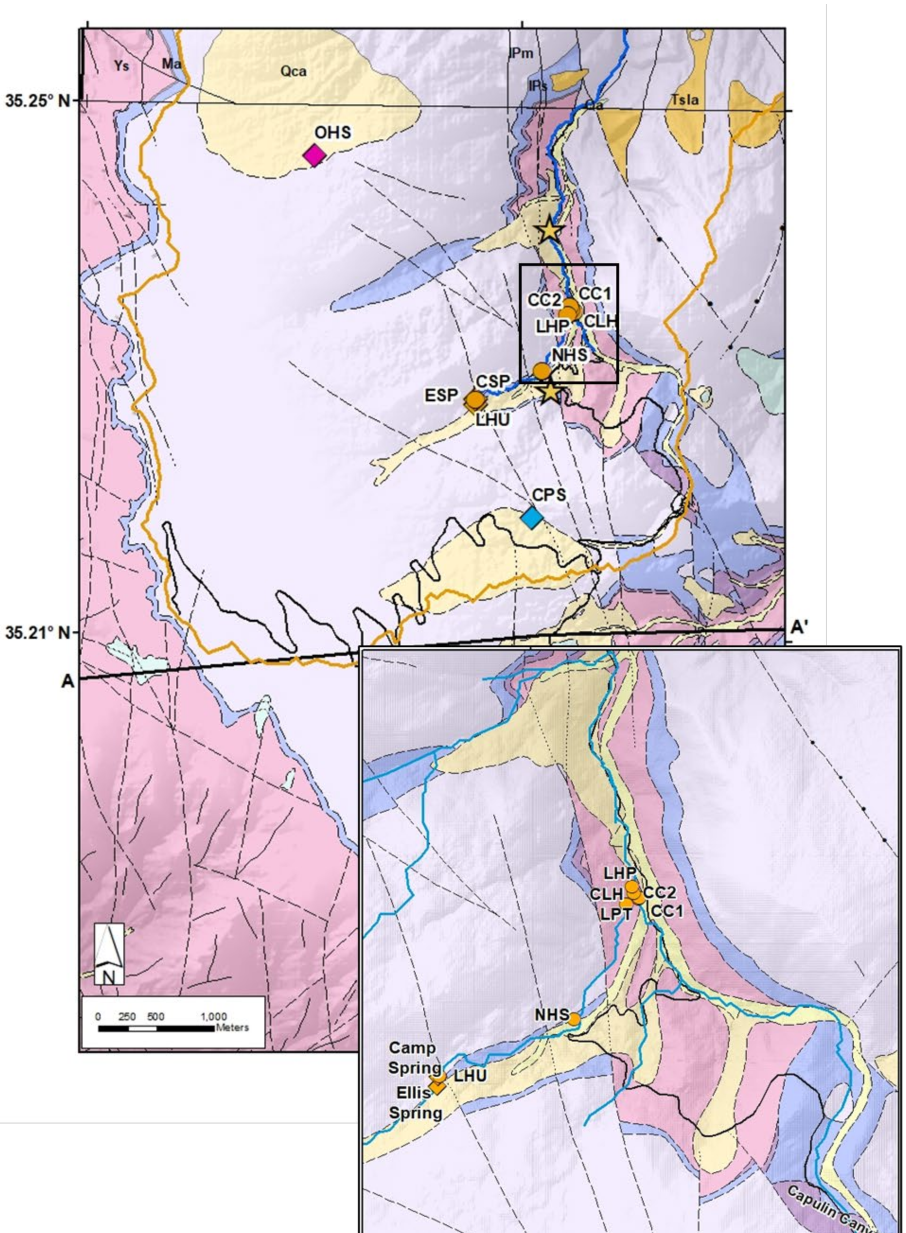

Figure 23 - Map depicting the geology of the northern and middle portions of the Las Huertas watershed. Capulin Spring (CPS), Ellis Spring (ESP), and Camp Spring (CSP) lie on colluvium over the Madera limestone. The site location cluster in the inset shows stream water sample locations on the Sandia granite (pink).

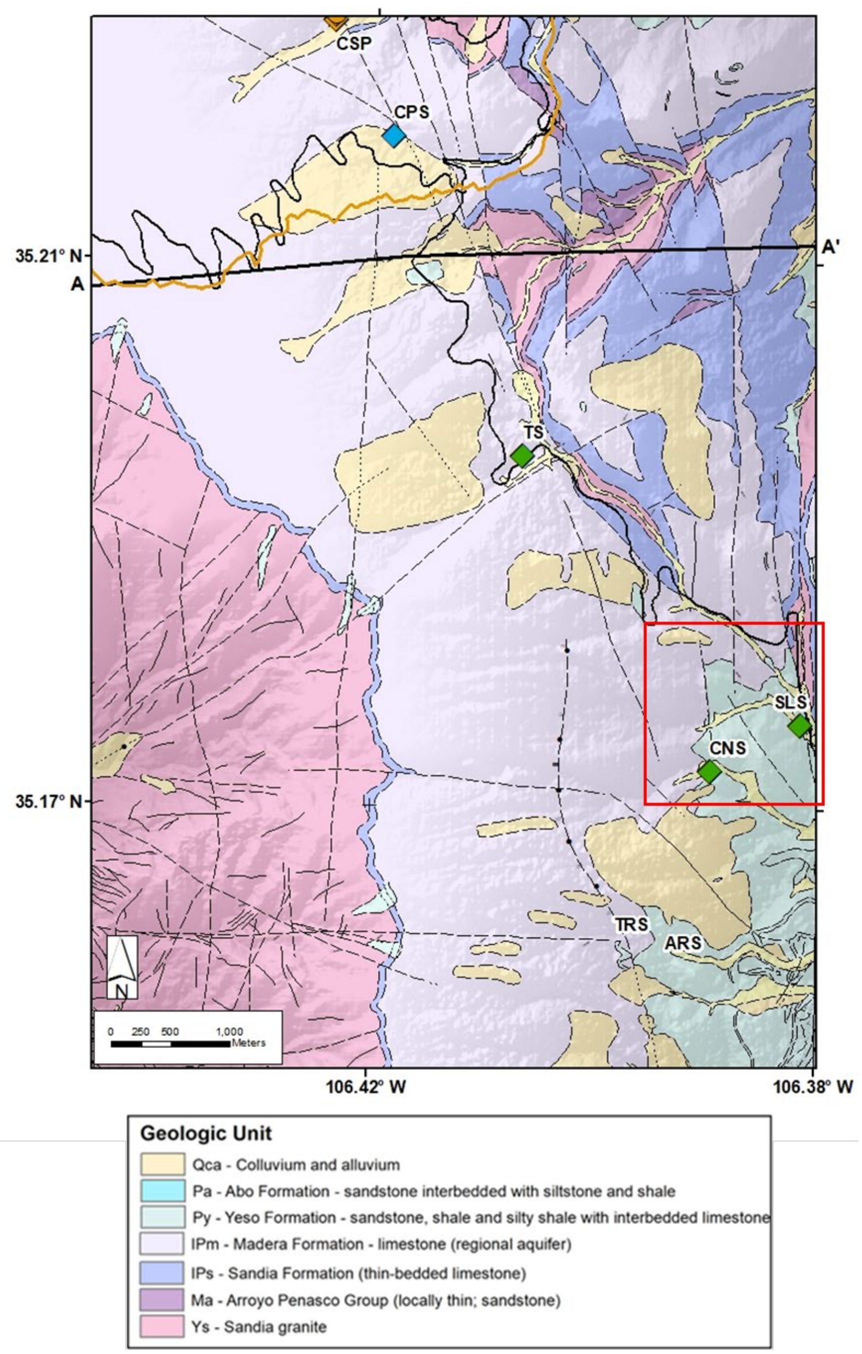

Figure 24 - Geologic map of the southern portion of the Sandia Mountains near Sandia Crest Road, Cienega Spring (CNS), and Sulphur Spring (SLS). CNS and SLS lie on contacts of alluvium (yellow) and the Abo and Yeso Formations (light green) stratigraphically above the Madera formation.

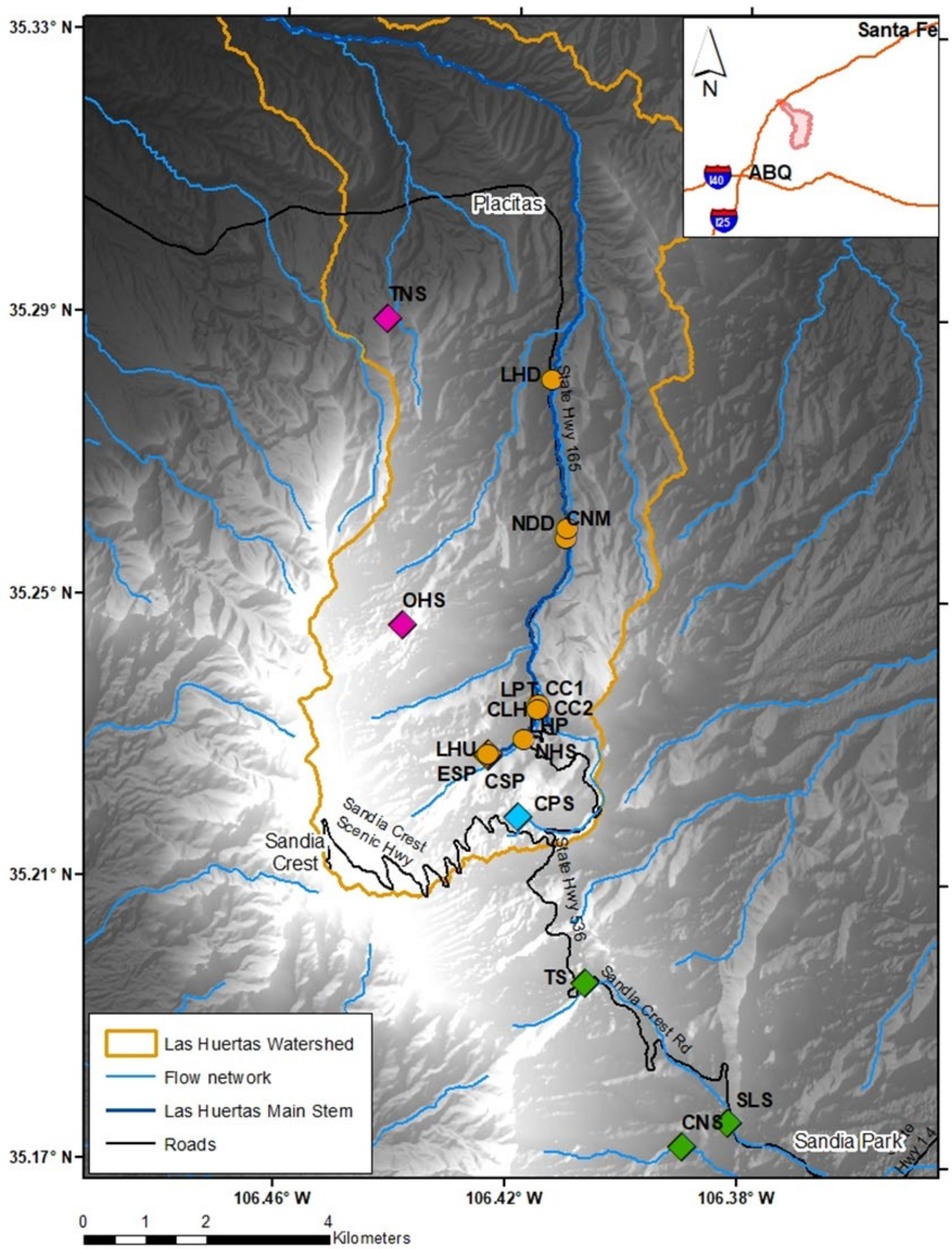

Figure 25 - Site map showing Las Huertas watershed, specific springs from the surrounding Sandia Mountains (Cienega Spring (CNC), Sulfur Spring (SLS), Tree Spring (TS), Osha Spring (OHS), and Tunnel Spring (TNS)), and drainage flow paths.

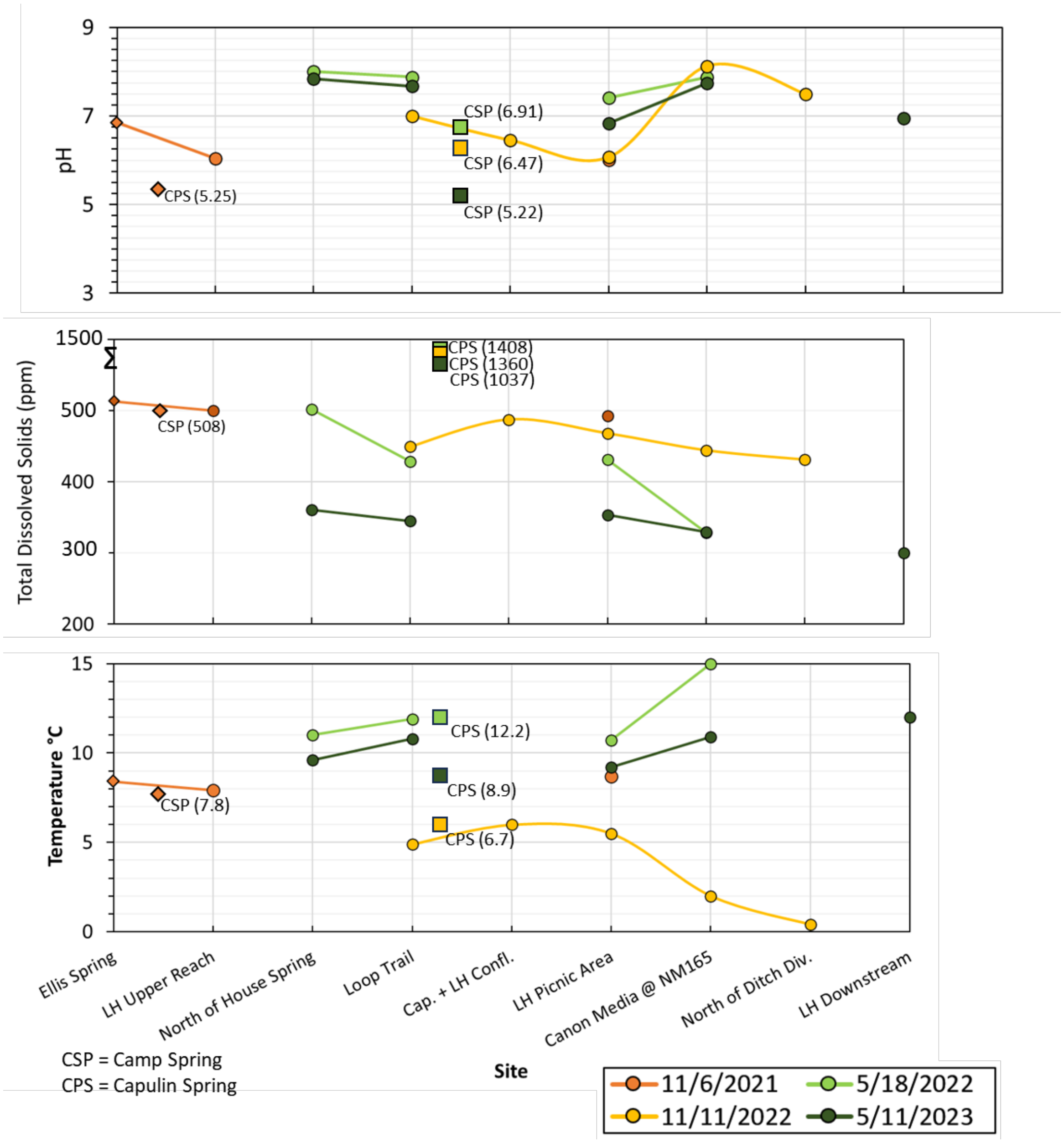

Figure 26 - Downstream plots showing measured parameters (TDS, Temperature, pH, and δD) and calculated Total Inorganic Carbon (DIC) with respect to location downstream from Capulin Spring (CPS), Ellis Spring (EPS) and Camp Spring (CSP) to Las Huertas Downstream (LHD) in the lower reaches of Las Huertas stream.

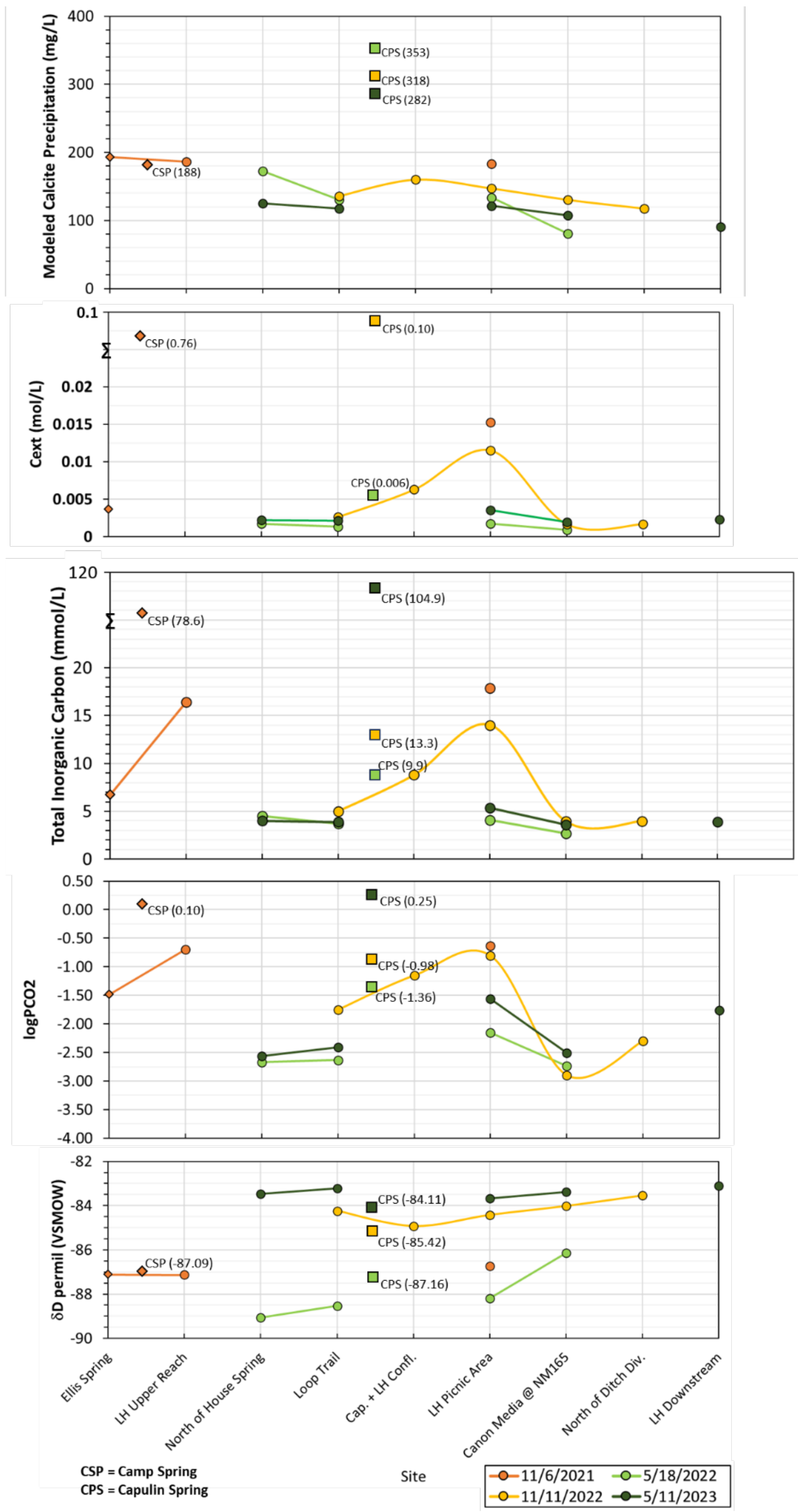

Figure 27 - Additional downstream plots with calculated PCO2, modeled calcite precipitation, external carbon, and total carbon with respect to the downstream location along the Las Huertas mainstem.